Sea Level Rise Scenarios and Inundation Maps for Selected Indian Coastal Cities

Sea Level Rise Scenarios and Inundation Maps for Selected Indian Coastal Cities

Centre for Study of Science, Technology and Policy (CSTEP)
July 2024

Designed and edited by CSTEP

Contributors: Anushiya J, Sai Venkata Ramana M, Pradeep M S, and Vidya S

This report should be cited as: CSTEP. (2024). Sea level rise scenarios and inundation maps for selected Indian coastal cities. (CSTEP-RR-2024-04)

July 2024

Center for Study of Science, Technology and Policy

Bengaluru

18, 10th Cross, Mayura Street
Papanna Layout, Nagashettyhalli
RMV II Stage, Bengaluru 560094
Karnataka (India)

Tel.: +91 (80) 6690 2500
Email: cpe@cstep.in

Noida

1st Floor, Tower-A
Smartworks Corporate Park
Sector 125, Noida 201303
Uttar Pradesh (India)

Acknowledgements

The authors would like to express their profound gratitude to Dr Mani Murali, Senior Principal Scientist, Council of Scientific and Industrial Research-National Institute of Oceanography (CSIR-NIO), Goa, and Mr Nagarajan R, Scientist and Head of GIS and Remote Sensing at the MS Swaminathan Research Foundation, Chennai. Their invaluable insights and meticulous review were instrumental in enhancing the quality of this work. The authors also extend their heartfelt appreciation to Dr Indu K Murthy, Sector Head, Climate, Environment, and Sustainability at CSTEP, and Dr Jai Asundi, the Executive Director of CSTEP, for their unwavering support and encouragement. The generous financial backing provided by Rohini Nilekani Philanthropies has been instrumental in the success of this study and is gratefully acknowledged. Lastly, the authors wish to acknowledge the significant contributions and critical reviews from various members of the CSTEP team that have greatly enriched this work.

Internal Review: Dr Indu K Murthy

Editorial Support: Ms Veena P

Report Design: Mr Alok Kumar Saha

Executive Summary

Background: Sea level rise (SLR) has been recognised as the most serious global threat. Continuing greenhouse gas (GHG) emissions are increasing global temperatures, causing thermal expansion of ocean water, and accelerating the melting of mountain glaciers and ice sheets, eventually raising sea levels. The Intergovernmental Panel on Climate Change (IPCC) has projected a global mean SLR of 1.3 to 1.6 m by 2100 under the high-emission scenario. Rising sea levels are a major hazard to coastal cities worldwide, including Indian coastal cities. Such cities in India have been economic hubs since the colonial era, with natural ports, religious monuments, cultural centres, and biodiversity or eco-sensitive hotspots. Continuing SLR will have a severe impact on these cities' resilience. There is, therefore, a need for information on inundation due to SLR irrespective of the spatial extent to frame suitable adaptation and risk mitigation strategies.

To address this need and to sensitise stakeholders on the extent of the problem, we have prepared a portfolio of SLR-induced inundation maps for selected Indian coastal cities and towns. This report presents critical information on SLR changes under historical and future climate scenarios, as well as inundation maps for 15 Indian coastal cities and towns. This information and the maps are aimed to serve as a valuable resource for research scholars and city planners and development officials involved in decision-making.

Methodology: A few Tier-I cities (Chennai and Mumbai), Tier-II cities (Haldia, Kozhikode, Kochi, Mangaluru, Thiruvananthapuram, and Visakhapatnam), and towns (Kanniyakumari, Panaji, Paradip, Puri, Thoothukudi, Udupi, and Yanam) were considered for the analysis. The approach is complementary to the plausible SLR scenarios in the IPCC Sixth Assessment Report (AR6). The observed SLR data for the selected tide gauge stations from the Permanent Service for Mean Sea Level (PSMSL) data bank and the projected ensemble model of IPCC AR6 Shared Socio-economic Pathways (SSPs) climate scenarios were used for site-specific SLR assessment. Observed SLR data for the historical period of 1987 to 2021 were analysed and plotted in combination with SLR under future scenarios till 2100. Subsequently, elevation-based inundation area mapping was performed using a digital elevation model (DEM) from Alaska Satellite Facility (ALOS) Phased Array Type L-Band Synthetic Aperture Radar (PALSAR) with a spatial resolution of 12.5 m to estimate the possible inundation area under medium- and high-emission SSP scenarios (SSP2-4.5 and SSP5-8.5, respectively) for 2040, 2060, 2080, and 2100. Finally, inundation areas for 2100 were quantified with respect to the land area land cover (LULC) for medium- and high-emission scenarios and spatially mapped for visual interpretation.

Historical SLR: An alarming rise in sea levels was noticed during the historical period in most cities and towns on the west and east coasts of India. Mumbai has experienced the maximum increase in sea levels (4.44 cm), followed by Haldia (2.726 cm), Visakhapatnam (2.381 cm), Kochi (2.213 cm), Paradip (0.717 cm), and Chennai (0.679 cm). Moreover, per year increase in sea levels was high in Mumbai (0.315 cm/year), Visakhapatnam (0.181 cm/year), Kochi (0.158 cm/year), and Paradip (0.108 cm/year).

Future SLR: Climate models used in this study project that the SLR will continue until the end of the century under all scenarios and all 15 cities and towns will experience increases in SLR. While SLR will be higher in Mumbai, Tier-II cities and towns such as Panaji, Udupi, Mangaluru, Kochi, Kozhikode, Kanniyakumari, and Thiruvanathapuram may also experience a high increase in sea levels under future climate change scenarios. Under the SSP2-4.5 (medium-emission) scenario, the SLR is projected to be 76.2 cm at Mumbai, followed by Panaji (75.5 cm), Udupi (75.3 cm), Mangaluru (75.2 cm), Kozhikode (75.1 cm), Kochi (74.9 cm), Thiruvananthapuram (74.7 cm), and Kanniyakumari (74.7 cm) by 2100.

Future inundation: SLR-induced inundation area and the affected LULCs vary across the selected cities and towns. By 2040, land subsidence would exceed 10% in Mumbai, Yanam, and Thoothukudi; 5%–10% in Panaji and Chennai; and 1%–5% in Kochi, Mangaluru, Visakhapatnam, Haldia, Udupi, Paradip, and Puri. While in 2100, the inundation would be higher in Mangaluru (Tier-II city), Haldia, Paradip, Thoothukudi, and Yanam (towns) than in Tier-I cities under the high-emission (SSP5-8.5) scenario.

These results emphasise the importance of considering localised SLR-induced inundation in informing a wide range of stakeholders on resilience actions in coastal cities. Further, such information would be useful in developing appropriate adaptation and risk mitigation strategies to reduce the effects of SLR, protect coastal communities, and promote sustainable coastal development in the face of climate change.

Table of Contents

1. Introduction **13**

1.1. Impacts of SLR 13

1.2. Trends of SLR in the Indian Coastline 14

2. Objectives **14**

3. Why Map SLR for Coastal Cities? **15**

4. Data and Methodology **17**

4.1. Relative SLR 17

4.2. Projected SLR-Induced Inundation Mapping for Tier-I Cities, Tier-II Cities, and Towns 18

4.3. Assessing Future SLR-Induced Inundation for LULC Classes 19

5. Results and Discussion **21**

5.1. Tier-I Cities 22

5.1.1. Chennai, Tamil Nadu 22

5.1.2. Mumbai, Maharashtra 23

5.2. Tier-II Cities 26

5.2.1. Haldia, West Bengal 26

5.2.2. Kochi, Kerala 28

5.2.3. Kozhikode, Kerala 29

5.2.4. Mangaluru, Karnataka 31

5.2.5. Thiruvananthapuram, Kerala 32

5.2.6. Visakhapatnam, Andhra Pradesh 34

5.3. Towns 39

5.3.1. Kanniyakumari, Tamil Nadu 39

5.3.2. Panaji, Goa 40

5.3.3. Paradip, Odisha 42

5.3.4. Puri, Odisha 43

5.3.5. Thoothukudi, Tamil Nadu 45

5.3.6. Udupi, Karnataka 46

5.3.7. Yanam, Puducherry 48

6. Conclusion **53**

7. References **55**

8. Appendices **61**

Tables

Table 4.1: Details of data from the tide gauge stations 18

Table 5.1: Historical SLR at the tide gauge stations 21

Table 5.2: Projected SLR (in cm) and impacted area (in sq. km) for Tier-I cities under different SSP scenarios for the considered years 25

Table 5.3: LULC-wise (existing) inundation area (in sq. km) for projected SLR by 2100 in Tier-I cities 25

Table 5.4: Projected SLR (in cm) and impacted area (in sq. km) for Tier-II cities under different SSP scenarios for the considered years 36

Table 5.5: LULC-wise (existing) inundation area (sq. km) for projected SLR by 2100 in Tier-II cities 37

Table 5.6: Projected SLR (in cm) and impacted area (in sq. km) for the selected towns under different SSP scenarios for the considered years 50

Table 5.7: LULC-wise (existing) inundation area (sq. km) for projected SLR by 2100 in the selected towns. 51

Figures

Figure 3.1: Tier-wise spatial distribution of Indian coastal cities and towns 16

Figure 4.1: Flow chart of the methodology 17

Figure 4.2: Flow chart of DEM processing and delineation of inundation maps 20

Figure 5.1: (a) Sea level rise during the historical period from the Chennai tide gauge station; (b) SLR projected under the future SSP scenarios for Chennai, Tamil Nadu 22

Figure 5.2: (a) Inundation area for projected SLR in Chennai, Tamil Nadu; (b) LULC-wise inundation for projected SLR by 2100 under the future SSP2-4.5 scenario in Chennai, Tamil Nadu 22

Figure 5.3: (a) Inundation area for projected SLR in Chennai, Tamil Nadu; (b) LULC-wise inundation for projected SLR by 2100 under the future SSP5-8.5 scenario in Chennai, Tamil Nadu 23

Figure 5.4: (a) Sea level rise during the historical period from the Mumbai tide gauge station; (b) SLR projected under the future SSP scenarios for Mumbai, Maharashtra 23

Figure 5.5: (a) Inundation area for projected SLR in Mumbai, Maharashtra; (b) LULC-wise inundation for projected SLR by 2100 under the future SSP2-4.5 scenario in Mumbai, Maharashtra 24

Figure 5.6: (a) Inundation area for projected SLR in Mumbai, Maharashtra; (b) LULC-wise inundation for projected SLR by 2100 under the future SSP5-8.5 scenario in Mumbai, Maharashtra 24

Figure 5.7: (a) Sea level rise during the historical period from the Haldia tide gauge station; (b) SLR projected under the future SSP scenarios for Haldia, West Bengal 26

Figure 5.8: (a) Inundation area for projected SLR in Haldia, West Bengal; (b) LULC-wise inundation for projected SLR by 2100 under the SSP2-4.5 scenario in Haldia, West Bengal 27

Figure 5.9: (a) Inundation area for projected SLR in Haldia, West Bengal; (b) LULC-wise inundation for projected SLR by 2100 under the SSP5-8.5 scenario in Haldia, West Bengal 27

Figure 5.10: (a) Sea level rise during the historical period from the Kochi tide gauge station; (b) SLR projected under the future SSP scenarios for Kochi, Kerala 28

Figure 5.11: (a) Inundation area for projected SLR in Kochi, Kerala; (b) LULC-wise inundation for projected SLR by 2100 under the future SSP2-4.5 scenario in Kochi, Kerala 28

Figure 5.12: (a) Inundation area for projected SLR in Kochi, Kerala; (b) LULC-wise inundation for projected SLR by 2100 under the future SSP5-8.5 scenario in Kochi, Kerala 29

Figure 5.13: (a) Sea level rise during the historical period from the Kochi tide gauge station; (b) SLR projected under the future SSP scenarios for Kozhikode, Kerala 29

Figure 5.14: (a) Area inundated due to SLR in Kozhikode, Kerala; (b) LULC-wise inundation by 2100 under the SSP2-4.5 scenario in Kozhikode, Kerala 30

Figure 5.15: (a) Inundation area for projected SLR in Kozhikode, Kerala; (b) LULC-wise inundation for projected SLR by 2100 under the future SSP5-8.5 scenario in Kozhikode, Kerala 30

Figure 5.16: (a) Sea level rise during the historical period from the Panambur tide gauge station; (b) SLR projected under the future SSP scenarios for Mangaluru, Karnataka 31

Figure 5.17: (a) Inundation area for projected SLR in Mangaluru, Karnataka; (b) LULC-wise inundation for projected SLR by 2100 under the SSP2-4.5 scenario in Mangaluru, Karnataka 31

Figure 5.18: (a) Inundation area for projected SLR in Mangaluru, Karnataka; (b) LULC-wise inundation for projected SLR by 2100 under the SSP5-8.5 scenario in Mangaluru, Karnataka 32

Figure 5.19: (a) Sea level rise during the historical period from the Kochi tide gauge station; (b) SLR projected under the future SSP scenarios for Thiruvananthapuram, Kerala 32

Figure 5.20: (a) Inundation area for projected SLR in Thiruvananthapuram, Kerala; (b) LULC-wise inundation by 2100 under the SSP2-4.5 scenario in Thiruvananthapuram, Kerala 33

Figure 5.21: (a) Inundation area for projected SLR in Thiruvananthapuram, Kerala; (b) LULC-wise inundation for projected SLR by 2100 under the SSP5-8.5 scenario in Thiruvananthapuram, Kerala........ 33

Figure 5.22: (a) Sea level rise during the historical period from the Visakhapatnam tide gauge station; (b) SLR projected under the future SSP scenarios for Visakhapatnam, Andhra Pradesh 34

Figure 5.23: (a) Inundation area for projected SLR in Visakhapatnam, Andhra Pradesh; (b) LULC-wise inundation for projected SLR by 2100 under the SSP2-4.5 scenario in Visakhapatnam, Andhra Pradesh 34

Figure 5.24: (a) Inundation area for projected SLR in Visakhapatnam, Andhra Pradesh; (b) LULC-wise inundation for projected SLR by 2100 under the SSP5-8.5 scenario in Visakhapatnam, Andhra Pradesh 35

Figure 5.25: (a) Sea level rise during the historical period from the Thoothukudi tide gauge station; (b) SLR projected under the future SSP scenarios for Kanniyakumari, Kerala........ 39

Figure 5.26: (a) Inundation area for projected SLR in Kanniyakumari, Tamil Nadu; (b) LULC-wise inundation for projected SLR by 2100 under the SSP2-4.5 scenario in Kanniyakumari, Tamil Nadu........ 39

Figure 5.27: (a) Inundation area for projected SLR in Kanniyakumari, Tamil Nadu; (b) LULC-wise inundation for projected SLR by 2100 under the SSP5-8.5 scenario in Kanniyakumari, Tamil Nadu........ 40

Figure 5.28: (a) Sea level rise during the historical period from the Murmugao tide gauge station; (b) SLR projected under the future SSP scenarios for Panaji, Goa........ 40

Figure 5.29: (a) Inundation area for projected SLR in Panaji, Goa; (b) LULC-wise inundation for projected SLR by 2100 under the SSP2-4.5 scenario in Panaji, Goa........ 41

Figure 5.30: (a) Inundation area for projected SLR in Panaji, Goa; (b) LULC-wise inundation for projected SLR by 2100 under the SSP5-8.5 scenario in Panaji, Goa........ 41

Figure 5.31: (a) Sea level rise during the historical period from the Paradip tide gauge station; (b) SLR projected under the future SSP scenarios for Paradip, Odisha........ 42

Figure 5.32: (a) Inundation area for projected SLR in Paradip, Odisha; (b) LULC-wise inundation for projected SLR by 2100 under the SSP2-4.5 scenario in Paradip, Odisha........ 42

Figure 5.33: (a) Inundation area for projected SLR in Paradip, Odisha; (b) LULC-wise inundation for projected SLR by 2100 under the SSP5-8.5 scenario in Paradip, Odisha........ 43

Figure 5.34: (a) Sea level rise during the historical period from the Paradip tide gauge station; (b) SLR projected under the future SSP scenarios for Puri, Odisha 43

Figure 5.35: (a) Inundation area for projected SLR in Puri, Odisha; (b) LULC-wise inundation for projected SLR by 2100 under the SSP2-4.5 scenario in Puri, Odisha 44

Figure 5.36: (a) Inundation area for projected SLR in Puri, Odisha; (b) LULC-wise inundation for projected SLR by 2100 under the SSP5-8.5 scenario in Puri, Odisha 44

Figure 5.37: (a) Sea level rise during the historical period from the Thoothukudi tide gauge station; (b) SLR projected under the future SSP scenarios for Thoothukudi, Tamil Nadu........ 45

Figure 5.38: (a) Inundation area for projected SLR in Thoothukudi, Tamil Nadu; (b) LULC-wise inundation for projected SLR by 2100 under the SSP2-4.5 scenario in Thoothukudi, Tamil Nadu........ 45

Figure 5.39: (a) Inundation area for projected SLR in Thoothukudi, Tamil Nadu; (b) LULC-wise inundation for projected SLR by 2100 under the SSP5-8.5 scenario in Thoothukudi, Tamil Nadu........ 46

Figure 5.40: (a) Sea level rise during the historical period from the Panambur tide gauge station; (b) SLR projected under the future SSP scenarios for Udupi, Karnataka 46

Figure 5.41: Inundation area for projected SLR in Udupi, Karnataka; (b) LULC-wise inundation for projected SLR by 2100 under the SSP2-4.5 scenario in Udupi, Karnataka 47

Figure 5.42: (a) Inundation area for projected SLR in Udupi, Karnataka; (b) LULC-wise inundation for projected SLR by 2100 under the SSP5-8.5 scenario in Udupi, Karnataka 47

Figure 5.43: (a) Sea level rise during the historical period from the Visakhapatnam tide gauge station; (b) SLR projected under the future SSP scenarios for Yanam, Puducherry 48

Figure 5.44: (a) Inundation area for projected SLR in Yanam, Puducherry; (b) LULC-wise inundation for projected SLR by 2100 under the SSP2-4.5 scenario in Yanam, Puducherry........ 48

Figure 5.45: (a) Inundation area for projected SLR in Yanam, Puducherry; (b) LULC-wise inundation for projected SLR by 2100 under the SSP5-8.5 scenario in Yanam, Puducherry........ 49

1. Introduction

The environment, ecosystems, human communities, and the economy are just a few of the many components of the Earth's system that are significantly impacted by climate change. Some of the clear signals of climate change are rising temperatures, melting ice and glaciers, changing precipitation patterns, extreme weather events, ocean acidification, and sea level rise (SLR).
Sea level rise is the gradual increase in the average height of the world's oceans and seas. It is determined by the rise in the water level in relation to the land (Church et al., 2001). The expansion of seawater is caused by heat and the influx of water from ice melting, as explained below.

- **Ocean thermal expansion**: Oceans absorb more than 90% of the heat trapped by accumulating greenhouse gases (GHGs)—the primary cause of Earth's warming (Titus et al., 1991). As a result, ocean temperatures increase and the water expands, resulting in SLR (Warrick & Oerlemans, 1990).
- **Ice melting**: The melting of ice from glaciers, ice caps, and ice sheets in Greenland and Antarctica is another cause of SLR (Leuliette & Nerem, 2016; Otosaka et al., 2022). Substantial melting of land-based ice blocks and glaciers due to rising global temperatures adds water to the oceans, thereby increasing global sea levels.

The past century has witnessed an increase in the rate of SLR, primarily because of human-induced climate change brought on by fossil-fuel burning and GHG emissions. Climate-change-induced SLR is one of the most serious concerns for low-lying coastal regions (Arkema et al., 2012). Between 1901 and 2018, the average worldwide sea level rose by 15 to 25 cm (6 to 10 inch), and it is predicted to further rise by 15 mm per year (10 to 20 mm per year) by 2100 (IPCC, 2019). The global average sea level reached a record high in 2022, rising 101.2 mm (4 inch) above 1993 levels. According to recent research, if emissions continue to rise at current rates, SLR may be significantly high by 2100—possibly rising by more than 2 m or 6.5 feet (NOAA, 2022).

1.1. Impacts of SLR

Sea level rise can have serious repercussions, especially in coastal cities and low-lying areas. The following are the possible effects of SLR:

- **Increased coastal erosion**: As the sea level rises, more frequent and extreme coastal floods (Yu et al., 2022) and storm surges (Houser et al., 2008) occur, which increase coastal erosion (Gopalakrishnan et al., 2016; Enríquez et al., 2017). This, in turn, may cause the loss of beaches, coastal habitats, and even entire settlements.
- **Coastal inundation and flooding**: Rising sea levels increase the risk of frequent and severe floods (Taherkhani et al., 2020) and inundation (Kanan et al., 2023) in low-lying coastal regions and islands.
- **Freshwater salinisation**: Freshwater sources, such as subterranean aquifers and river deltas, are susceptible to salinisation due to SLR (Werner & Simmons, 2009). This infiltration may contaminate drinking water sources and reduce agricultural output (Remya et al., 2018; Schneider & Asch, 2020).
- **Coastal community displacement**: Low-lying coastal communities are at risk of land flooding due to SLR (Nicholls et al., 2011). The resulting displacement of such communities would necessitate the use of adaptation and relocation strategies.
- **Coastal habitat loss**: Sea level rise is especially dangerous for coastal ecosystems, such as mangroves, salt marshes, and coral reefs (Saintilan et al., 2023). These habitats offer crucial

nurseries (Von Holle et al., 2019), breeding grounds, and shelter from coastal erosion. The disappearance of such habitats due to SLR may adversely affect fisheries and biodiversity (Arkema et al., 2013).

- **Infrastructure vulnerability**: Sea level rise puts coastal infrastructure, such as buildings, roads, airports, and ports, in danger. Higher water levels and more frequent flooding raise the risk of infrastructure disruption and damage, necessitating expensive repairs and modifications (Keenan et al., 2018).
- **Impacts on the economy**: With industries such as tourism (Yong, 2021), fishing, and shipping, coastal regions contribute majorly to the world economy. These industries may be affected by SLR, which could result in financial losses and higher adaptation and infrastructure protection expenditures (Lincke & Hinkel, 2018; Seeteram et al., 2023).

1.2. Trends of SLR in the Indian Coastline

Sea level rise varies by location across the world, which is due to modifications to atmospheric and/or oceanic circulation: the Indian coast is no exception. Unnikrishnan et al. (2006) used tide gauge observations over various periods and estimated the SLR at selected stations along the Indian coast (Mumbai, Kochi, Chennai, and Vishakhapatnam) to be under approximately 1 mm/year. A recent report by the Ministry of Earth Sciences (MoES, 2020) estimated an SLR of 1.7 mm/year in the Indian Ocean, with a rate of 3.3 mm/year from 1993 to 2015. Extreme sea level (ESL) has become more frequent and intense along the Indian Ocean coastline as a result of SLR. A 2–3-fold increase has been observed in ESL occurrence, with higher risk in the Arabian Sea coastline and the Indian Ocean islands (Sreeraj et al., 2022). Prasanth Kumar et al. (2021) used sea level anomaly altimeter data to report that the sea level is continuously rising in the Indian coastline, with a higher acceleration in the Arabian Sea (Jyothi et al., 2023). Although significant progress has been achieved in recent years, gaps remain in knowledge and information on SLR and its impacts, particularly at scales such as cities (IPCC, AR6, 2022). As a significant portion of the world's population and economic activity are concentrated across coastal cities and settlements (C&S), these are far more vulnerable to a variety of climate- and ocean-compounded hazard risks that are driven by climate change than inland C&Ss. Small towns along rivers and estuaries, small island states with a maritime population, large cities serving as important transportation and financial hubs in coastal deltas, megacities, and megaregions with multiple coastal megacities are examples of C&Ss (IPCC, AR6, 2022).

2. Objectives

This study aims to assess changes in SLR for selected coastal cities and towns under current and future climate change scenarios and map the inundation in these cities and towns. The following are the specific objectives of the study:

- Study the historical changes in relative SLR.
- Study the changes in relative SLR under future climate change scenarios.
- Estimate SLR-induced probable inundation area in coastal cities and towns for future scenarios.
- Assess land use land cover (LULC) that will be affected by SLR by 2100.

3. Why Map SLR for Coastal Cities?

Sea level rise, combined with rapid urbanisation, has considerably increased risks to the coastal cities. By 2050, over 800 million people (10% of the world and 13% of the total urban population), living in more than 570 coastal cities, will be at risk of at least 0.5 m of SLR and coastal flooding (UCCRN technical report, 2018). India, surrounded by the Indian Ocean, Arabian Sea, and Bay of Bengal, has a 7,517-km coastline, making SLR a crucial concern to the country. About 170 million people or 15.5% of the nation's population are spread across nine coastal states and union territories (Gujarat, Maharashtra, Goa, Karnataka, Kerala, Tamil Nadu, Andhra Pradesh, Odisha, and West Bengal). India's coastline has 13 major seaports and 180 smaller busy ports. Furthermore, India's coastal cities are habitation hubs with significant cultural, spiritual, and economic activities, including fishing, trading, and tourism.

Several studies have indicated that rising sea levels will biogeographically affect the coastal region, and impacts such as inundation, flood, and storm damage will lead to morphological changes and land claims (Carretero et al., 2013; Gesch, 2018; Pariartha et al., 2023; Taherkhani et al., 2020). Saltwater intrusion induced by SLR both upstream and into coastal aquifers will threaten urban drinking water supplies and contaminate agricultural soils (Rotzoll & Fletcher, 2013).

Moreover, the impacts of SLR and coastal flooding would vary according to a city's geography, social structure, urban development patterns, and economic make-up. The increasing urbanisation trend, particularly along the coast, is closely associated with vulnerability due to climate change drivers. Low-lying coastal towns are now more exposed and vulnerable to SLR and ESL occurrences due to human-induced non-climatic drivers, such as historical and current population and settlement patterns and subsidence (Oppenheimer et al., 2019).

In this study, 15 cities and towns from the east and west coast of India were selected for analysis; these cities and towns belong to three categories[1]—Tier-I city (thriving urban centres), Tier-II city (emerging urban centres), and towns (growing urban centres). Tier-I cities considered in this study are Mumbai and Chennai, which are major metropolitan cities known for their robust economies, well-developed infrastructure, and significant contributions to the country's gross domestic product. The included Tier-II cities are Kozhikode, Kochi, Haldia, Mangaluru, Thiruvananthapuram, and Visakhapatnam, while the considered towns are Kanniyakumari, Udupi, Panaji, Paradip, Puri, Thoothukudi, and Yanam. The geographic locations of the chosen coastal cities and towns are shown in Figure 3.1. The diverse nature of the selected cities and towns with respect to area, population, and other characteristics is presented in Appendix 1.

[1] Classified on the basis of population size, economic development, infrastructure, educational institutions, healthcare facilities, and administrative importance.

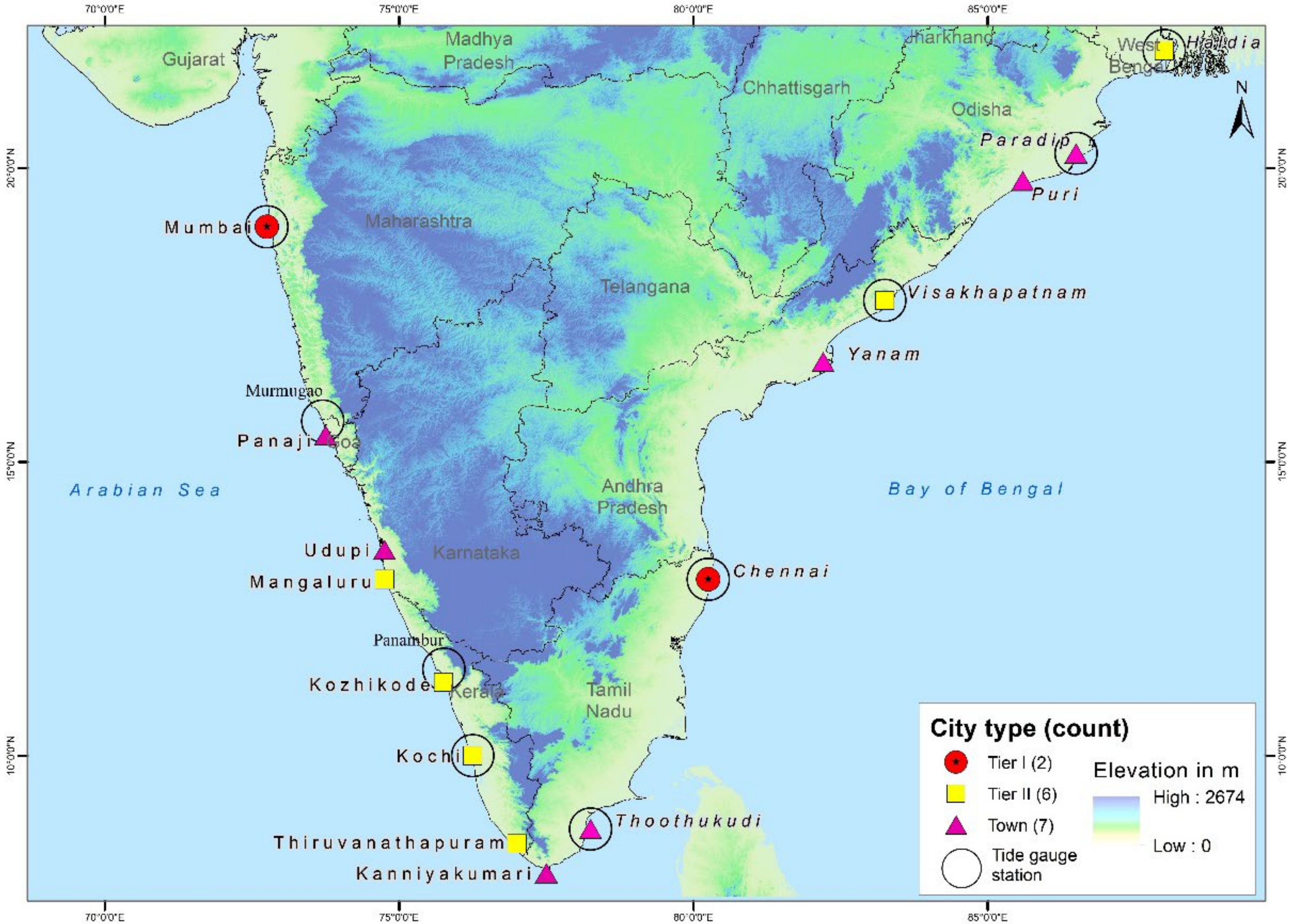

Figure 3.1: Tier-wise spatial distribution of Indian coastal cities and towns

4. Data and Methodology

This study analysed the changes in historical and future SLR for 15 coastal cities and towns and developed spatial information on future inundation. A three-phase approach, involving the assessment of relative SLR under historical and future climate scenarios, mapping of SLR-induced inundation for future climate scenarios, and the calculation of LULC-wise inundation areas, was adopted. A flow chart detailing the steps is presented in Figure 4.1.

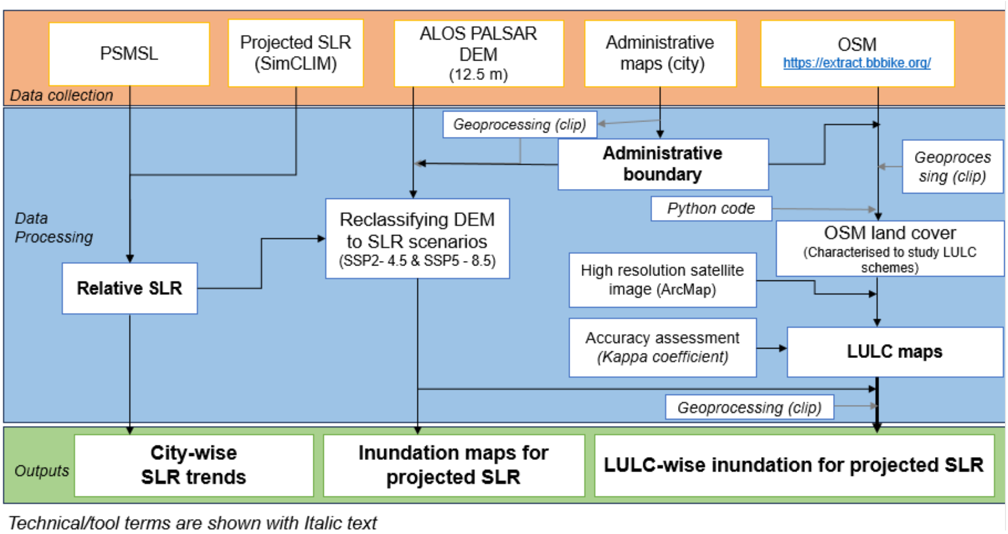

Figure 4.1: Flow chart of the methodology

4.1. Relative SLR

The relative sea level change at a coastal location is determined by the sum of global, regional, and local influences (Nicholls & Leatherman, 1996; Nicholls, 2002). To assess relative sea level changes[2] along the coastal cities under historical and future climate scenarios, historical and projected SLR data from the SimCLIM tool were utilised. Annual mean sea level observation data for selected tide gauge stations (Figure 3.1 and Table 4.1) along the Indian coastline were obtained from the Permanent Service for Mean Sea Level (PSMSL)[3] data bank. Continuous data for all available periods were considered to find the changes in historical SLR. Details of tide gauge stations, data availability, data completeness, and the nearby cities and towns are provided in Table 4.1.

The SimCLIM AR6 for Desktop[4], an integrated assessment modelling system, was utilised for generating SLR projections for selected coastal cities and towns by employing the pattern-scaling method[5]. This approach, essential at various scales and scenarios, incorporates comparisons of standardised spatial patterns from different general circulation models (GCMs) as outlined by Santer et al. (1990). It effectively leverages data from the latest Coupled Model Intercomparison Project Phase 6 (CMIP6), aligning with the IPCC's Sixth Assessment Report (AR6).

[2] Relative sea level change refers to the fluctuations in the ocean's elevation relative to the adjacent land at a particular site, showing if the sea level is increasing or decreasing in relation to the land.
[3] PSMSL is the global archive for data on long-term sea level changes obtained from tide gauges and bottom pressure recorders (https://psmsl.org/).
[4] SimCLIM Data Manual 4, 2017 (https://www.climsystems.com/)
[5] In climate projections, the pattern-scaling method uses simple models to approximate complex GCM responses. Although main errors crop in from non-linear local responses and GCM variability, the method remains effective for regional projections.

Renowned research institutions contribute to this valuable dataset, which showcases diverse levels of spatial resolution and includes a range of Shared Socio-economic Pathways (SSPs) for the IPCC AR6. The data is meticulously standardised to a 720 × 360 grid format, with a 0.5° resolution in longitude and latitude, by utilising advanced methods of pattern scaling and bilinear interpolation. This methodology has proven to be highly useful for comprehensive risk assessments of climate change especially as more GCM outputs become publicly available (Mitchell, 2003; Li et al., 2009), thereby complementing the insights of Warrick (2009).

The SimCLIM tool has 39 GCMs (Appendix 2) from CMIP6 and the ability to execute scenarios for all SSPs—SSP1-1.9, SSP1-2.6, SSP2-4.5, SSP3-7.0, and SSP5-8.5 scenarios (Appendix 3). All 39 GCMs were used to build an ensemble, and SLR changes with medium confidence (about 5 out of 10 chance) were computed for all SSP scenarios until 2100 (SimCLIM, 2011). For further analysis and mapping, the SLR was calculated for selected tide gauge stations over the past 30 years and plotted

Table 4.1: Details of data from the tide gauge stations

Station	Tide gauge station		City type		
	Period	Completeness (%)	Tier I	Tier II	Town
Chennai	1916–2016	61.14	Chennai		
Mumbai	1878 –2020	88.29	Mumbai		
Kochi	1939 –2019	85.34		Kozhikode, Kochi, Thiruvananthapuram	
Thoothukudi	1967 –2021	55.72			Kanniyakumari, Thoothukudi
Panambur	1977 –2021	77.17		Mangaluru	Udupi
Visakhapatnam	1937 –2021	83.63		Visakhapatnam	Yanam
Paradip	1967 –2021	77.98			Puri, Paradip
Haldia	1971–2020	94.93		Haldia	
Murmugao	1969–2020	72.6			Panaji

4.2. Projected SLR-Induced Inundation Mapping for Tier-I Cities, Tier-II Cities, and Towns

Inundation along the coast increases as relative sea levels rise. In this context, the inundation area refers to the area where emerging lands are submerged by seawater due to relative SLR. Elevation-based assessments have often been used to identify low-lying coastal lands over broad areas and assess the effects of rising sea levels (Gesch, 2018; Malik & Abdalla, 2016; Small et al., 2018; Titus & Richman, 2001). A digital elevation model (DEM) of Alaska Satellite Facility (ALOS) Phased Array Type L-Band Synthetic Aperture Radar (PALSAR)[6] with a spatial resolution of 12.5 m was used to demarcate and compute the probable submerged land area (Xie et al., 2013) under

[6] Alaska Satellite Facility - Distributed Active Archive Center https://asf.alaska.edu/datasets/daac/alos-palsar/

projected SLR scenarios (SSP2-4.5 and SSP5-8.5) for 2040, 2060, 2080, and 2100 in the ArcGIS platform (Figure 4.2).

DEM processing

The DEM was pre-processed to avoid imperfections and obtain a more precise version. Sinks (and peaks)[7] are often errors due to the resolution of data or rounding of elevations to the nearest integer value (Tarboton. et al., 1991). To overcome this, the DEM was processed using spatial analyst tools Fill and Sink.

Raster reclassification

The DEM from ALOS PALSAR offers higher resolution and greater vertical accuracy compared with other DEMs such as the Advanced Spaceborne Thermal Emission and Reflection Radiometer (ASTER), Shuttle Radar Topography Mission (SRTM), and Cartosat-1 (Gautam, 2023; Raman, 2023). Peer-reviewed studies, as mentioned in Appendix 6, have reported that the vertical accuracy of the ALOS PALSAR DEM ranges between 4.76 and 5 m; this variation is attributed to different terrain types (Gautam, 2023). This study considered DEM values from 0 (coastal line) to 5 m as 1 m. Further, a reclassification of the DEM was performed to identify areas with values less than 1 m. The ALOS DEM's minimum pixel value over ocean areas is −95, which was considered as zero elevation. Utilising Map Algebra expressions in the Raster Calculator tool, the DEM was reclassified to delineate the desired inundation cells, generating new rasters in accordance with the SSPs, SLR, and the years under consideration.

Raster to polygon and SLR scenarios

The reclassified raster layers were converted to a polygon using the Raster to Polygon conversion tool in ArcGIS, followed by the assessment of the inundation area for each city's and town's boundary under future climate scenarios in four time slices. The administrative maps (Appendix 4) of all cities and towns were geo-rectified and considered in the study.

4.3. Assessing Future SLR-Induced Inundation for LULC Classes

An LULC map was prepared for the selected cities and towns in near real-time (2022) by using reliable open-source data—OpenStreetMap (OSM)[8] (Calazans et al., 2017; Fonte & Martinho, 2017; Schultz et al., 2017). Atal Mission for Rejuvenation and Urban Transformation (AMRUT, 2016)[9] and National Remote Sensing Centre, Indian Space Research Organisation (ISRO), LULC[10] classification schemes were used to assign exclusive LULC classes (Appendix 5). Gaps in the base map—the LULC map for 2022 built using OSM—were filled using the visual interpretation method by utilising high-resolution satellite data in ArcMap[11] environment. We used 'attribute-based text replace' python code to geocode OSM land cover classes with respect to the LULC scheme. The primary LULC classes were identified as agriculture, green space, industrial, urban, wasteland, wetland, and waterbodies by using the Level-III classification scheme.

[7] A sink is a specific area in a DEM that is surrounded by higher elevation values on all sides, making it a local minimum in the elevation data. Peak is a specific area in a DEM that is surrounded by low elevation values on all sides (ArcGIS pro 2024).

[8] OpenStreetMap offers a freely accessible geographic database that is regularly updated and maintained by a community of volunteers through open collaboration (https://www.openstreetmap.org/).

[9] AMRUT mission includes measures for urban reforms and capacity building. It strives to provide basic infrastructure in selected cities and towns with respect to non-motorised urban transport, water supply, storm water drainage, sewerage and septage management, and green spaces and parks (AMRUT, 2016).

[10] NRSC - 2019, Document control number: NRSC-RSA-LRUMG-JUN-2019-TR-1320-V1

[11] Service Layer Credits: Source: Esri, Maxar, Earthstar Geographics, and the GIS User Community

The accuracy of the identified LULCs was quantitatively assessed to determine how effectively they are classified with respect to the referenced data (Arumugam et al., 2021; Rwanga & Ndambuki, 2017). This study followed one of the widely used (Ganjirad & Bagheri, 2024; Lyons et al., 2018) statistical measures to quantify the accuracy of LULCs—the Kappa coefficient. This coefficient offers a more rigorous assessment than other methods, such as overall accuracy, by accounting for LULC chance agreements (Appendix 7; Jamal & Ahmad, 2020).

Finally, city-level LULCs were clipped with inundation layers for 2100 to visualise the inundation area for the end of this century. The LULC-wise specific inundation statistics were computed to comprehend the potential land loss under each category.

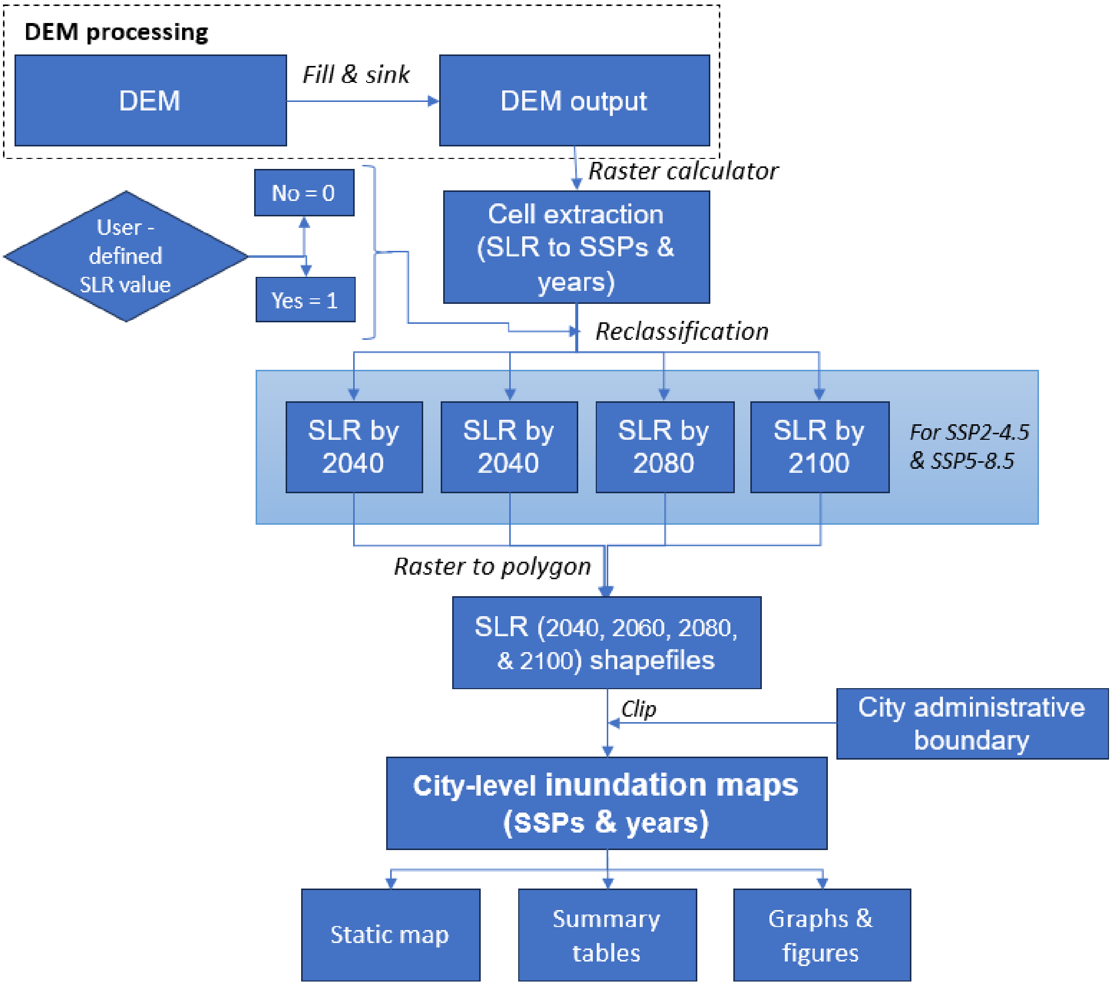

Figure 4.2: Flow chart of DEM processing and delineation of inundation maps

5. Results and Discussion

The SLR changes over the historical period along the Indian coastline indicate alarming trends. The majority of the tide gauge stations situated on the east and west coasts show increasing trends in SLR. The maximum SLR (4.44 cm; 0.31 cm per year) over the past 30 years was observed at the Mumbai station, followed by Haldia (2.72 cm), Visakhapatnam (2.38 cm), Kochi (2.21 cm), Paradip (0.72 cm), Chennai (0.68 cm), and Murmugao (0.36 cm) stations. However, the SLR per year is higher at the Paradip station than at the Chennai and Murmugao stations. Both Thoothukudi and Panambur stations exhibit a negative trend in SLR over the 30-year (1992–2021) period. Table 5.1 lists the SLR changes (in cm) for selected tide gauge stations over the past 30 years. Scientific reasons behind the negative trend in SLR at the Panambur and Thoothukudi stations (mentioned as 'less than 0' in the table) need to be explored.

Table 5.1: Historical SLR at the tide gauge stations

Tide gauge stations	Period	Total SLR (in cm)	Average SLR per year (in cm)
Chennai	1987–2016	0.679	0.066
Kochi	1990–2019	2.213	0.158
Haldia	1991–2020	2.726	0.096
Mumbai	1991–2020	4.441	0.315
Murmugao	1991–2020	0.359	0.033
Panambur	1992–2021	Less than 0	0.091
Paradip	1992–2021	0.717	0.108
Thoothukudi	1992–2021	Less than 0	0.003
Visakhapatnam	1992–2021	2.381	0.181

This section presents city-wise and town-wise historical SLR, future SLR changes for five SSP scenarios until 2100, and likely inundation maps for medium- (SSP2-4.5) and high-emission (SSP5-8.5) scenarios by 2100.

5.1. Tier-I Cities

5.1.1. Chennai, Tamil Nadu

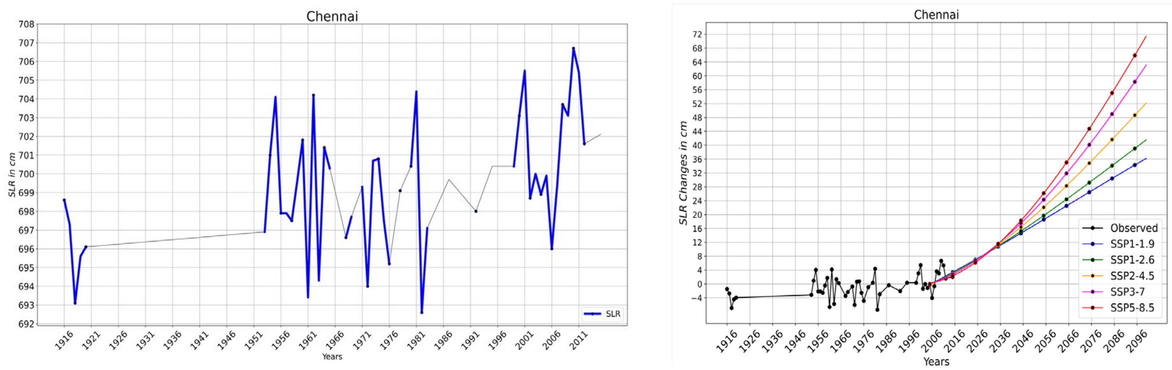

Figure 5.1: (a) Sea level rise during the historical period from the Chennai tide gauge station; (b) SLR projected under the future SSP scenarios for Chennai, Tamil Nadu

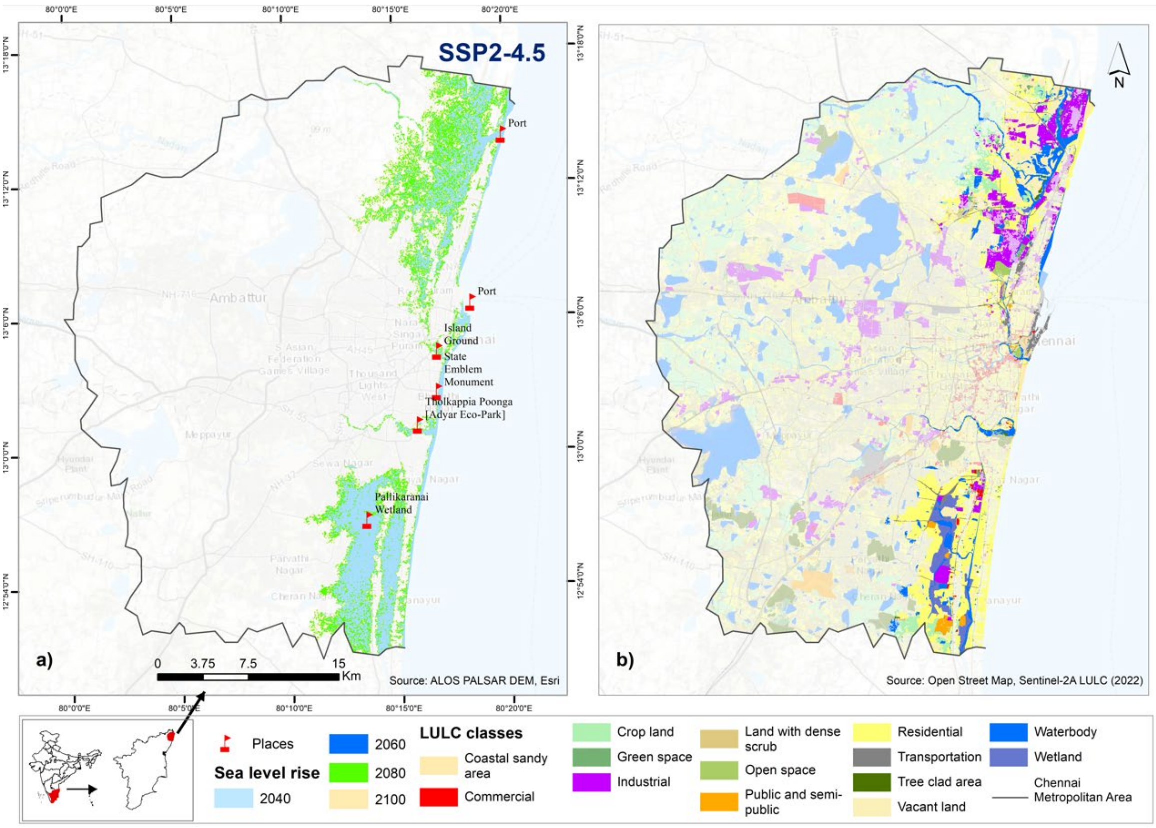

Figure 5.2: (a) Inundation area for projected SLR in Chennai, Tamil Nadu; (b) LULC-wise inundation for projected SLR by 2100 under the future SSP2-4.5 scenario in Chennai, Tamil Nadu

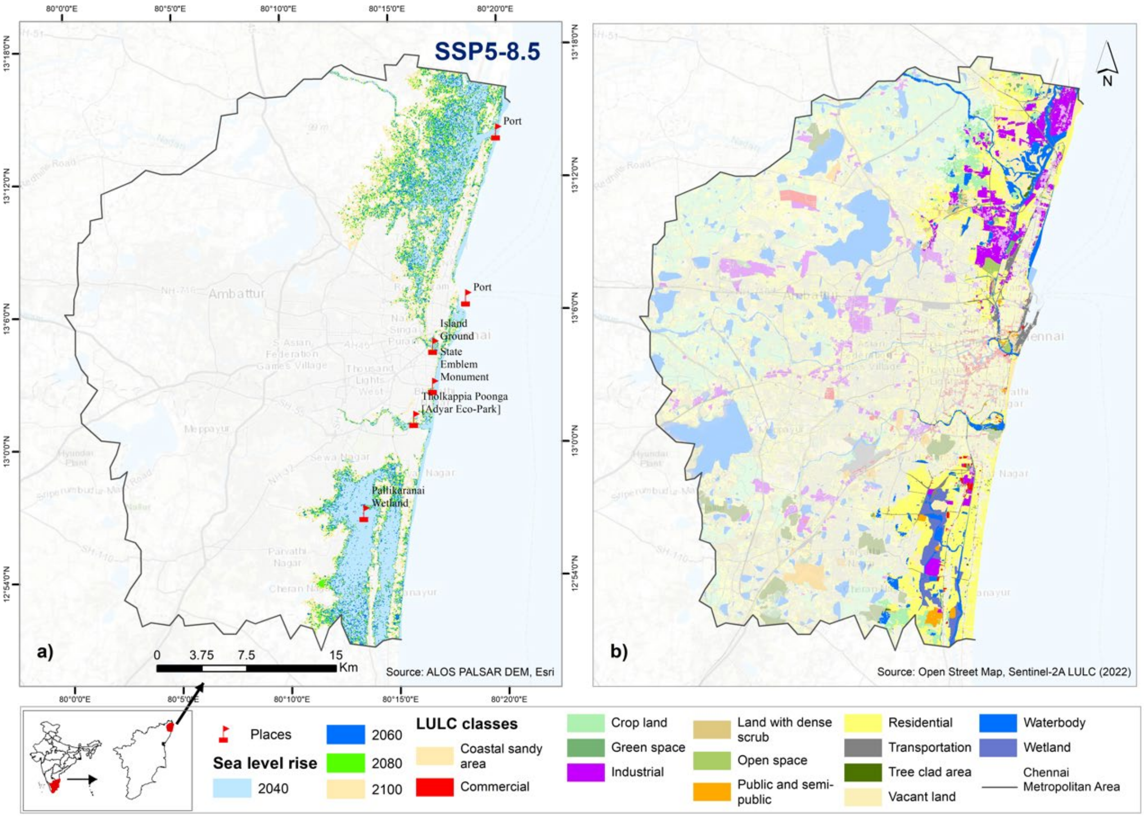

Figure 5.3: (a) Inundation area for projected SLR in Chennai, Tamil Nadu; (b) LULC-wise inundation for projected SLR by 2100 under the future SSP5-8.5 scenario in Chennai, Tamil Nadu

5.1.2. Mumbai, Maharashtra

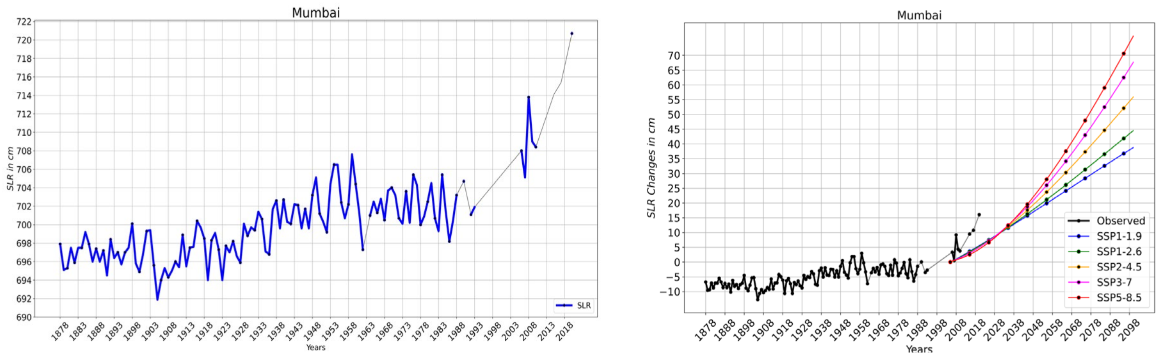

Figure 5.4: (a) Sea level rise during the historical period from the Mumbai tide gauge station; (b) SLR projected under the future SSP scenarios for Mumbai, Maharashtra

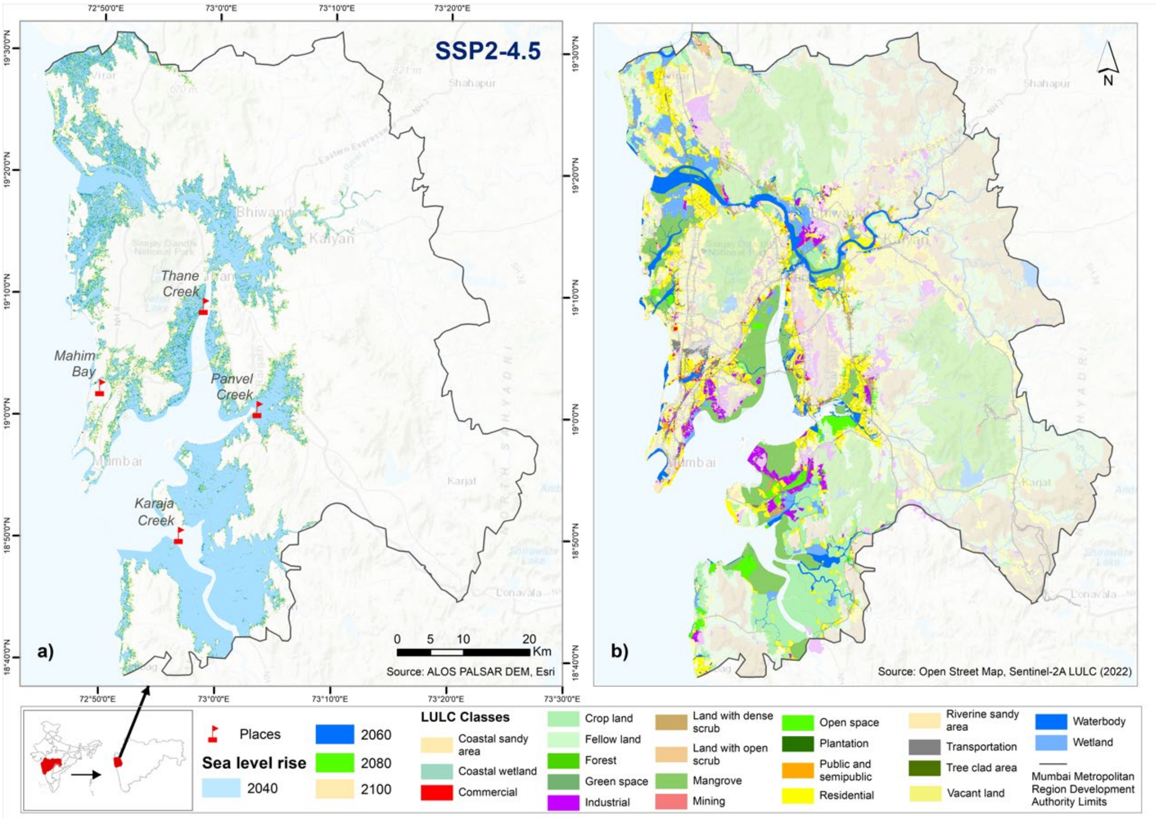

Figure 5.5: (a) Inundation area for projected SLR in Mumbai, Maharashtra; (b) LULC-wise inundation for projected SLR by 2100 under the future SSP2-4.5 scenario in Mumbai, Maharashtra

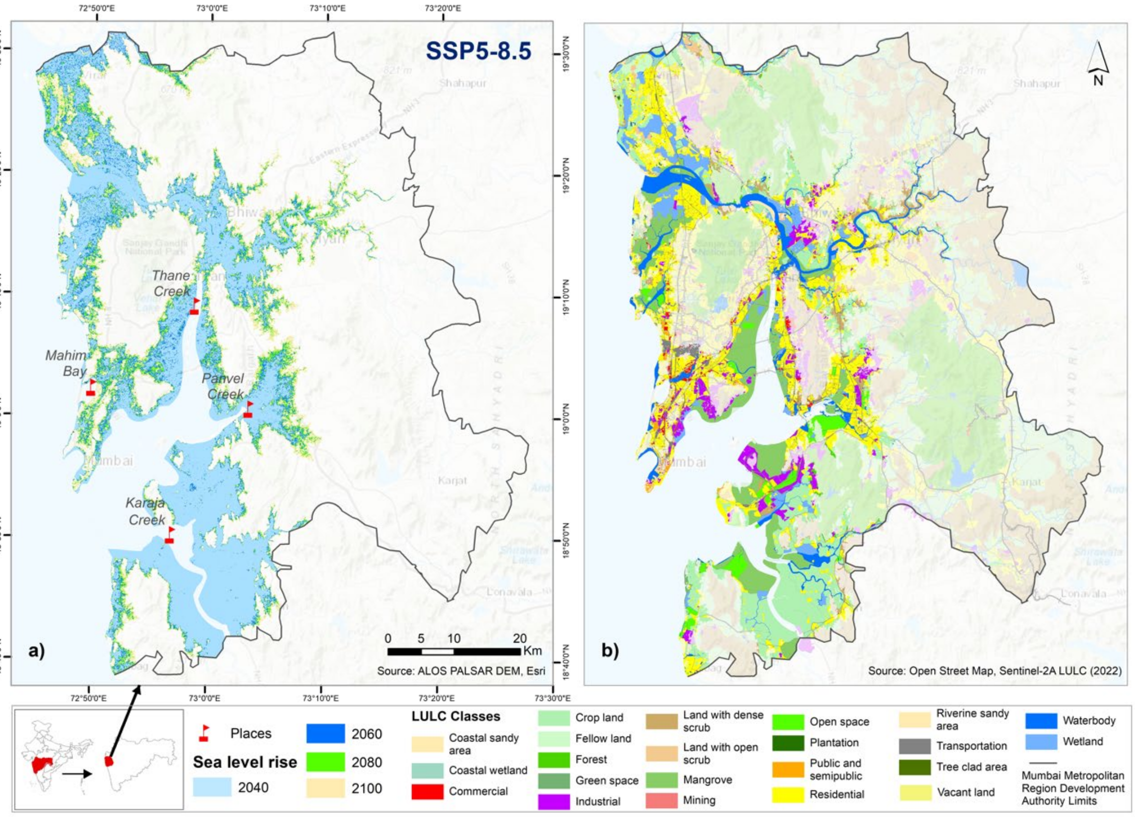

Figure 5.6: (a) Inundation area for projected SLR in Mumbai, Maharashtra; (b) LULC-wise inundation for projected SLR by 2100 under the future SSP5-8.5 scenario in Mumbai, Maharashtra

Table 5.2: Projected SLR (in cm) and impacted area (in sq. km) for Tier-I cities under different SSP scenarios for the considered years

City	SSP	2040		2060		2080		2100	
		SLR	Area	SLR	Area	SLR	Area	SLR	Area
Chennai	SSP2-4.5	17.40	86.66	32.70	114.31	51.00	159.28	71.20	207.04
	SSP5-8.5	18.70	86.77	32.70	119.48	64.90	154.66	94.70	215.77
Mumbai	SSP2-4.5	18.60	727.83	35.00	826.83	54.60	914.03	76.20	1,055.07
	SSP5-8.5	20.00	829.72	41.90	1,003.09	69.50	1,159.05	101.40	1,377.13

Table 5.3: LULC-wise (existing) inundation area (in sq. km) for projected SLR by 2100 in Tier-I cities

LULC	Chennai		Mumbai	
	SSP2-4.5	SSP5-8.5	SSP2-4.5	SSP5-8.5
Agriculture	11.57	16.78	230.45	314.85
Green area	4.34	5.25	40.15	49.25
Industrial	22.01	26.75	45.30	66.94
Urban	101.73	126.70	260.23	350.03
Waste land	4.15	5.02	45.30	70.65
Waterbody	53.03	25.04	243.44	315.28
Wetland	10.21	10.23	190.20	210.13

As per these results, SLR poses a threat to both Mumbai and Chennai under historical and future climatic scenarios.

SLR and inundation in Chennai

- Increasing sea level trend of around 0.67 cm was observed over the past three decades (1987–2016), with an annual rise of 0.066 cm.
- SSP2-4.5 scenario
  - Sea level is projected to increase by 17.4 cm, 32.7 cm, 51 cm, and 71.2 cm by 2040, 2060, 2080, and 2100, respectively.
  - Inundation of 7.29% (86.6 sq. km) by 2040, 9.65% (114.31 sq. km) by 2060, 15.11% (159.28 sq. km) by 2080, and 16.90% (207.04 sq. km) by 2100 may occur.
- SSP5-8.5 scenario
  - Sea level rise is projected to be 18.7 cm, 32.7 cm, 64.9 cm, and 94.7 cm by 2040, 2060, 2080, and 2100, respectively.
  - Inundation of 7.30% (86.77 sq. km) by 2040, 10.05% (119.48 sq. km) by 2060, 13.01% (154.66 sq. km) by 2080, and 18.15% (215.77 sq. km) by 2100 is projected.

- All LULCs would be affected by SLR by the end of the century.
  - Adyar Eco-Park, Island Ground, State Emblem Monument, and Pallikaranai wetland and port would be at high risk, with notable areas under habitation and waterbodies.

SLR and inundation in Mumbai

- Historical data show an increasing sea level trend of around 4.44 cm over the past three decades (1991–2020), with an annual rise of 0.314 cm.
- SSP2-4.5 scenario
  - Sea level rise is projected to be 18.6 cm, 35 cm, 54.6 cm, and 76.2 cm by 2040, 2060, 2080, and 2100, respectively.
  - Inundation is estimated to be 11.50% (727.83 sq. km) by 2040, 13.07% (826.83 sq. km) by 2060, 14.04% (914.03 sq. km) by 2080, and 16.67% (1,055.07 sq. km) by 2100.
- SSP5-8.5 scenario
  - Sea level rise is projected to be 20 cm, 41.9 cm, 69.5 cm, and 101.4 cm by 2040, 2060, 2080, and 2100, respectively.
  - Inundation of 13.11% (829.72 sq. km) by 2040, 15.85% (1,003.09 sq. km) by 2060, 18.32% (1,159.05 sq. km) by 2080, and 21.76% (1,377.13 sq. km) by 2100 may occur.
- All LULCs would be affected by SLR by the end of the century, and much of this area comes under urban, industrial, waterbody, and wetland categories.
  - Thane Creek, Karanja Creek, Panvel Creek, and Mahim Bay would be at high risk, with a notable area under airport, habitation, wetland, mangrove, and agriculture.

5.2. Tier-II Cities

Tier-II cities are smaller than major metropolitan areas but significant in terms of population and economy. Kozhikode, Kochi, Mangaluru, Thiruvananthapuram, Visakhapatnam, and Haldia were considered in this study. Except for Visakhapatnam and Haldia, the remaining cities are on the western coastline. Of these cities, tide gauge stations are only available at Kochi and Visakhapatnam. Therefore, the nearest stations were considered for analysing the historical SLR for Kozhikode, Mangaluru, and Haldia (Table 4.1).

5.2.1. Haldia, West Bengal

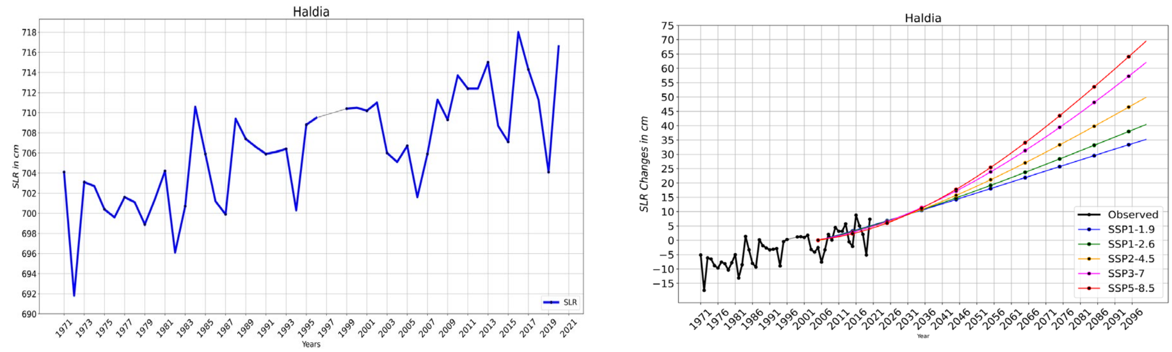

Figure 5.7: (a) Sea level rise during the historical period from the Haldia tide gauge station; (b) SLR projected under the future SSP scenarios for Haldia, West Bengal

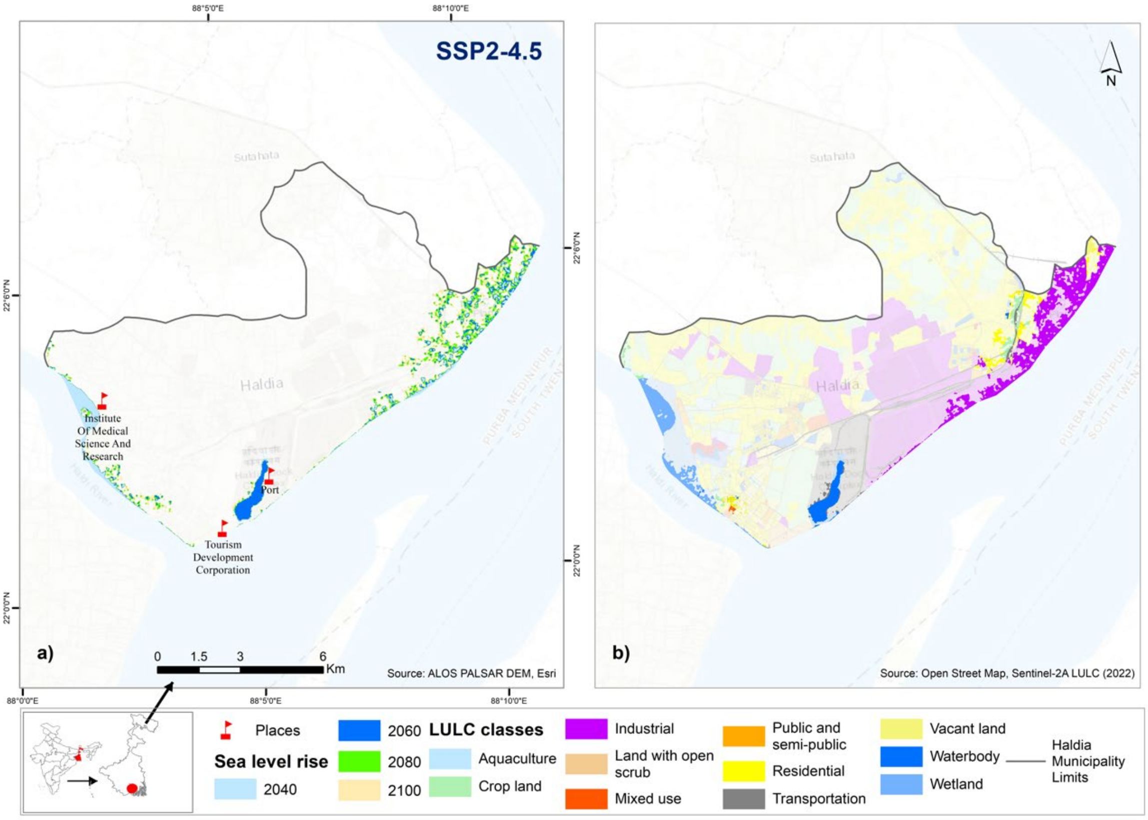

Figure 5.8: (a) Inundation area for projected SLR in Haldia, West Bengal; (b) LULC-wise inundation for projected SLR by 2100 under the SSP2-4.5 scenario in Haldia, West Bengal

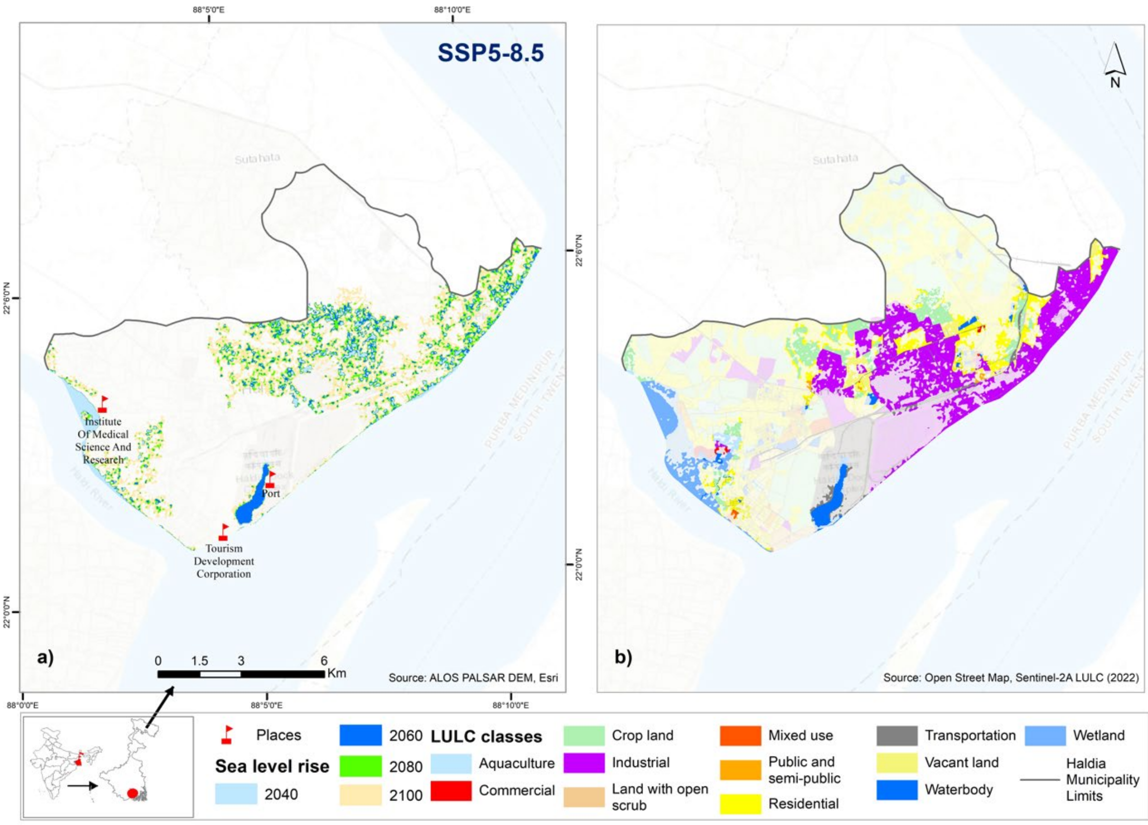

Figure 5.9: (a) Inundation area for projected SLR in Haldia, West Bengal; (b) LULC-wise inundation for projected SLR by 2100 under the SSP5-8.5 scenario in Haldia, West Bengal

5.2.2. *Kochi, Kerala*

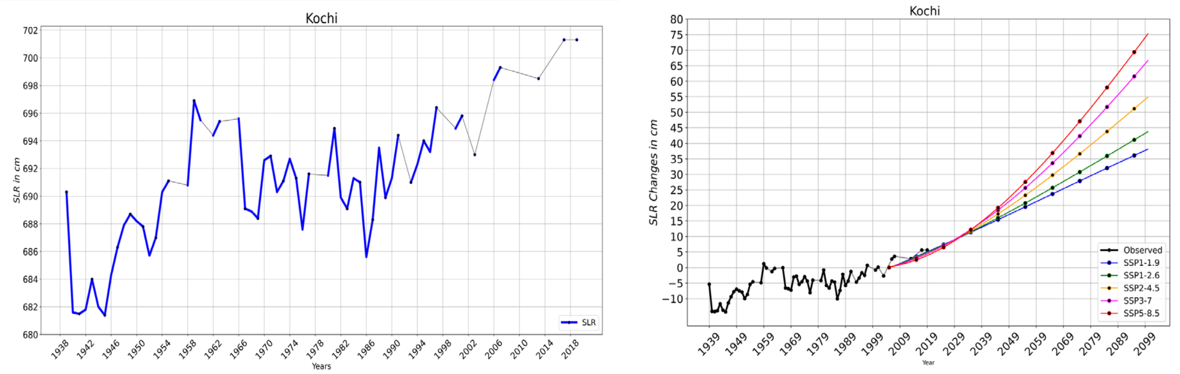

Figure 5.10: (a) Sea level rise during the historical period from the Kochi tide gauge station; (b) SLR projected under the future SSP scenarios for Kochi, Kerala

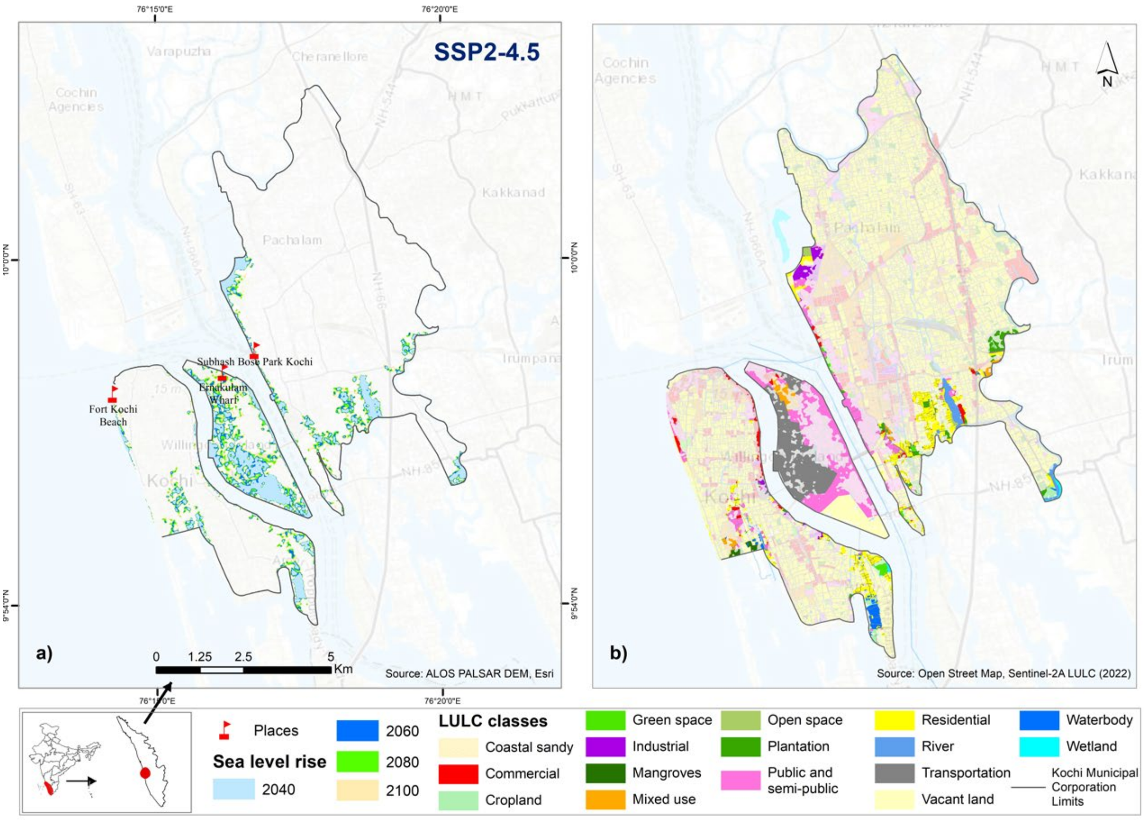

Figure 5.11: (a) Inundation area for projected SLR in Kochi, Kerala; (b) LULC-wise inundation for projected SLR by 2100 under the future SSP2-4.5 scenario in Kochi, Kerala

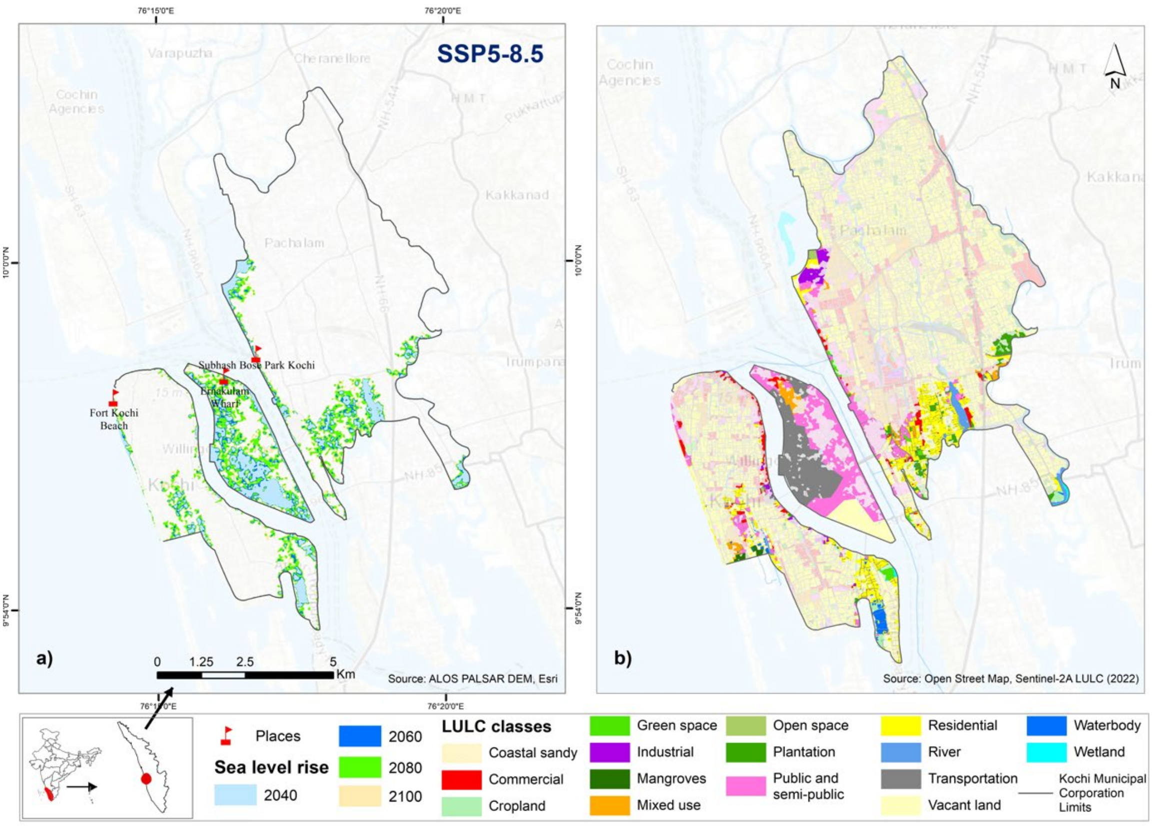

Figure 5.12: (a) Inundation area for projected SLR in Kochi, Kerala; (b) LULC-wise inundation for projected SLR by 2100 under the future SSP5-8.5 scenario in Kochi, Kerala

5.2.3. Kozhikode, Kerala

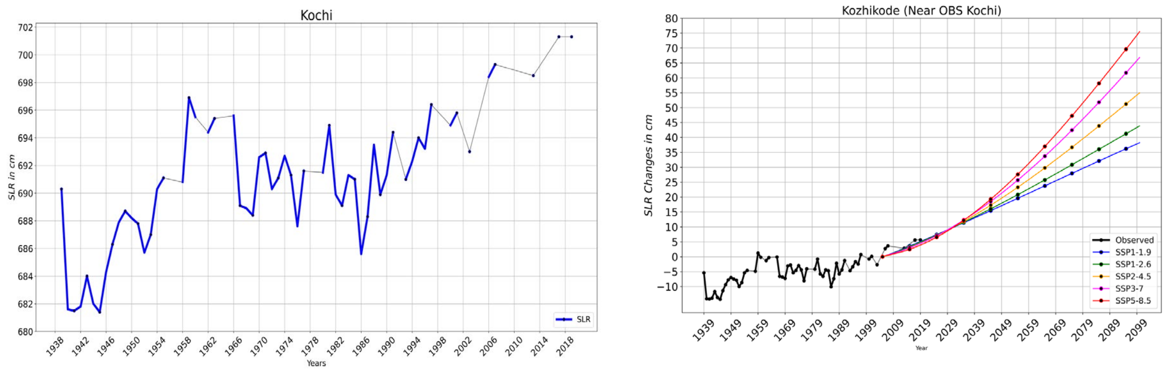

Figure 5.13: (a) Sea level rise during the historical period from the Kochi tide gauge station; (b) SLR projected under the future SSP scenarios for Kozhikode, Kerala

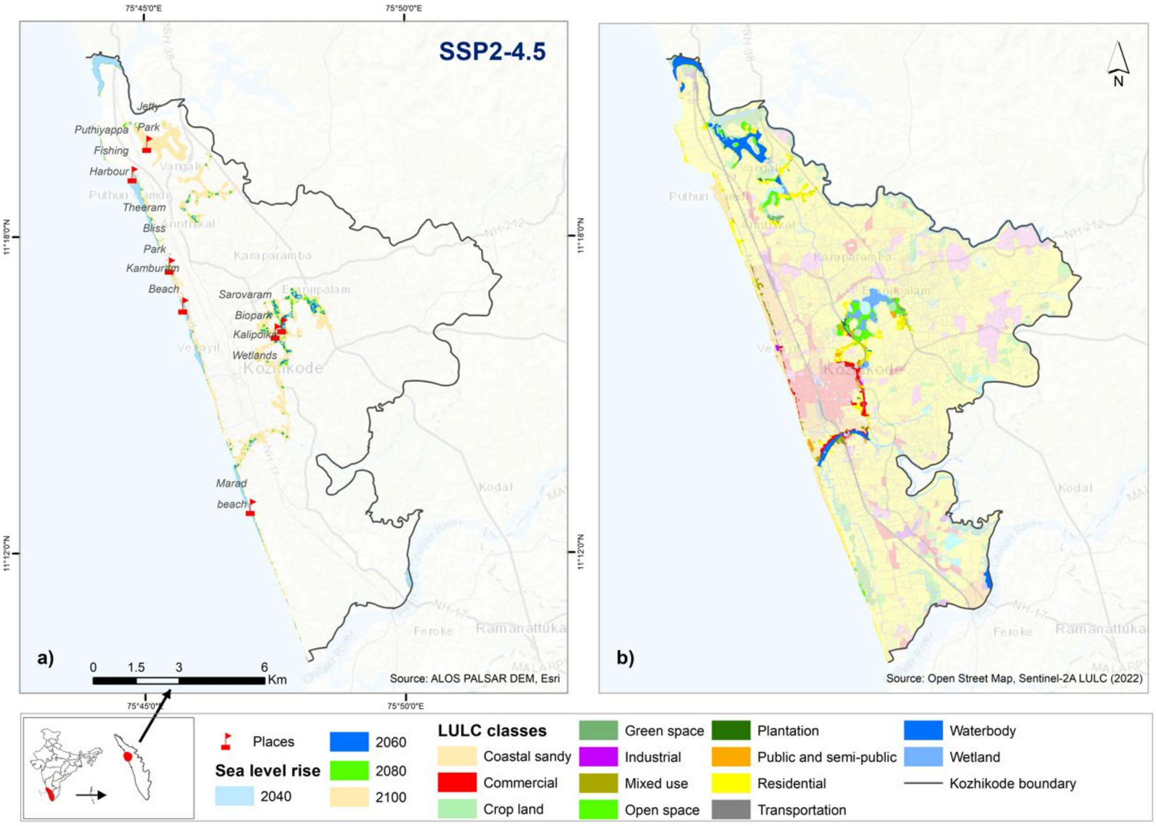

Figure 5.14: (a) Area inundated due to SLR in Kozhikode, Kerala; (b) LULC-wise inundation by 2100 under the SSP2-4.5 scenario in Kozhikode, Kerala

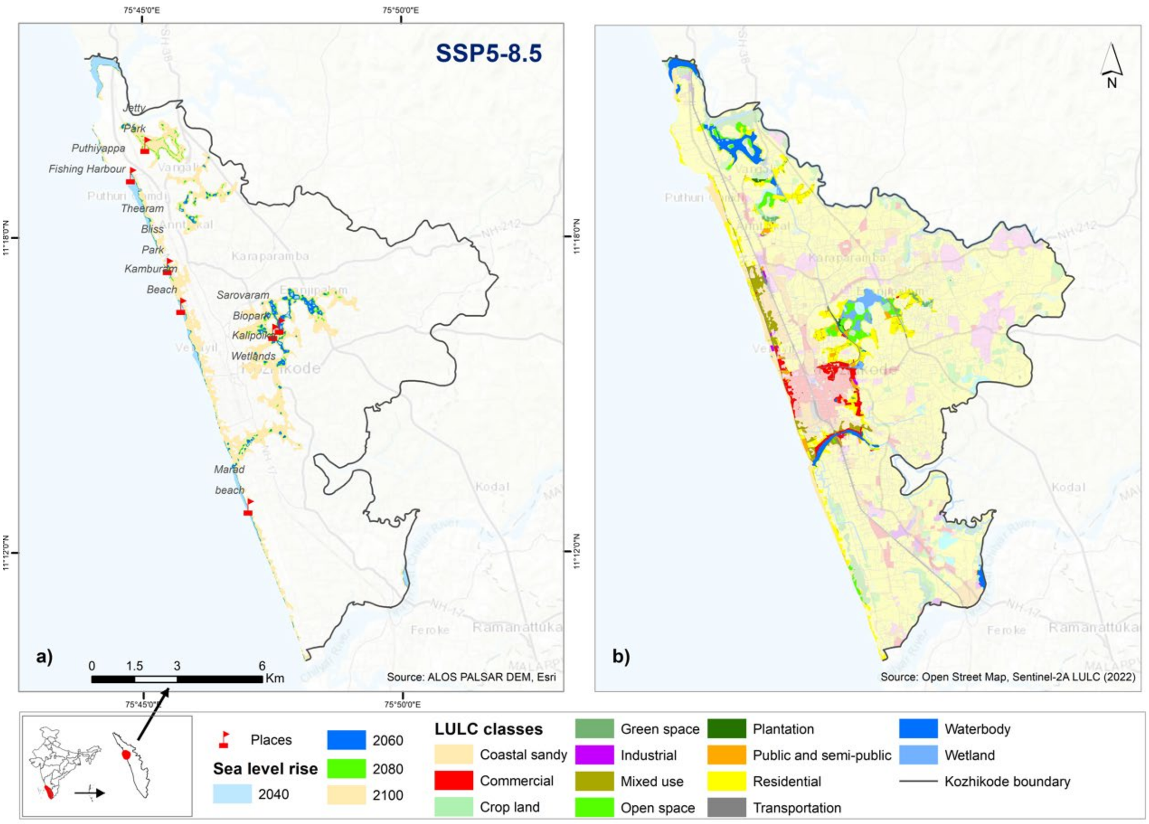

Figure 5.15: (a) Inundation area for projected SLR in Kozhikode, Kerala; (b) LULC-wise inundation for projected SLR by 2100 under the future SSP5-8.5 scenario in Kozhikode, Kerala

5.2.4. Mangaluru, Karnataka

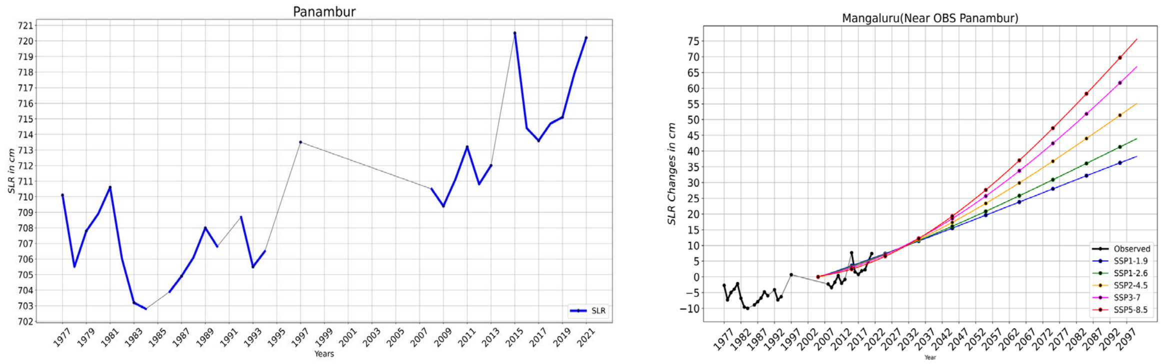

Figure 5.16: (a) Sea level rise during the historical period from the Panambur tide gauge station; (b) SLR projected under the future SSP scenarios for Mangaluru, Karnataka

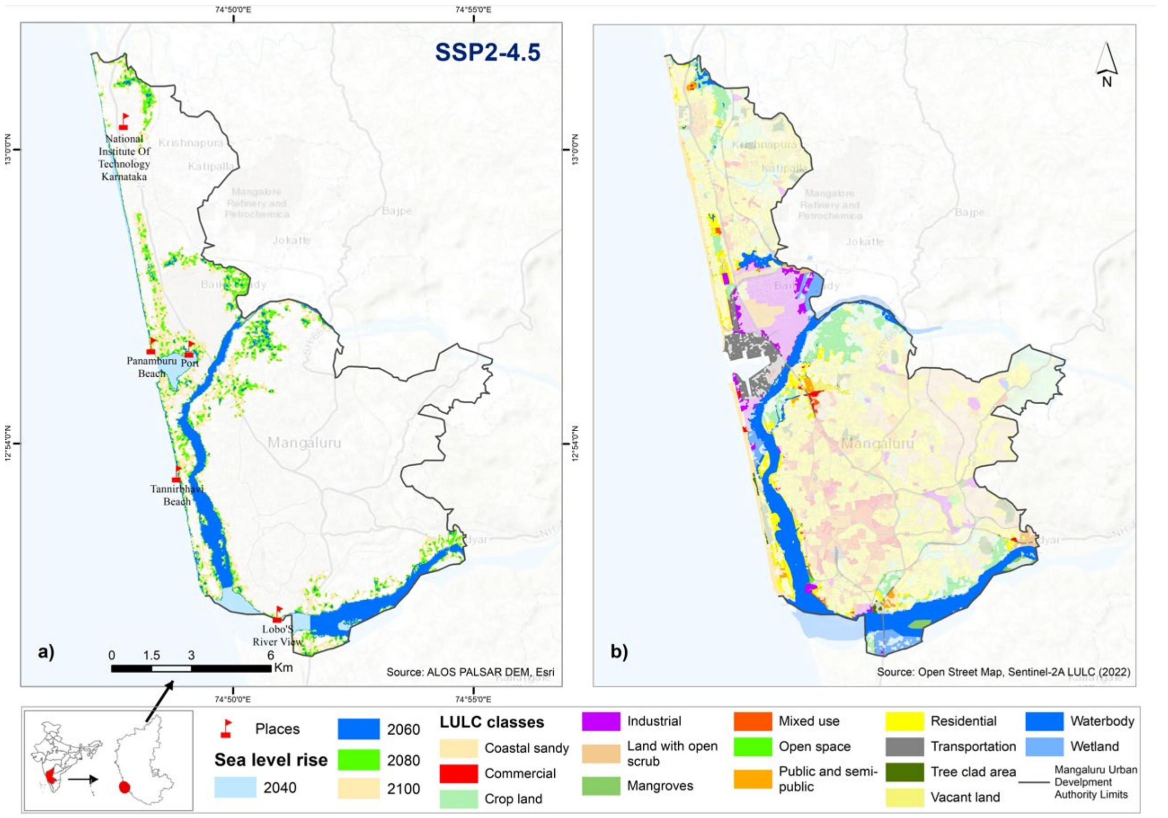

Figure 5.17: (a) Inundation area for projected SLR in Mangaluru, Karnataka; (b) LULC-wise inundation for projected SLR by 2100 under the SSP2-4.5 scenario in Mangaluru, Karnataka

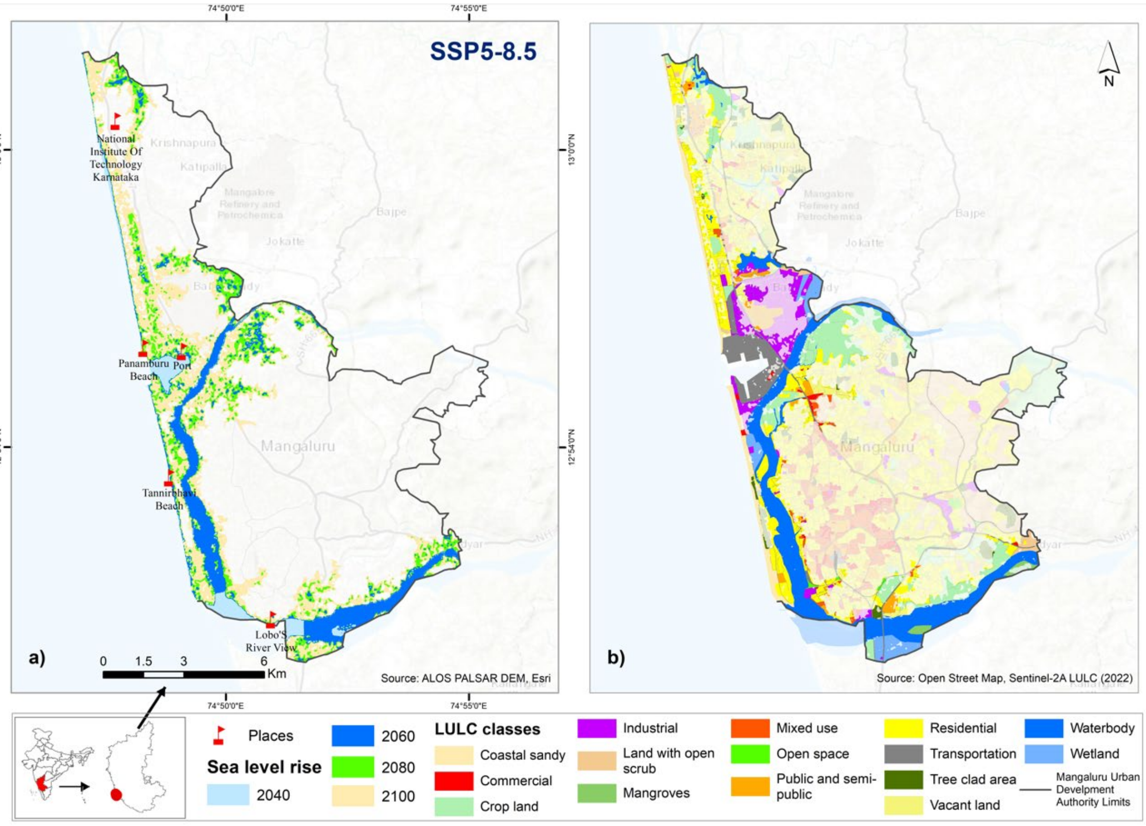

Figure 5.18: (a) Inundation area for projected SLR in Mangaluru, Karnataka; (b) LULC-wise inundation for projected SLR by 2100 under the SSP5-8.5 scenario in Mangaluru, Karnataka

5.2.5. *Thiruvananthapuram, Kerala*

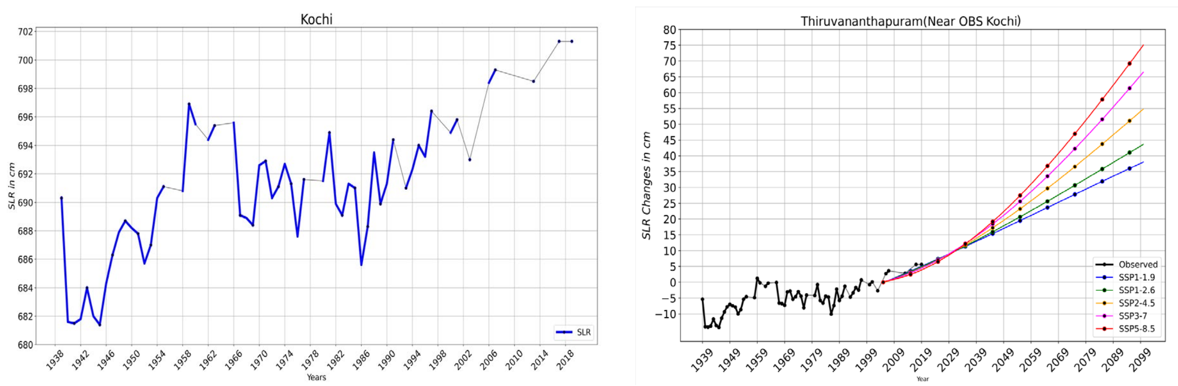

Figure 5.19: (a) Sea level rise during the historical period from the Kochi tide gauge station; (b) SLR projected under the future SSP scenarios for Thiruvananthapuram, Kerala

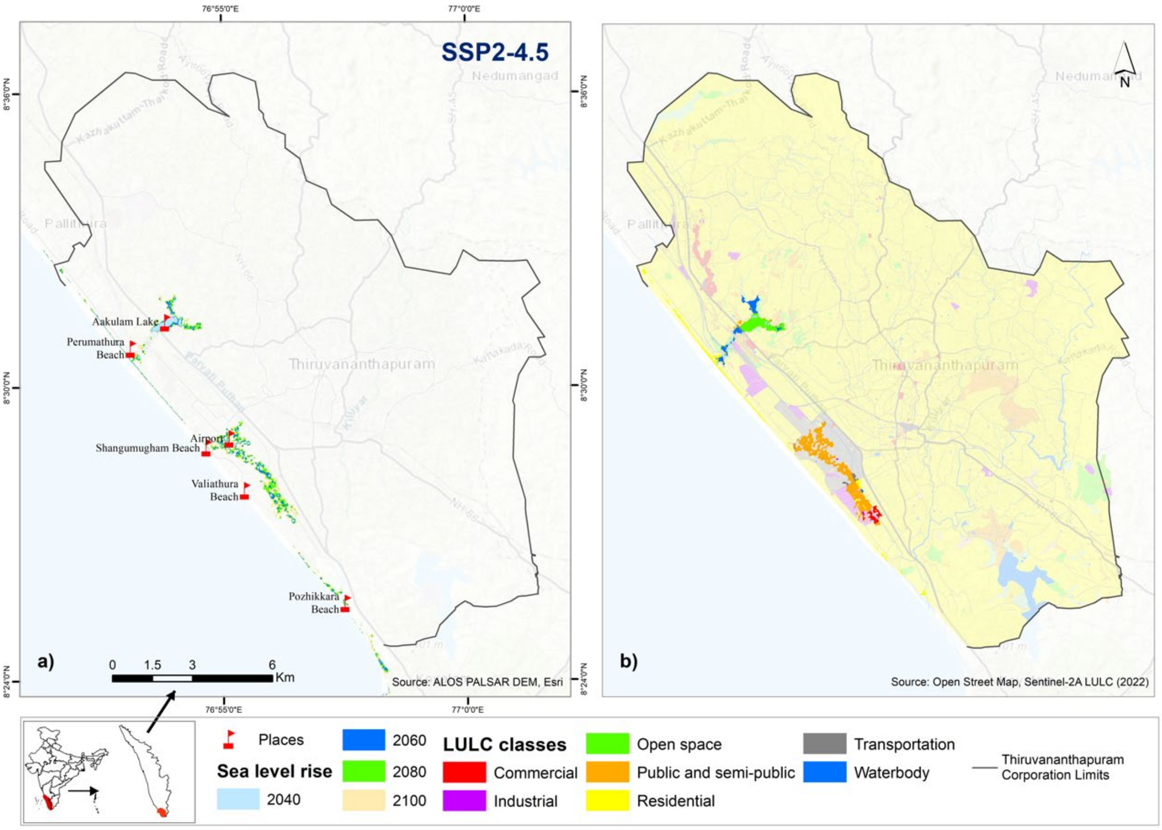

Figure 5.20: (a) Inundation area for projected SLR in Thiruvananthapuram, Kerala; (b) LULC-wise inundation by 2100 under the SSP2-4.5 scenario in Thiruvananthapuram, Kerala

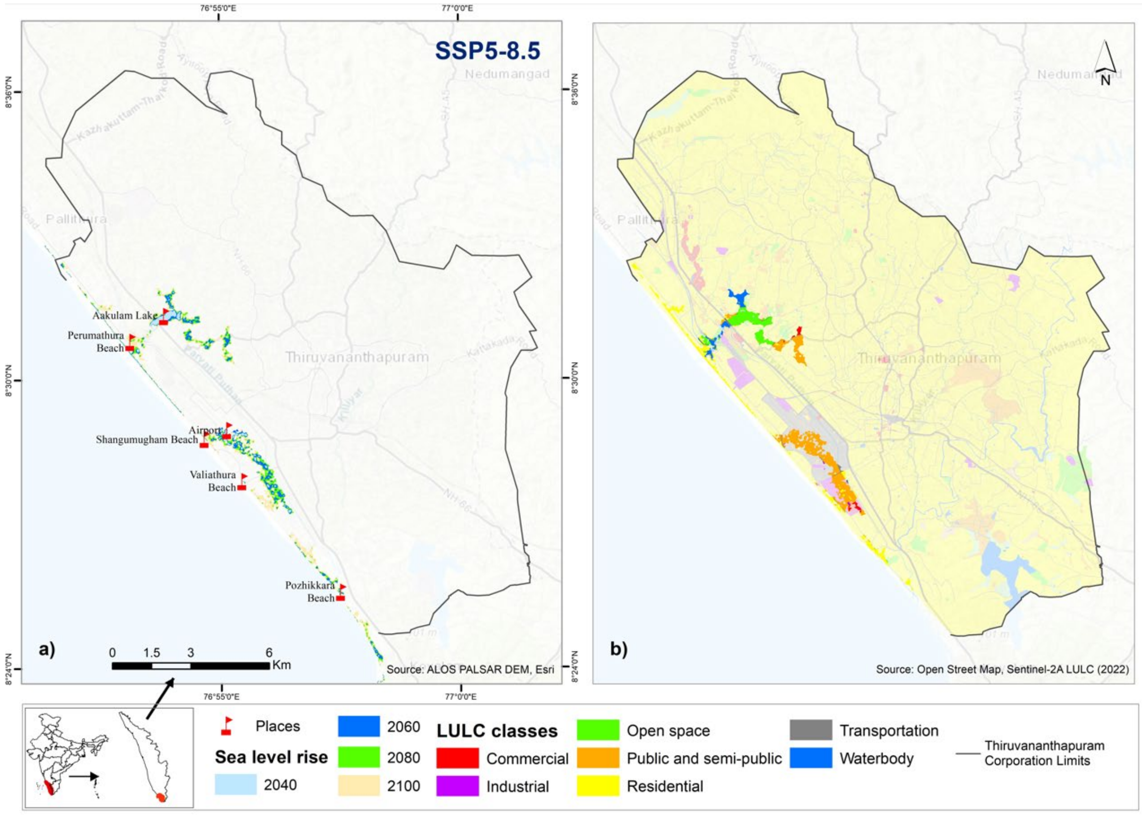

Figure 5.21: (a) Inundation area for projected SLR in Thiruvananthapuram, Kerala; (b) LULC-wise inundation for projected SLR by 2100 under the SSP5-8.5 scenario in Thiruvananthapuram, Kerala

5.2.6. Visakhapatnam, Andhra Pradesh

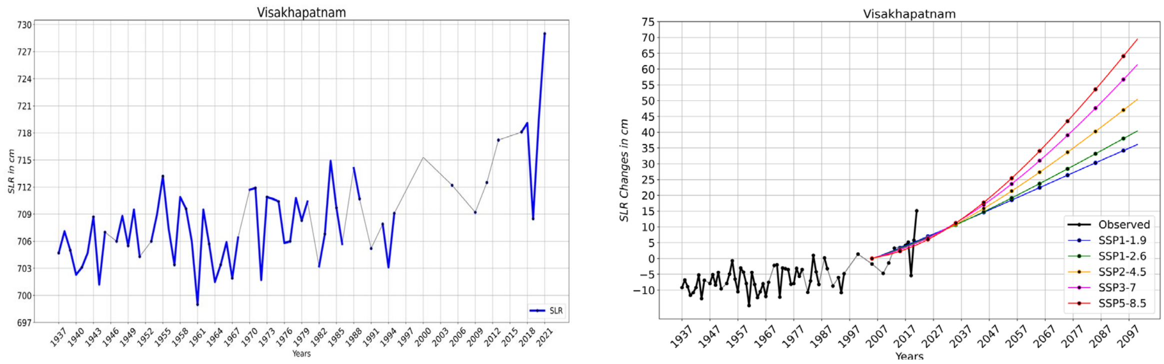

Figure 5.22: (a) Sea level rise during the historical period from the Visakhapatnam tide gauge station; (b) SLR projected under the future SSP scenarios for Visakhapatnam, Andhra Pradesh

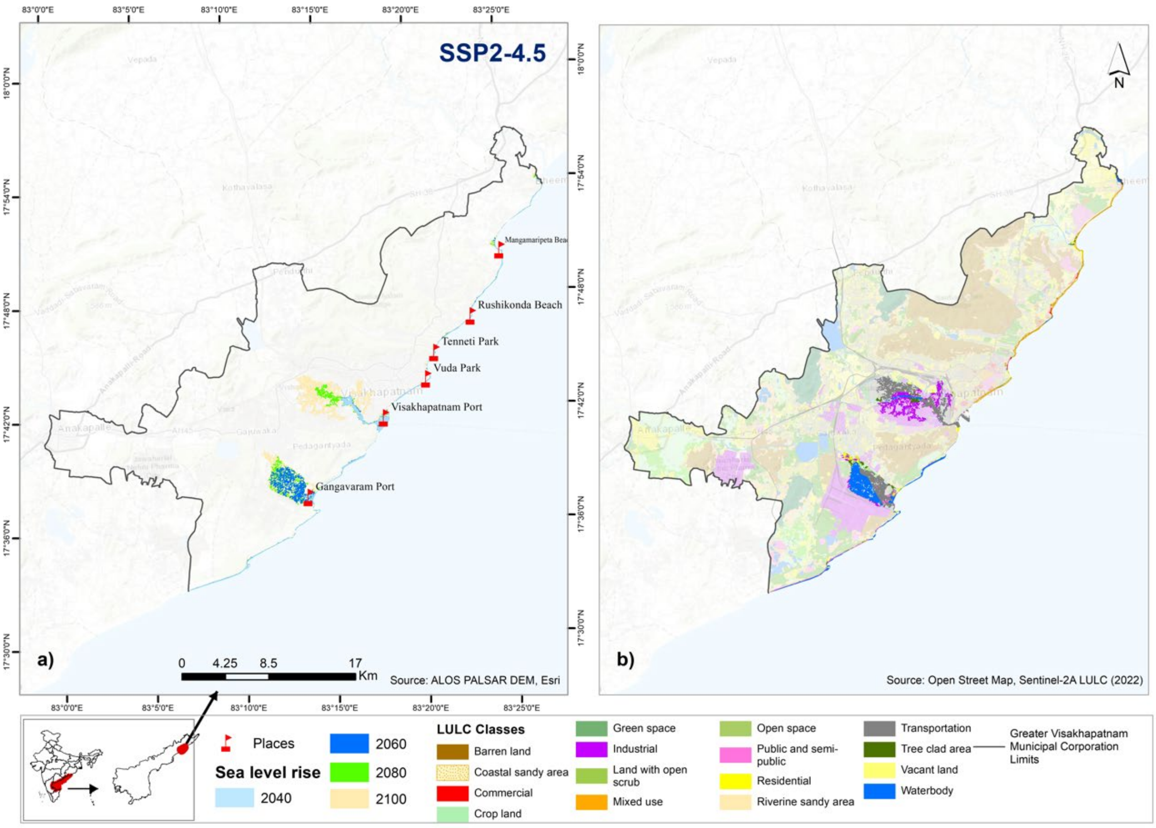

Figure 5.23: (a) Inundation area for projected SLR in Visakhapatnam, Andhra Pradesh; (b) LULC-wise inundation for projected SLR by 2100 under the SSP2-4.5 scenario in Visakhapatnam, Andhra Pradesh

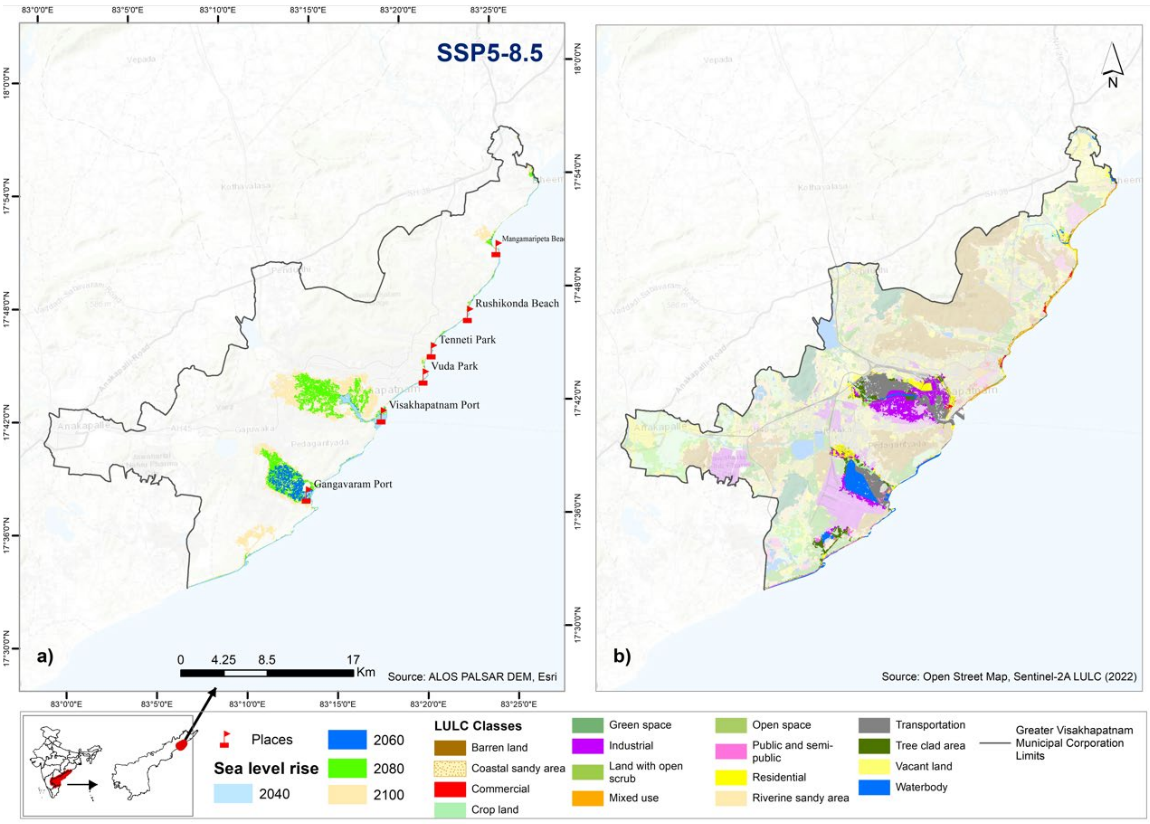

Figure 5.24: (a) Inundation area for projected SLR in Visakhapatnam, Andhra Pradesh; (b) LULC-wise inundation for projected SLR by 2100 under the SSP5-8.5 scenario in Visakhapatnam, Andhra Pradesh

Table 5.4: Projected SLR (in cm) and impacted area (in sq. km) for Tier-II cities under different SSP scenarios for the considered years

City	SSP	2040		2060		2080		2100	
		SLR	Area	SLR	Area	SLR	Area	SLR	Area
Haldia	SSP2-4.5	16.7	2.16	31.4	4.28	48.9	6.71	68.3	9.37
	SSP5-8.5	18	3.37	37.5	7.44	62.3	13.02	90.9	27.86
Kochi	SSP2-4.5	18.3	4.95	34.5	6.8	53.7	9.12	74.9	11.55
	SSP5-8.5	19.7	5.08	41.2	7.04	68.9	12.55	100	15.61
Kozhikode	SSP2-4.5	18.3	1.32	34.5	1.74	53.8	2.33	75.1	8.75
	SSP5-8.5	19.7	1.32	41.2	2.35	68.4	3.27	99.9	13.89
Mangaluru	SSP2-4.5	18.3	3.43	34.6	12.67	53.9	19.55	75.2	30.75
	SSP5-8.5	19.8	3.42	41.3	14.17	68.6	23.61	100.1	44.18
Thiruvananthapuram	SSP2-4.5	18.2	0.68	34.4	1.35	53.5	2.53	74.7	3.97
	SSP5-8.5	19.6	0.68	41	2	68.1	3.44	99.4	5.95
Visakhapatnam	SSP2-4.5	16.7	6.96	31.5	13.29	49.1	18.18	68.6	32.44
	SSP5-8.5	18	7.43	37.7	13.14	62.5	33.35	91.3	61.58

Table 5.5: LULC-wise (existing) inundation area (sq. km) for projected SLR by 2100 in Tier-II cities

LULC	Haldia		Kochi		Kozhikode		Mangaluru		Thiruvananthapuram		Visakhapatnam	
	SSP 2-4.5	SSP 5-8.5	SSP 2-4.5	SSP 5-8.5	SSP 2-4.5	SSP 5-8.5	SSP 2-4.5	SSP 5-8.5	SSP 2-4.5	SSP 5-8.5	SSP 2-4.5	SSP 5-8.5
Agriculture	0.52	3.94	0.57	0.77	0.24	0.38	5.26	7.65	-	-	0.48	1.28
Green area	-	-	0.25	0.31	1.22	1.63	0.19	0.39	0.4	0.8	1.24	4.96
Industrial	4.53	13.14	0.37	0.49	0.04	0.09	1.24	2.89	2.75	4.1	5.94	13.58
Urban	1.54	6.36	9.38	13.01	3.23	7.42	7.82	15.6	2.38	3.4	14.2	28.18
Waste land	0.01	0.02	0.07	0.07	1.3	1.4	2.69	3.13	-	-	2.6	3.9
Waterbody	0.94	1.34	0.74	0.78	2.03	2.2	11.46	12	0.82	1.01	7.98	9.68
Wetland	1.83	3.06	0.17	0.18	0.69	0.77	2.09	2.52	-	-	-	-

All cities show increasing sea level trends under the historical climate scenario. Future projections indicate continuing SLR till the end of the century.

- Historical data indicate an SLR of 2.213 cm in Kochi over the past three decades (1990–2019), with an annual increase of 0.158 cm. In Visakhapatnam and Haldia, there was an SLR of 2.381 (with an annual increase of 0.181 cm) and 2.726 cm (with annual rise of 0.096) from 1992 to 2021, respectively.

- SSP2-4.5 scenario
  - Sea level rise is projected to be 16.7–18.3 cm by 2040, 31.5–34.6 cm by 2060, 49.1–53.8 cm by 2080, and 68.6–75.2 cm by 2100.
  - Area-wise inundation mapping reveals the following:
- Highest inundation would occur in Visakhapatnam—1.02 % (6.96 sq. km) by 2040, 1.95% (13.29 sq. km) by 2060, 2.67% (18.18 sq. km) by 2080, and 4.76% (32.44 sq. km) by 2100; followed by Kochi 1.15% (4.95 sq. km) by 2040, 1.60% (6.80 sq. km) by 2060, 2.85% (9.12 sq. km) by 2080, and 3.55% (11.55 sq. km) by 2100; Mangaluru 2.59% (3.43 sq. km) by 2040, 9.56% (12.67 sq. km) by 2060, 14.75% (19.55 sq. km) by 2080, and 23.21% (30.75 sq. km) by 2100; and Kozhikode 0.74% (1.32 sq. km) by 2040, 0.97% (1.74 sq. km) by 2060, 1.30% (2.33 sq. km) by 2080, and 4.89% (8.75 sq. km) by 2100
  - Urban areas in these cities are the most vulnerable to SLR-induced inundation.

- SSP5-8.5 scenario
  - Under this scenario, SLR is projected to be 18–19.8 cm by 2040, 37.7–41.3 cm by 2060, 62.5–68.9 cm by 2080, and 91.3–100.1 cm by 2100.
  - The rise would be the highest for Mangaluru (100.1 cm), followed by Kochi (100 cm), Kozhikode (99.9 cm), Thiruvananthapuram (99.4 cm), Visakhapatnam (91.3 cm), and Haldia (90.9 cm) by 2100 under the high-emission scenario by 2100.
  - Among the Tier-II cities, SLR is projected to be the lowest in Visakhapatnam and Haldia under both climate scenarios and by all time slices.
- Highest inundation would occur in Visakhapatnam 1.09% (7.43 sq. km) by 2040, 1.93% (13.14 sq. km) by 2060, 4.89% (33.35 sq. km) by 2080, and 9.03% (61.58 sq. km) by 2100; followed by Kochi 1.15% (5.08 sq. km) by 2040, 1.60% (7.04 sq. km) by 2060, 2.85% (12.55 sq. km) by 2080, and 3.55% (15.61 sq. km) by 2100; Mangaluru 2.58% (3.42 sq. km) by 2040, 10.69% (14.17 sq. km) by 2060, 17.82% (23.61 sq. km) by 2080, and 33.34% (44.18 sq. km) by 2100; Kozhikode 0.74% (1.32 sq. km) by 2040, 1.31% (2.35 sq. km) by 2060, 1.83% (3.27 sq. km) by 2080, and 7.76% (13.89 sq. km) by 2100; and Haldia 3.09% (3.37 sq. km) by 2040, 6.29% (7.44 sq. km) by 2060, 11.94% (13.02 sq. km) by 2080, and 25.56% (27.86 sq. km) by 2100.
  - Urban areas in these cities are the most vulnerable to SLR-induced inundation. However, in Haldia, industrial areas would face the highest risk of inundation.
  - Some of the notable places projected to be under inundation are the following:
  - Kozhikode: Marad and Kamburam beach, Theeram Bliss park, Puthiyappa fishing harbour, and Jetty park.
  - Kochi: Airport, Ernakulam Wharf, Fort Kochi beach, and Subhash Bose park. Visakhapatnam: Port, VUDA Tenneti park, and Rushikonda and Mangamaripeta beach.
  - Thiruvananthapuram: Airport, Pozhikkara beach, Valiathura beach, Shangumugham beach, Perumathura beach, and Akkulam lake.
  - Mangaluru: Tannirbhavi beach, Panambur beach, port, and Lobo's River View.

5.3. Towns

Towns are municipalities that are smaller and less developed than Tier-I and Tier-II cities. The specific criteria may change over time, but generally, a town in India has lesser population and economic opportunities than Tier-I and Tier-II cities. In this study, seven towns—Kanniyakumari, Panaji, Paradip, Puri, Thoothukudi, Udupi, and Yanam—were considered to assess the SLR change. Some of these towns (Udupi, Panaji, Puri, and Yanam) do not have tide gauge stations. Therefore, the nearest stations (Visakhapatnam, Panambur, Murmugao, and Paradip) were considered for the analysis (Table 4.1).

5.3.1. Kanniyakumari, Tamil Nadu

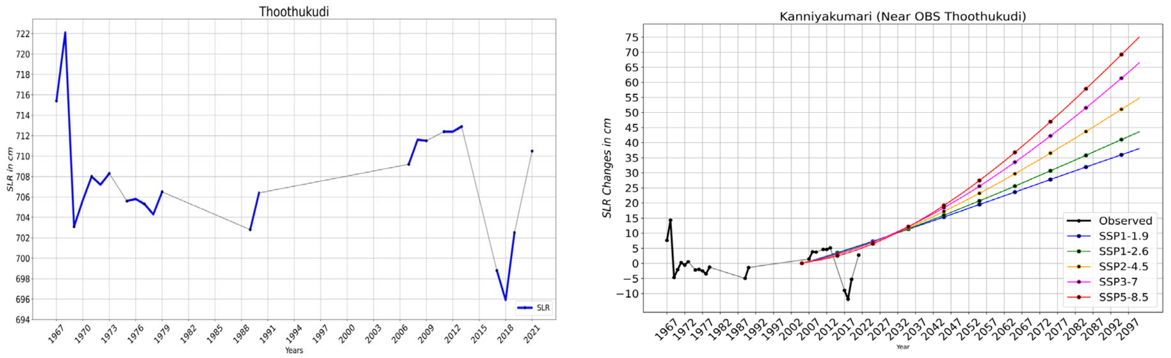

Figure 5.25: (a) Sea level rise during the historical period from the Thoothukudi tide gauge station; (b) SLR projected under the future SSP scenarios for Kanniyakumari, Kerala

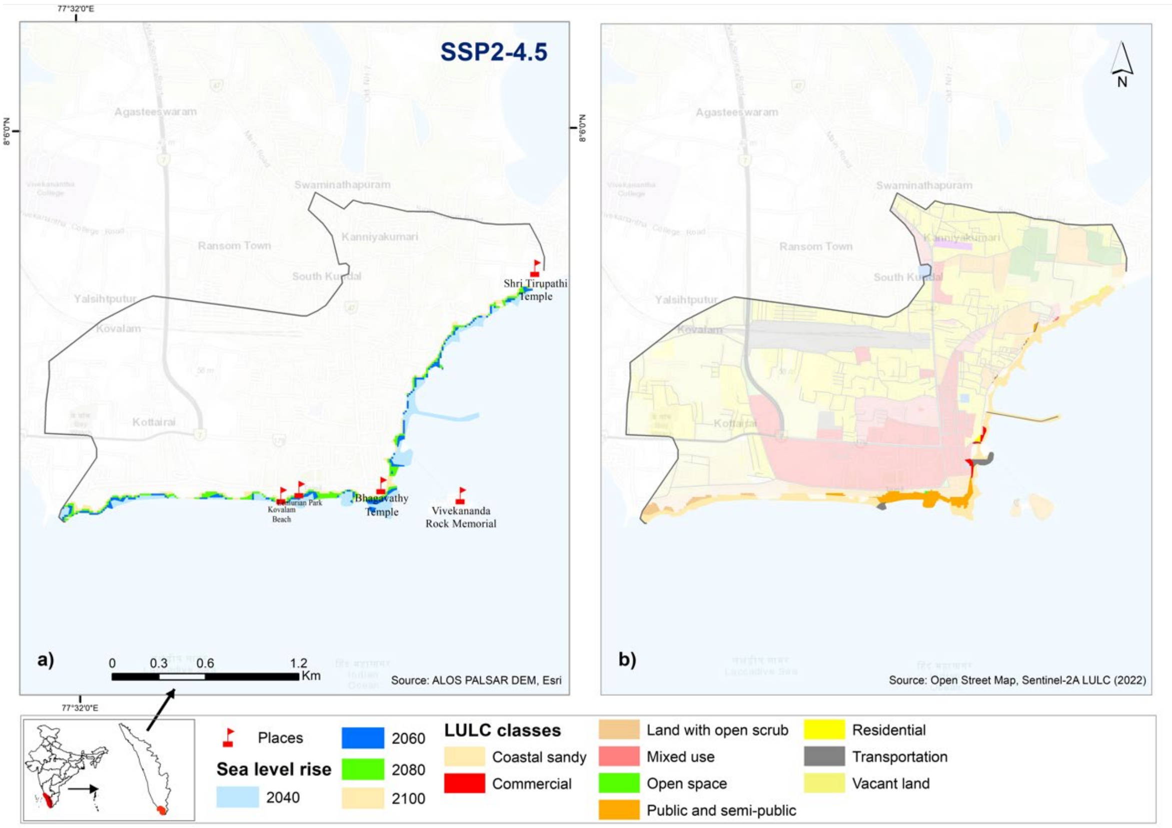

Figure 5.26: (a) Inundation area for projected SLR in Kanniyakumari, Tamil Nadu; (b) LULC-wise inundation for projected SLR by 2100 under the SSP2-4.5 scenario in Kanniyakumari, Tamil Nadu

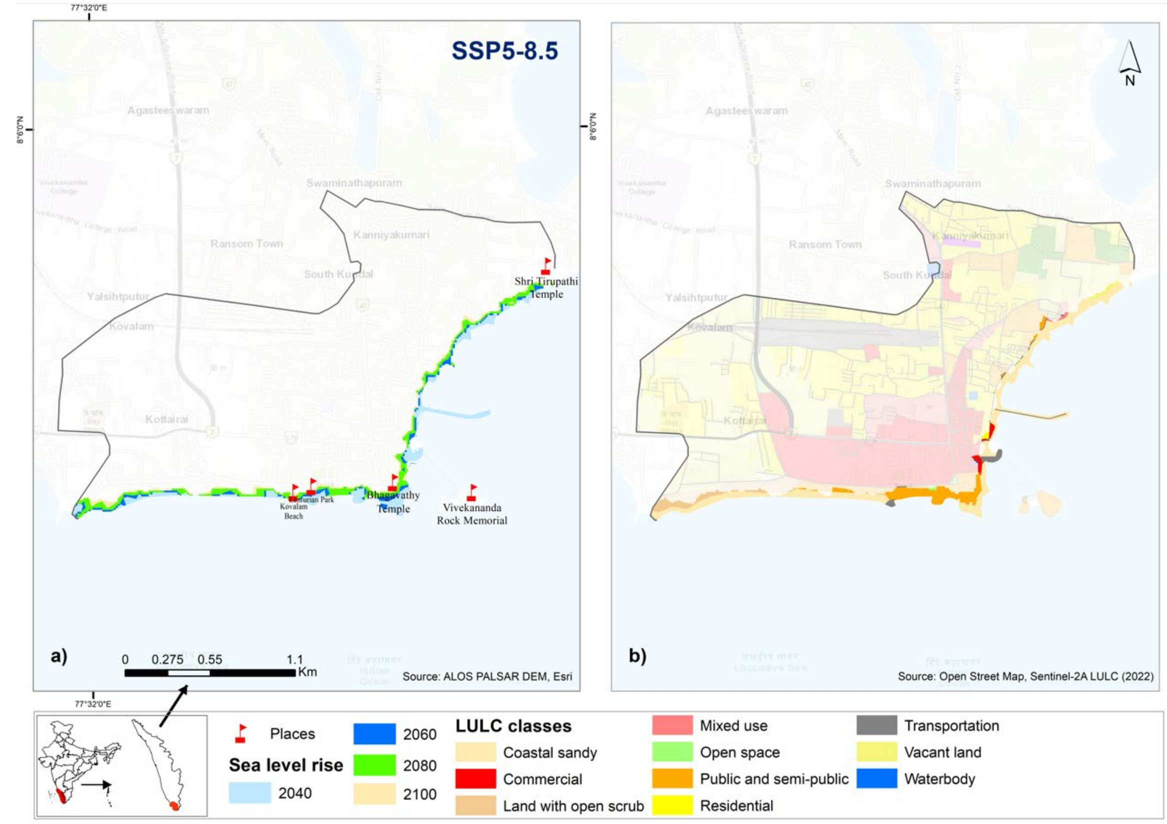

Figure 5.27: (a) Inundation area for projected SLR in Kanniyakumari, Tamil Nadu; (b) LULC-wise inundation for projected SLR by 2100 under the SSP5-8.5 scenario in Kanniyakumari, Tamil Nadu

5.3.2. Panaji, Goa

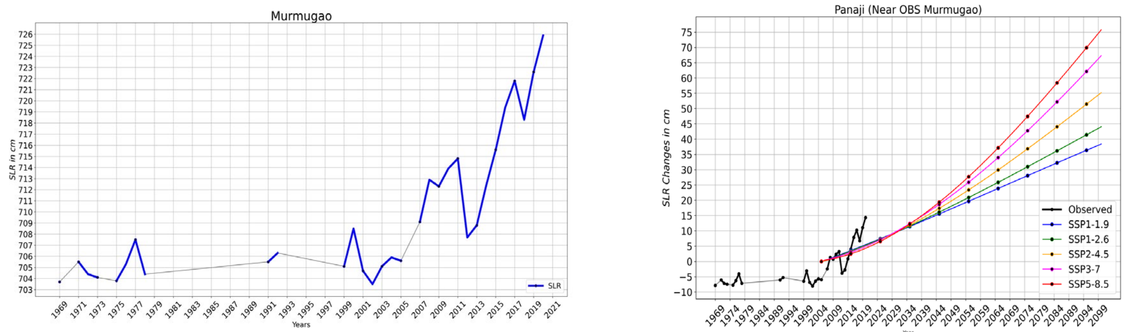

Figure 5.28: (a) Sea level rise during the historical period from the Murmugao tide gauge station; (b) SLR projected under the future SSP scenarios for Panaji, Goa

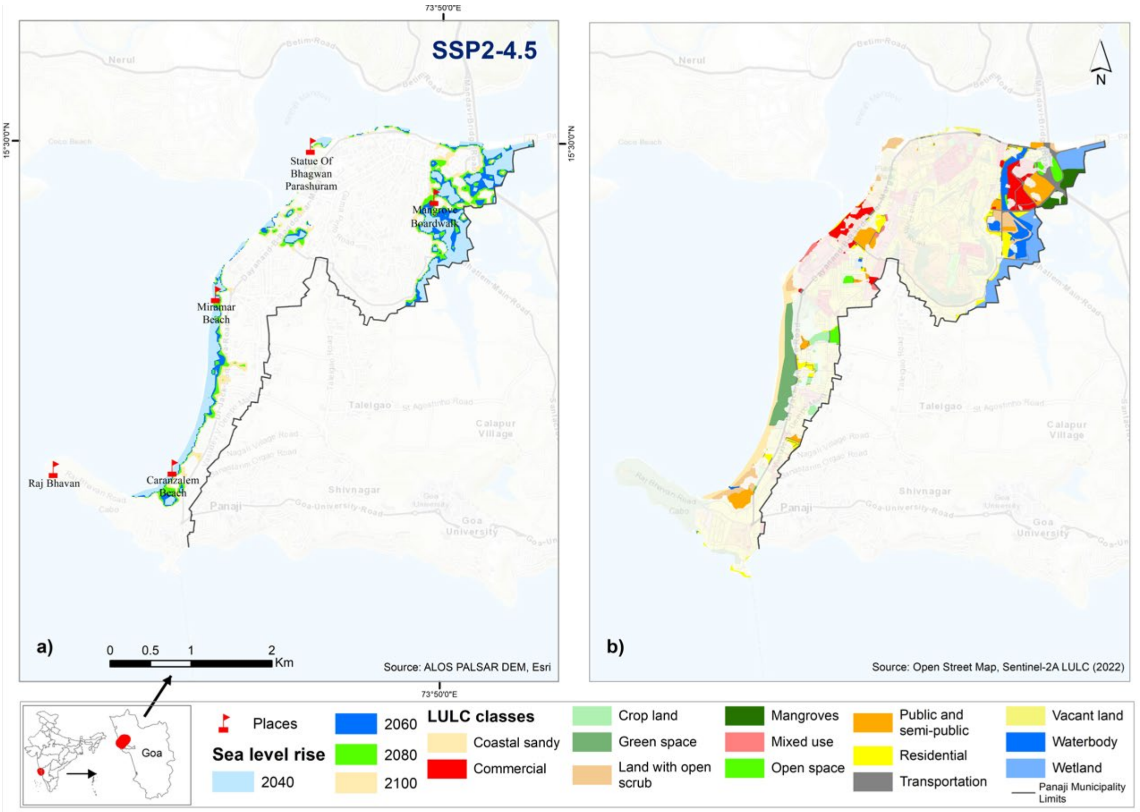

Figure 5.29: (a) Inundation area for projected SLR in Panaji, Goa; (b) LULC-wise inundation for projected SLR by 2100 under the SSP2-4.5 scenario in Panaji, Goa

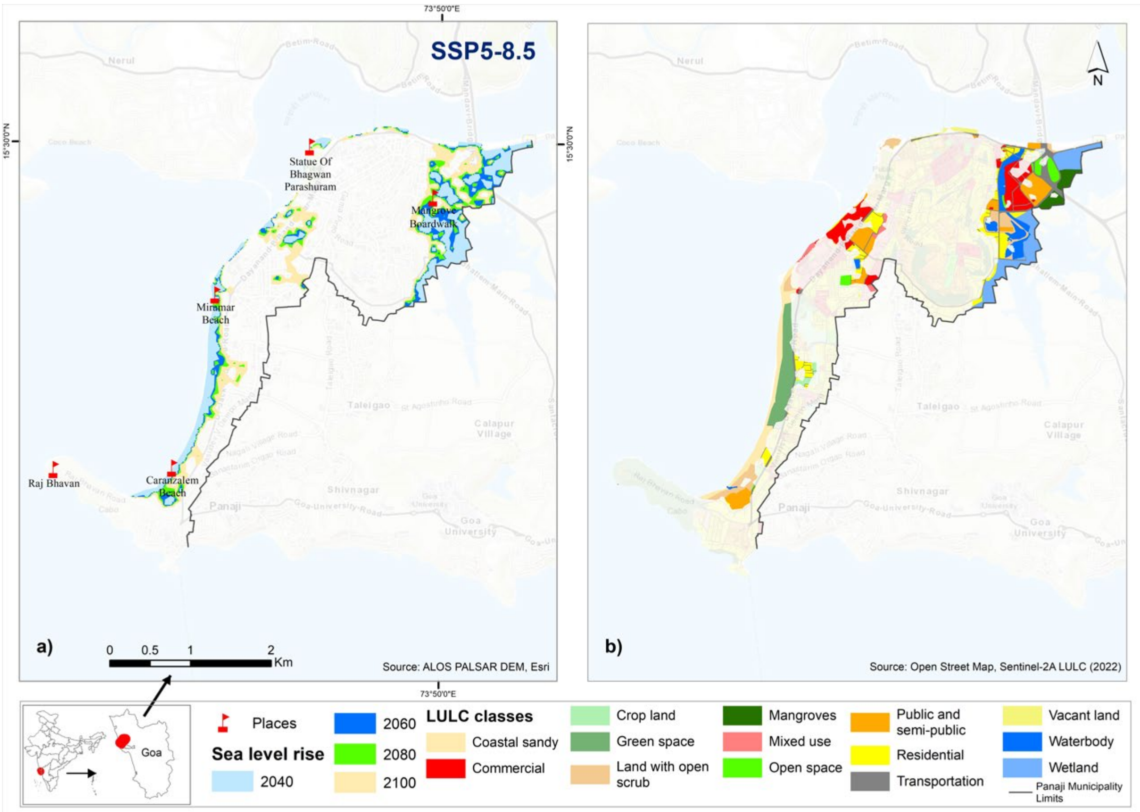

Figure 5.30: (a) Inundation area for projected SLR in Panaji, Goa; (b) LULC-wise inundation for projected SLR by 2100 under the SSP5-8.5 scenario in Panaji, Goa

5.3.3. Paradip, Odisha

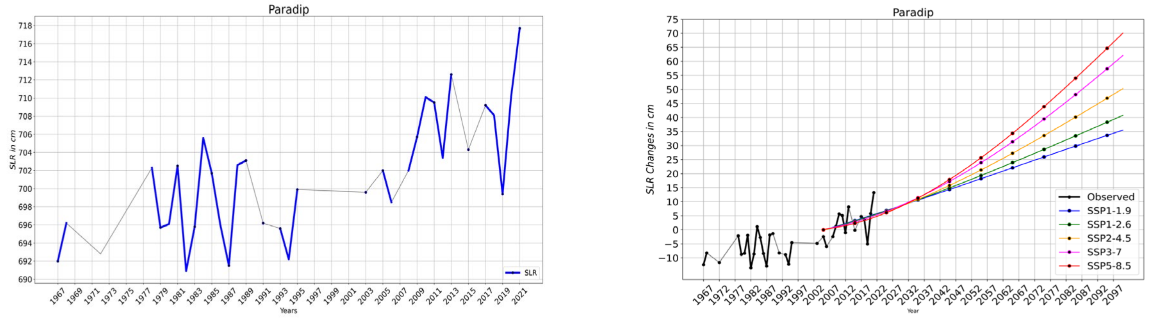

Figure 5.31: (a) Sea level rise during the historical period from the Paradip tide gauge station; (b) SLR projected under the future SSP scenarios for Paradip, Odisha

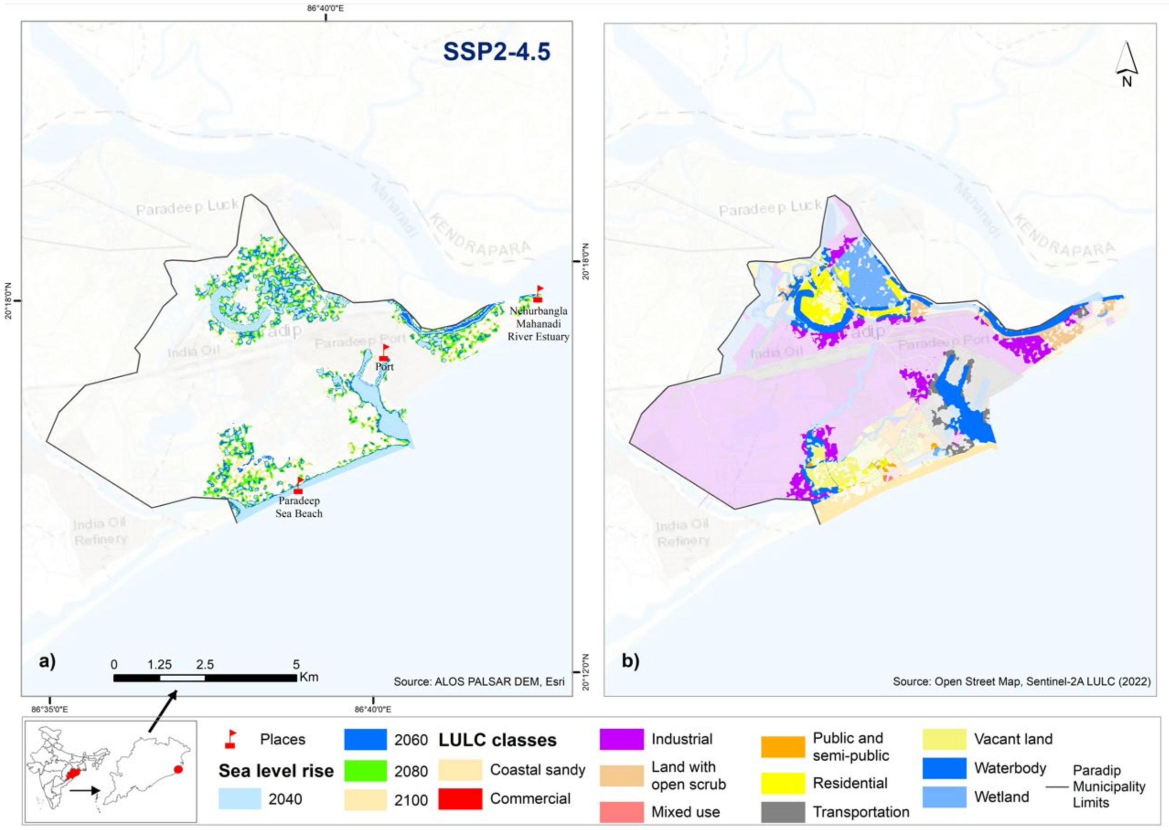

Figure 5.32: (a) Inundation area for projected SLR in Paradip, Odisha; (b) LULC-wise inundation for projected SLR by 2100 under the SSP2-4.5 scenario in Paradip, Odisha

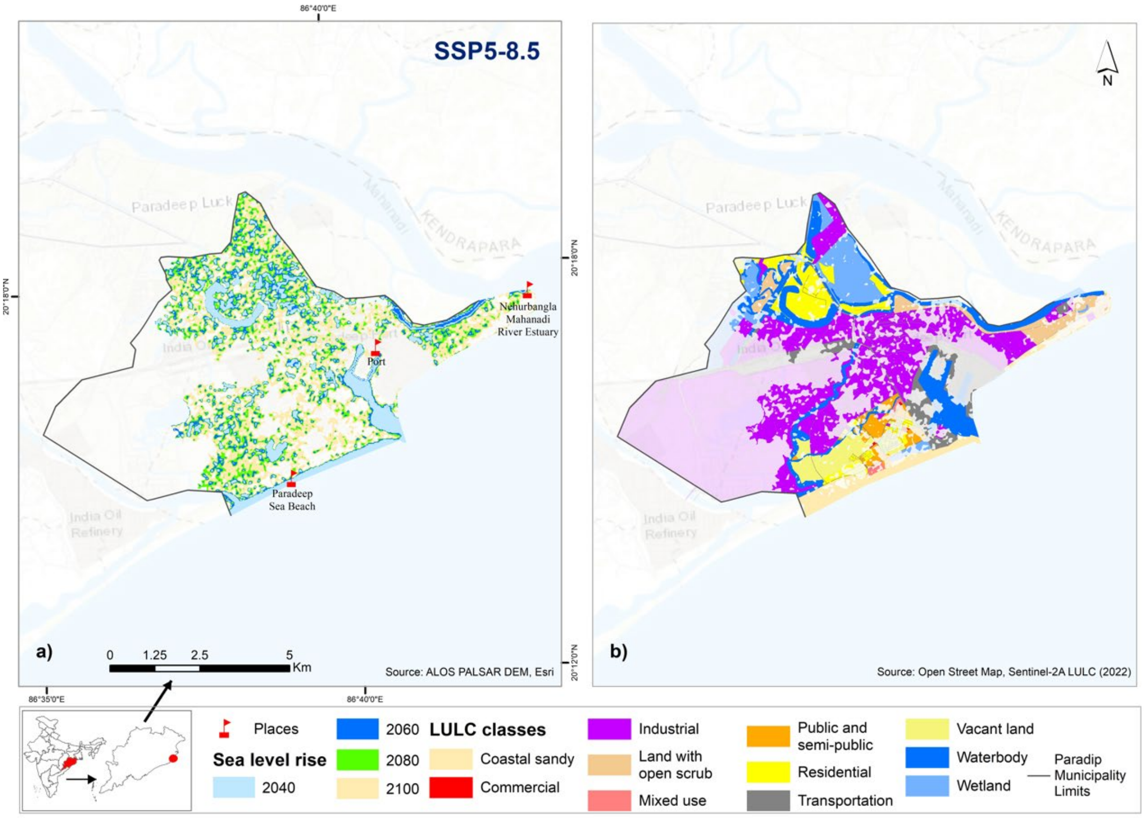

Figure 5.33: (a) Inundation area for projected SLR in Paradip, Odisha; (b) LULC-wise inundation for projected SLR by 2100 under the SSP5-8.5 scenario in Paradip, Odisha

5.3.4. Puri, Odisha

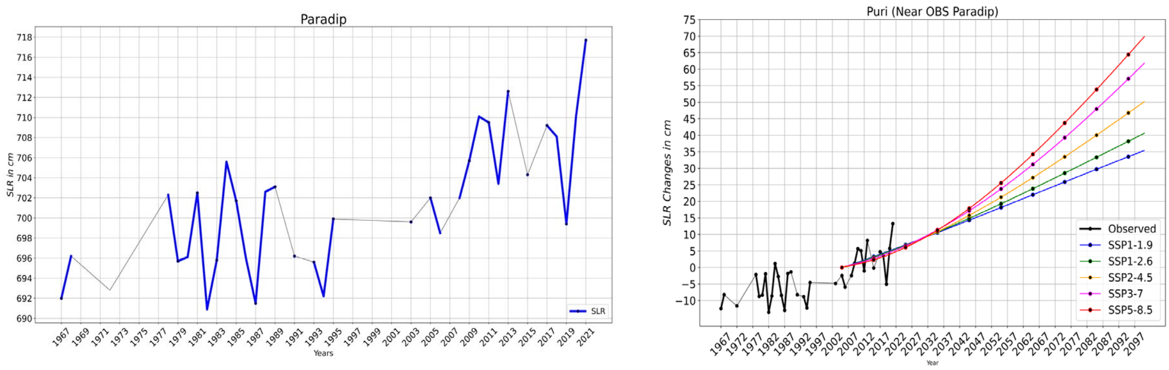

Figure 5.34: (a) Sea level rise during the historical period from the Paradip tide gauge station; (b) SLR projected under the future SSP scenarios for Puri, Odisha

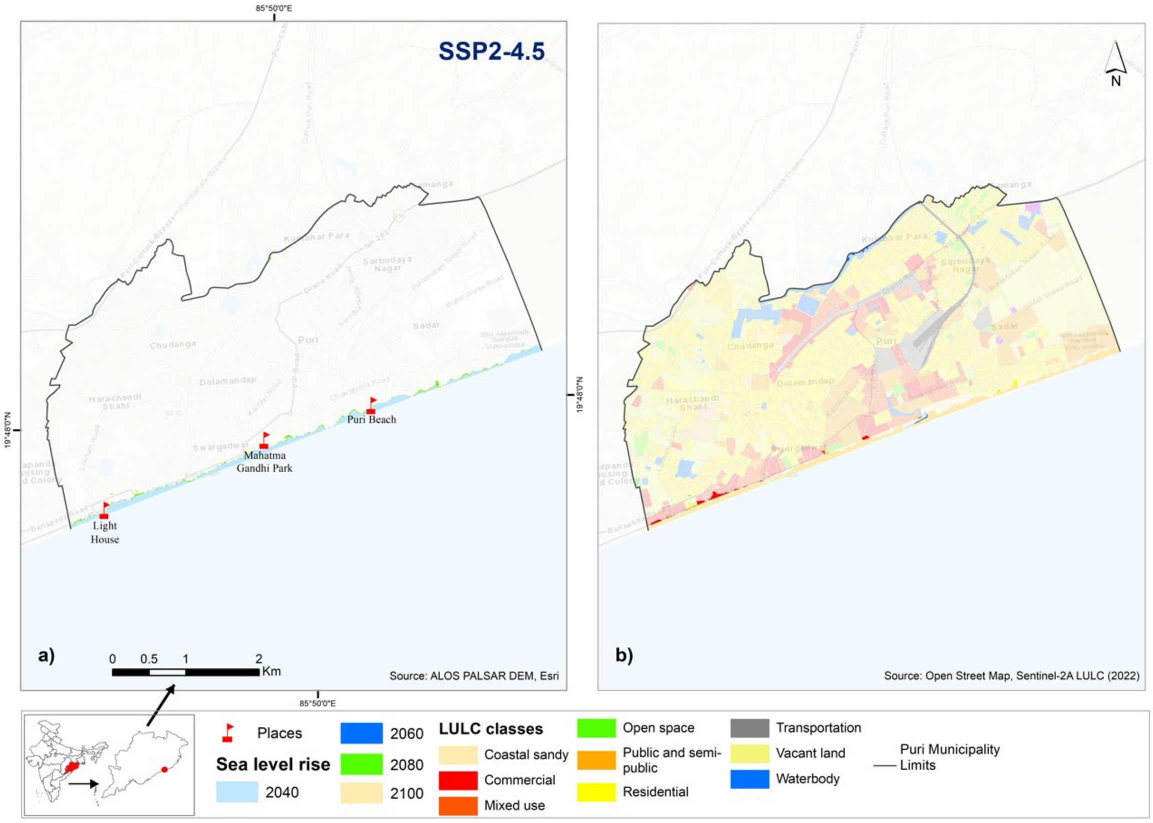

Figure 5.35: (a) Inundation area for projected SLR in Puri, Odisha; (b) LULC-wise inundation for projected SLR by 2100 under the SSP2-4.5 scenario in Puri, Odisha

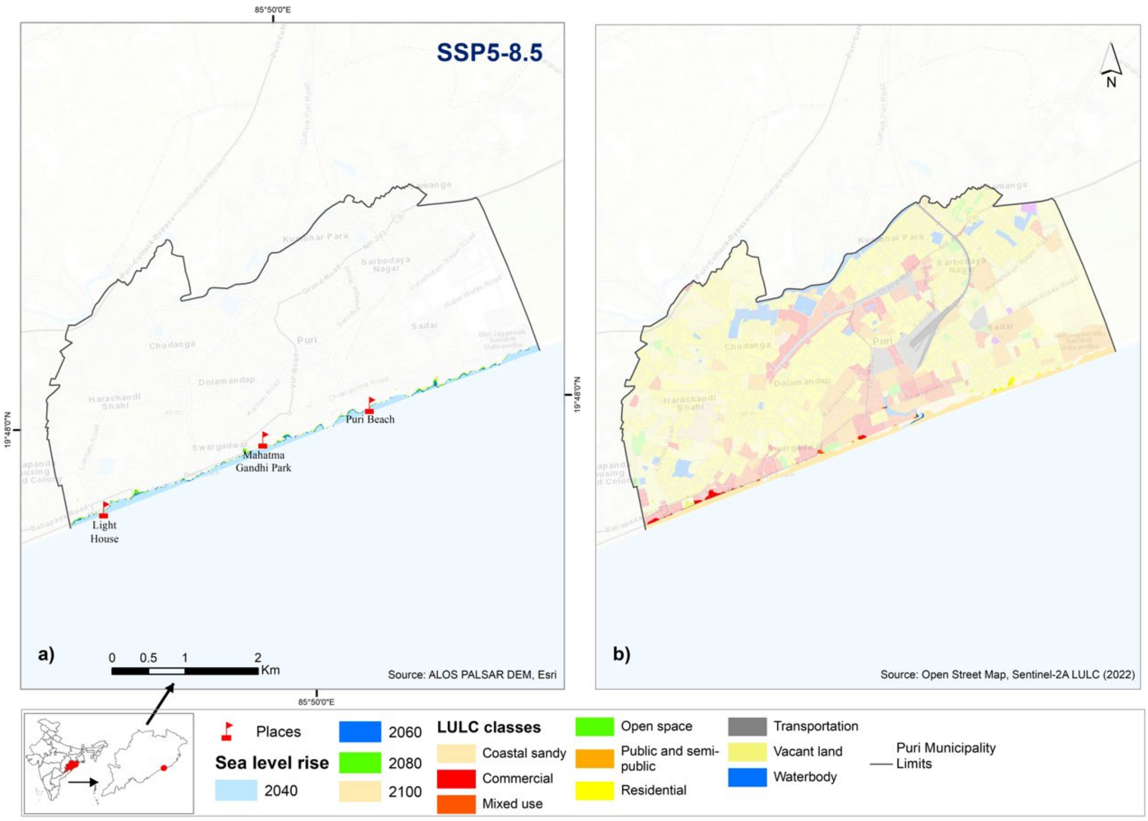

Figure 5.36: (a) Inundation area for projected SLR in Puri, Odisha; (b) LULC-wise inundation for projected SLR by 2100 under the SSP5-8.5 scenario in Puri, Odisha

5.3.5. Thoothukudi, Tamil Nadu

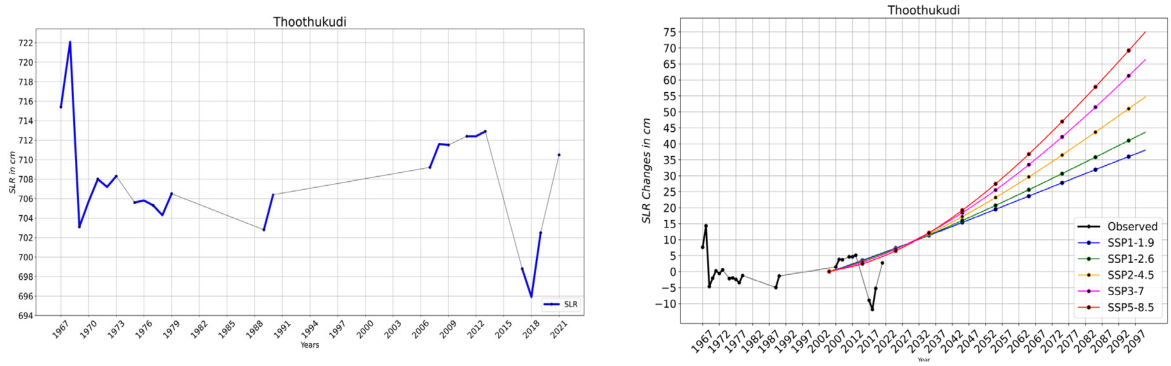

Figure 5.37: (a) Sea level rise during the historical period from the Thoothukudi tide gauge station; (b) SLR projected under the future SSP scenarios for Thoothukudi, Tamil Nadu

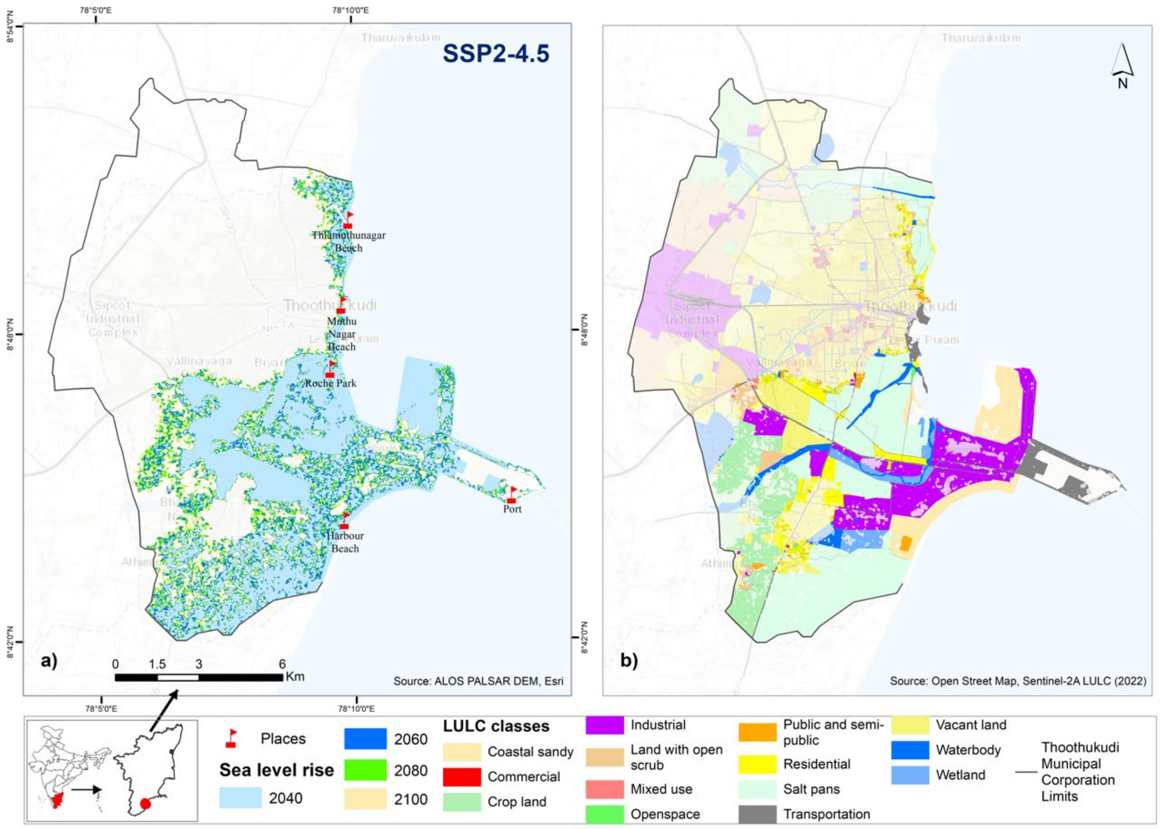

Figure 5.38: (a) Inundation area for projected SLR in Thoothukudi, Tamil Nadu; (b) LULC-wise inundation for projected SLR by 2100 under the SSP2-4.5 scenario in Thoothukudi, Tamil Nadu

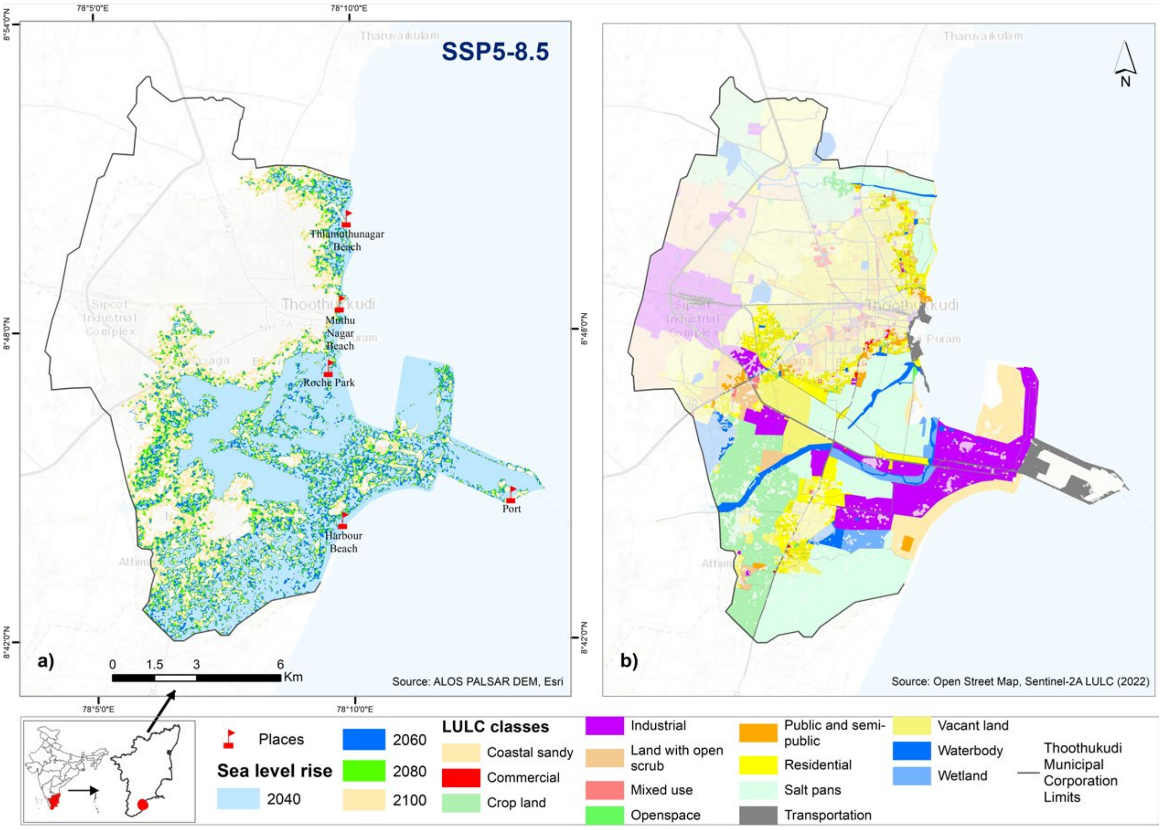

Figure 5.39: (a) Inundation area for projected SLR in Thoothukudi, Tamil Nadu; (b) LULC-wise inundation for projected SLR by 2100 under the SSP5-8.5 scenario in Thoothukudi, Tamil Nadu

5.3.6. Udupi, Karnataka

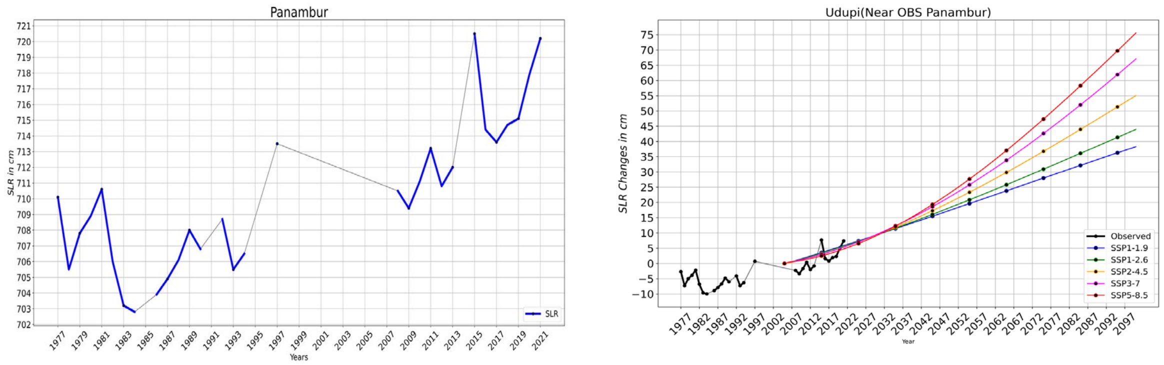

Figure 5.40: (a) Sea level rise during the historical period from the Panambur tide gauge station; (b) SLR projected under the future SSP scenarios for Udupi, Karnataka

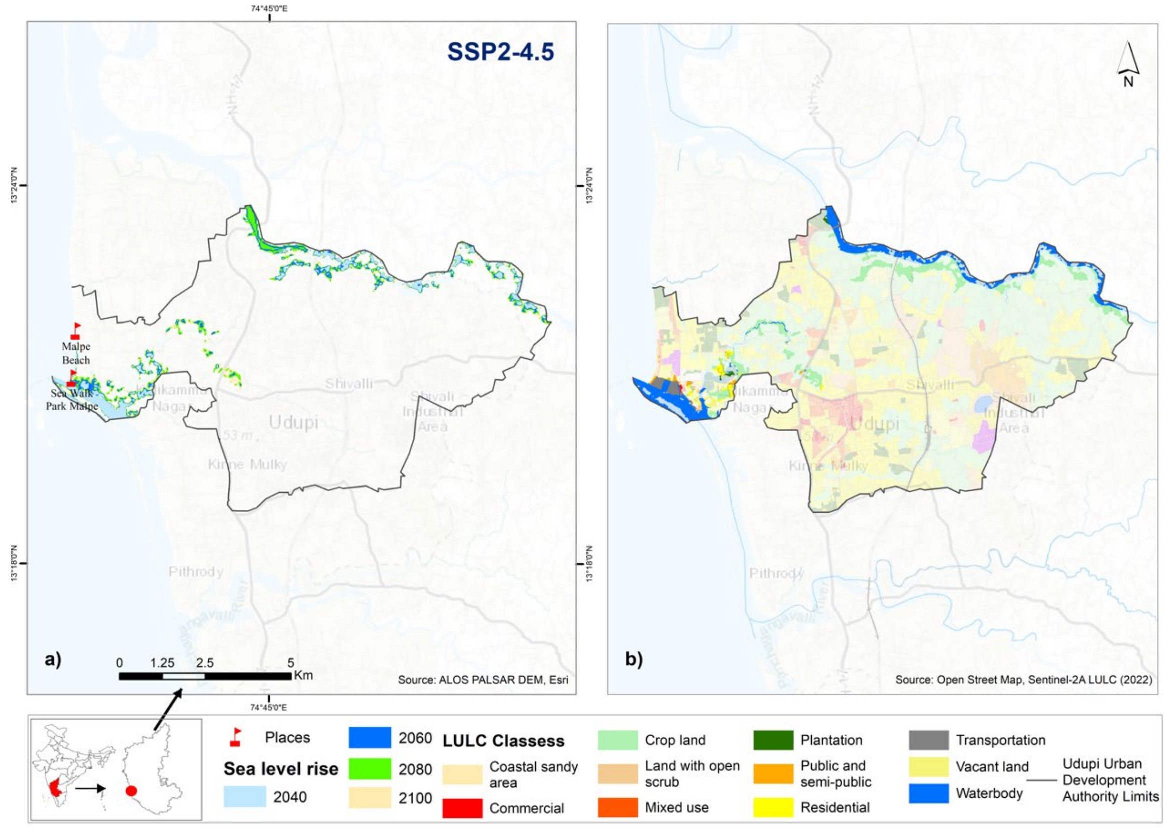

Figure 5.41: Inundation area for projected SLR in Udupi, Karnataka; (b) LULC-wise inundation for projected SLR by 2100 under the SSP2-4.5 scenario in Udupi, Karnataka

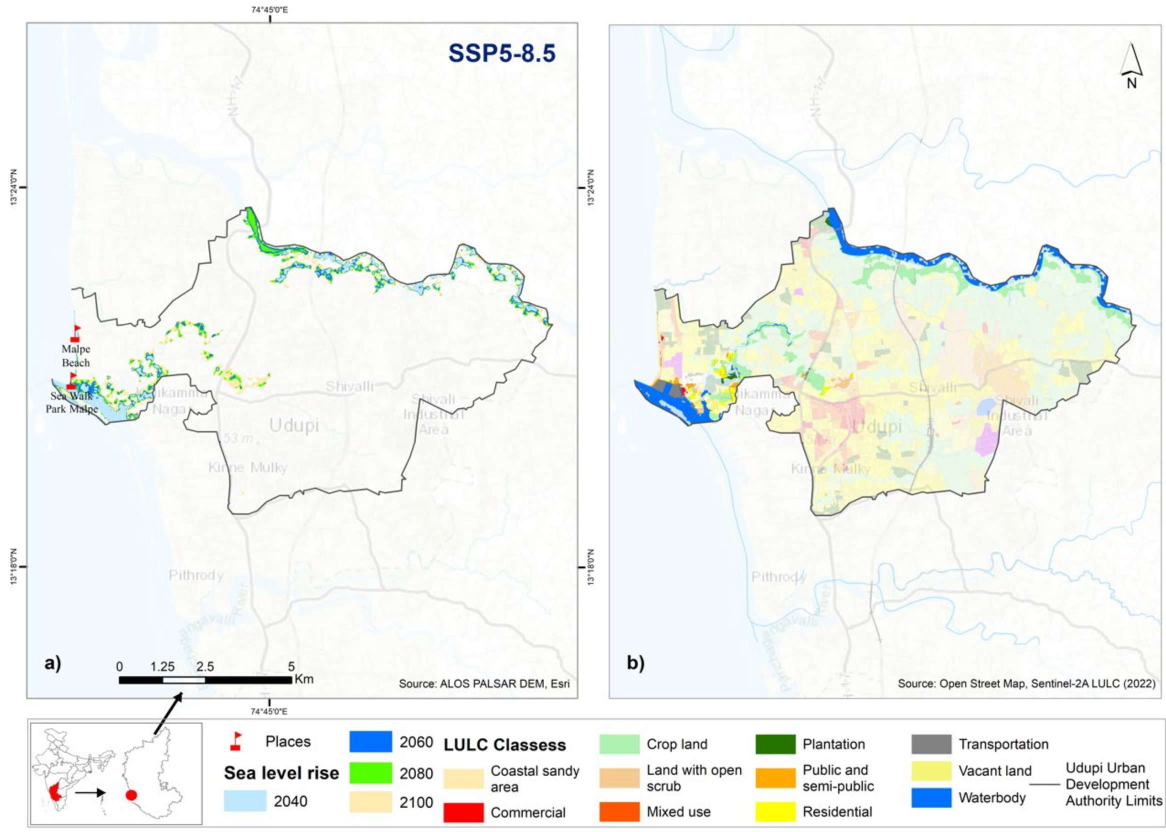

Figure 5.42: (a) Inundation area for projected SLR in Udupi, Karnataka; (b) LULC-wise inundation for projected SLR by 2100 under the SSP5-8.5 scenario in Udupi, Karnataka

5.3.7. Yanam, Puducherry

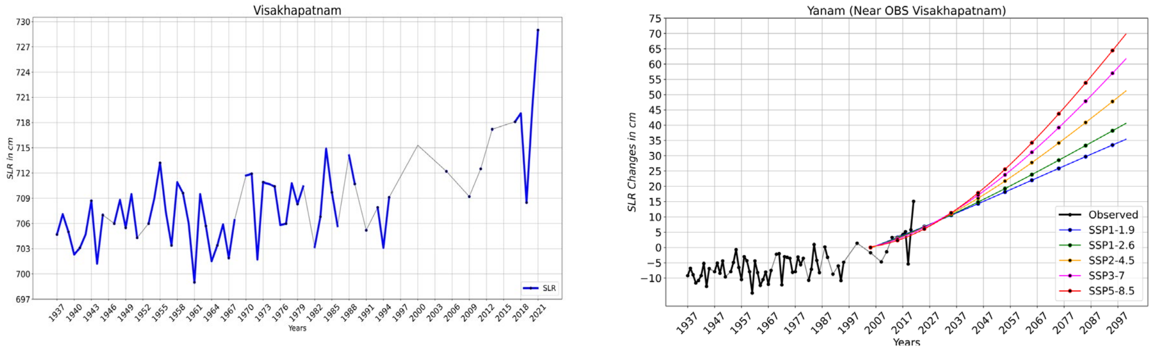

Figure 5.43: (a) Sea level rise during the historical period from the Visakhapatnam tide gauge station; (b) SLR projected under the future SSP scenarios for Yanam, Puducherry

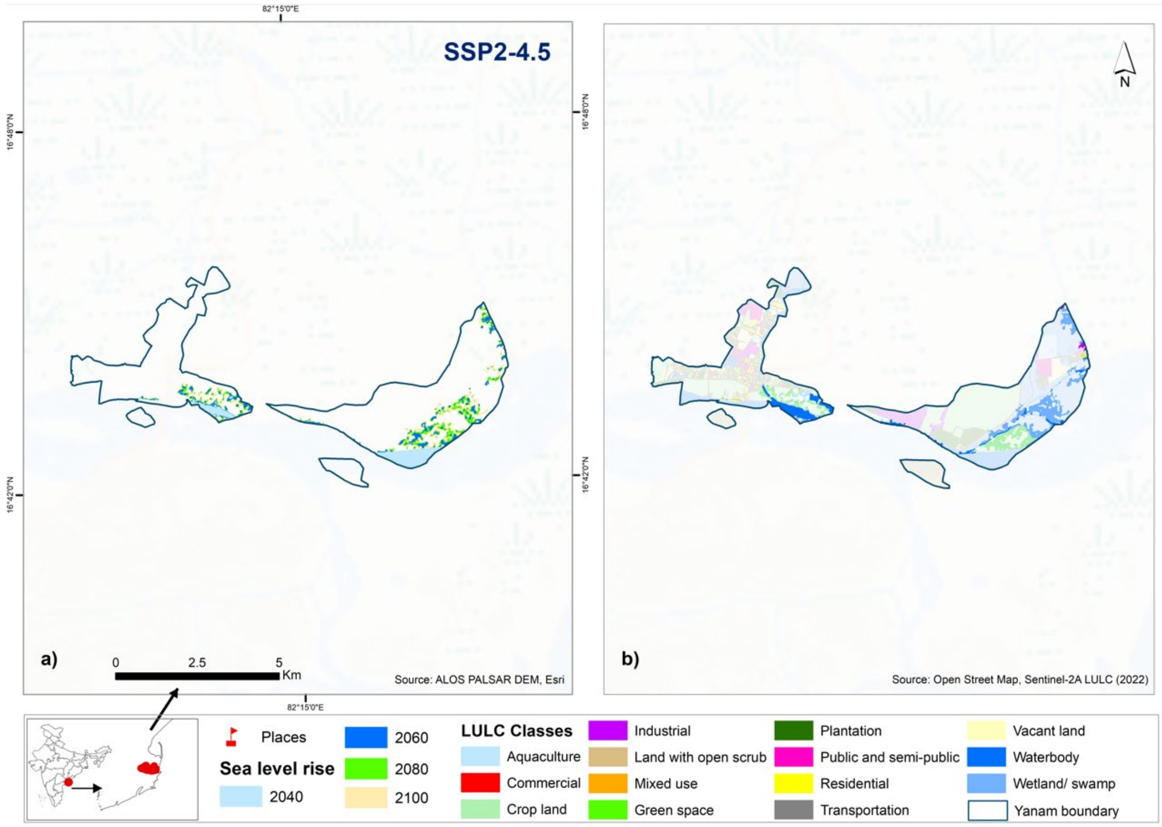

Figure 5.44: (a) Inundation area for projected SLR in Yanam, Puducherry; (b) LULC-wise inundation for projected SLR by 2100 under the SSP2-4.5 scenario in Yanam, Puducherry

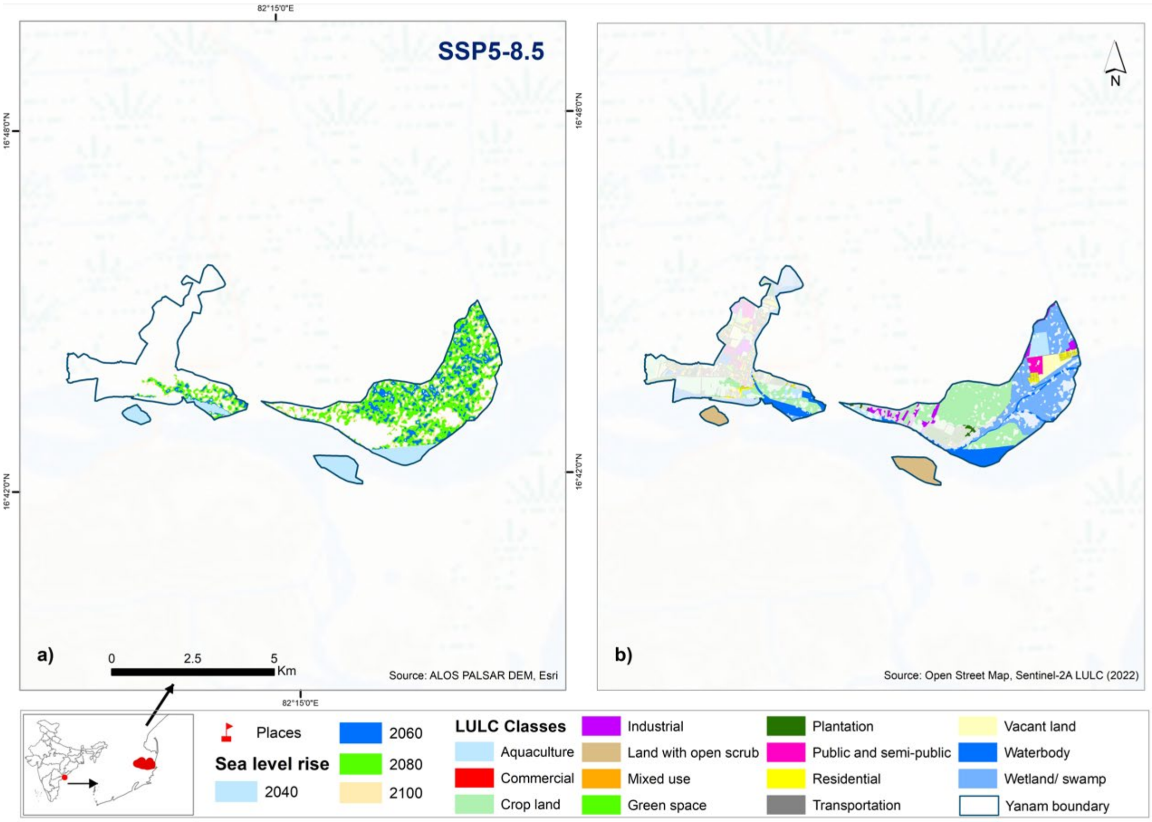

Figure 5.45: (a) Inundation area for projected SLR in Yanam, Puducherry; (b) LULC-wise inundation for projected SLR by 2100 under the SSP5-8.5 scenario in Yanam, Puducherry

Table 5.6: Projected SLR (in cm) and impacted area (in sq. km) for the selected towns under different SSP scenarios for the considered years

City	SSPs	2040		2060		2080		2100	
		SLR	Area	SLR (in cm)	Area	SLR	Area	SLR (in cm)	Area
Kanniyakumari	SSP2-4.5	18.2	0.1	34.3	0.14	43.5	0.18	74.7	0.2
	SSP5-8.5	19.6	0.09	41	0.18	68	0.21	99.3	0.23
Panaji	SSP2-4.5	18.4	0.78	34.7	1.1	54	1.42	75.5	1.63
	SSP5-8.5	19.8	0.78	41.5	1.1	68.8	1.42	100.4	1.88
Paradip	SSP2-4.5	16.8	4.39	31.7	6.95	49.4	10.11	69	13.01
	SSP5-8.5	18.2	5.5	37.9	9.48	62.9	15.21	91.9	27.58
Puri	SSP2-4.5	16.7	0.37	31.6	0.37	49.2	0.4	68.6	0.45
	SSP5-8.5	18.1	0.36	37.7	0.39	62.6	0.42	91.3	0.49
Thoothukudi	SSP2-4.5	18.2	41.56	34.3	52.23	53.4	62.08	74.6	68.55
	SSP5-8.5	19.3	44.1	40.9	55.45	67.9	66.65	92.2	81.64
Udupi	SSP2-4.5	18.4	1.76	34.6	2.85	53.9	4.24	75.3	5.38
	SSP5-8.5	19.8	1.82	41.4	2.92	68.6	4.06	100.2	6.84
Yanam	SSP2-4.5	17	3.08	32	4.39	49.8	5.77	69.5	8.32
	SSP5-8.5	18.3	3.21	38.2	5.96	63.4	12.87	92.5	15.49

Table 5.7: LULC-wise (existing) inundation area (sq. km) for projected SLR by 2100 in the selected towns.

LULC	Kanniyakumari		Panaji		Paradip		Puri		Thoothukudi		Udupi		Yanam	
	SSP2-4.5	SSP5-8.5	SSP2-4.5	SSP5-8.5	SSP2-4.5	SSP5-8.5	SSP2-4.5	SSP5-8.5	SSP2-4.5	SSP5-8.5	SSP2-4.5	SSP5-8.5	SSP2-4.5	SSP5-8.5
Agriculture	-	-	0.32	0.34	-	0.01	-	-	7.18	9.85	2.34	3.09	1.08	4.84
Green area	-	-	0.23	0.28	-	0.23	0	0	0.1	0.16	-	-	-	-
Industrial	-	-	-	-	2.32	9.73	-	-	10.93	12.44	-	0	0.05	1.24
Urban	0.1	0.1	0.58	0.73	2.99	6.53	0.04	0.07	14.75	20.91	0.72	0.99	0.08	1.03
Waste land	0.1	0.1	0.35	0.37	2.31	3.1	0.4	0.42	7.3	7.7	0.09	0.29		
Waterbody	-	-	0.15	0.16	5.39	5.28	0.01	0	2.22	2.95	2.23	2.47	4.54	4.95
Wetland	-	-	-	-	-	2.7	0	0	26.07	27.63	0	0	1.62	4.38

All towns except Thoothukudi, Kanniyakumari, and Udupi (analysed with respect to the Panambur tide gauge station) show increasing SLR under the historical climate scenario. Future projections of SLR indicate an increase till the end of the century.

- Historical data show an SLR of 0.359 cm with an annual rise of 0.033 cm in Murmugao over the past three decades (1991–2020). Paradip witnessed an SLR of 0.717 cm and an annual rise of 0.108 cm over the past three decades (1992–2021).
    - Decreasing trends in SLR were observed in Thoothukudi and Panambur during 1992–2021. However, this does not imply a decrease in overall sea levels but rather a slow rate of increase.
- SSP2-4.5 scenario
    - Sea level rise would be 16.7–18.4 cm by 2040, 31.4–34.7 cm by 2060, 48.9–54 cm by 2080, and 68.6–75.5 cm by 2100 for the selected towns.
    - Highest SLR is projected in Kanniyakumari (75.7 cm), followed by Panaji (75.6 cm) and Thoothukudi (75.5 cm) by 2100.The least rise is projected in Puri (68.6 cm).
- SSP5-8.5 scenario
    - Sea level rise would be 18–19.8 cm by 2040, 37.5–41.5 cm by 2060, 62.3–68.8 cm by 2080, and 90.9–100.4 cm by 2100 for the selected towns.
    - Sea level rise is projected to be the highest for Panaji (100.4 cm), followed by Udupi (100.2 cm), Kanniyakumari (99.3 cm), Yanam (92.5 cm), Thoothukudi (92.2 cm), Paradip (91.9 cm), and Puri (91.3 cm) by 2100.
- Inundation mapping shows the following:
    - Inundation induced by SLR would be high in Thoothukudi 12.49% (44.10 sq. km) by 2040, 15.71% (55.45 sq. km) by 2060, 18.88% (66.65 sq. km) by 2080, and 23.12% (81.64 sq. km) by 2100, followed by Paradip 5.24% (5.50 sq. km) by 2040, 9.03% (9.48 sq. km) by 2060, 14.49% (15.21 sq. km) by 2080, and 26.11% (27.58 sq. km) by 2100, and Yanam 2.67% (3.21 sq. km) by 2040, 4.28% (5.96 sq. km) by 2060, 5.95% (12.87 sq. km) by 2080, and 10.02% (15.49 sq. km) by 2100 under the SSP5-8.5 scenario. Further, Kanniyakumari is projected to have the least area inundated.
    - Puri, Panaji, and Udupi would experience less inundation.
    - Among all types of land use, industrial areas in Thoothukudi and Panaji would face the highest risk of inundation. However, in Udupi, agricultural land is projected to have the highest inundation risk.
    - Agriculture, fishing, aquaculture, and fish habitats would face potential threats from the rising sea levels, which may lead to financial and social challenges.

6. Conclusion

Data on sea levels during the historical period clearly indicate SLR, which is projected to continue till the end of the century. To cope with the continuing SLR and its impacts, it is important to build capacities among city planners and decision-makers to use SLR information and critical inundation data while planning; this work is an effort in that direction. The SLR observations and projections are largely in agreement with the literature available for major cities and the country (MoES, 2020).

An increasing trend in SLR was observed in most cities and towns over the past 30 years. In the west coast, an increasing trend was observed for Mumbai, Kochi, and Murmugao stations, whereas the Panambur station showed a negative trend during this period. On the east coast, Haldia, Paradip, Visakhapatnam, and Chennai stations showed an increasing trend in SLR, whereas a negative trend was observed for Thoothukudi during the 30-year period. Historical SLR was observed to be the maximum in Mumbai, followed by Haldia, Visakhapatnam, Kochi, Paradip, and Chennai. Further, per year increase in sea levels was high in Mumbai, Visakhapatnam, Kochi, and Paradip.

Multi-model ensemble of IPCC-AR6 GCMs indicate an increase in sea level till the end of the century for all cities and towns under all future climate scenarios (including medium- and high-emission scenarios). Among the 15 cities and towns, this increase is projected to be more in Mumbai, Kozhikode, Kochi, Mangaluru, Thiruvananthapuram, Panaji, Udupi, and Kanniyakumari.

The projected changes in sea levels will lead to inundation in low-lying areas. The SLR-induced inundation maps from this study indicate LULC subsidence under future climate scenarios. By 2100, the inundation would be higher in Tier-II cities (Mangaluru and Haldia) and towns (Paradip, Thoothukudi, and Yanam) than in Tier-I cities (Chennai and Mumbai) under the high-emission scenario. Compared with other cities and towns (except Kanniyakumari), Thiruvananthapuram is projected to have less overall inundation area (1.86% to 2.78%) under future climate scenarios; however, the city may experience a much higher urban area subsidence (22.32%). By 2100, around 10% of Chennai's current urban land use will be under the risk of inundation. Such inundation will contribute to soil erosion and put coastal cities and their habitations, ecosystems, infrastructure, communities, and livelihoods at risk of destruction.

Flooding events are already happening quite frequently in Indian cities. Under future climate scenarios, SLR-induced inundation will lead to extended coastal flooding, with serious impacts on key sectors such as water, agriculture, forest and biodiversity, and health. The beaches, backwaters, and mangrove forests in coastal cities are particularly at risk, impacting biodiversity and tourism. The cities heavily relying on agriculture, fishing, and aquaculture operations will incur financial losses and face social challenges. Moreover, towns (Haldia, Udupi, Panaji, and Yanam) with significant agricultural areas, wetlands, and waterbodies will face subsidence due to SLR. Large and minor ports in these coastal cities would also experience an increased risk of SLR hazards.

Evidence on SLR and inundation under future scenarios is a prerequisite for cities to plan for and implement solutions in response to SLR-induced inundation risks. This study provides SLR information for coastal cities, including growing urban centres, coupled with possible LULC-wise inundation scenarios by using the available satellite images (12.5 m spatial resolution) and climate datasets. This information on SLR and inundation is essential for decision-makers to understand the SLR impacts and develop city action plans for buffering SLR effects. The high-risk hotspot mapping performed in this study for the 15 cities and towns is a useful resource for stakeholders in urban development, disaster risk reduction, and coastal management. However, using spatial resolution images with high vertical accuracy will be advantageous for city level assessments and further actions at the cadastral level. Such an exercise helps frame appropriate adaptation and risk mitigation strategies that would reduce the effects of SLR, safeguard coastal communities, and promote sustainable coastal development in the face of climate change.

7. References

Adiri, Z., Lhissou, R., Maacha, L., Jilali, A., Talbi, E. H., Jellouli, A., & Chakouri, M. (2022). Comparison of ASTER GDEM3, SRTM3, NASADEM, TanDEM-X90, AW3D30, and ALOS PALSAR data with TanDEM-X12: a case study of Tagragra of Akka inlier, Moroccan Anti-Atlas. *Arabian Journal of Geosciences, 15(21),* 1654.

Alahmadi, F. S. (2018). Evaluation of global digital elevation model ALOS/PALSAR using aerial LiDAR.

Arabameri, A., Pradhan, B., Rezaei, K., & Lee, C.-W. (2019). Assessment of landslide susceptibility using statistical- and artificial intelligence-based FR–RF integrated model and multiresolution *DEMs. Remote Sensing, 11(9),* Article 9. https://doi.org/10.3390/rs11090999

Arkema, K. K., Guannel, G., Verutes, G., Wood, S. A., Guerry, A., Ruckelshaus, M., Kareiva, P., Lacayo, M., Silver, J. M. (2013). Coastal habitats shield people and property from sea-level rise and storms. *Nature climate change, 3(10), 913–918.*

Arumugam, T., Yadav, R. L., & Kinattinkara, S. (2021). Assessment and predicting of LULC by Kappa analysis and CA Markov model using RS and GIS techniques in Udham Singh Nagar District, India [Preprint]. https://doi.org/10.21203/rs.3.rs-141832/v1

Ministry of Earth Sciences. (2020). *Assessment of climate change over the Indian region: A report of the Ministry of Earth Sciences (MoES), Government of India.* Springer Singapore. doi:10.1007/978-981-15-4327-2.

Bendib, A. (2021). High-resolution Alos Palsar for the characterization of water storage at the Fountaine Des Gazelles Dam in Biskra, Eastern Algeria. *Journal of the Indian Society of Remote Sensing,* 49(8), 1927–1938. https://doi.org/10.1007/s12524-021-01365-y

Bethel, M. B., Brien, L. F., Esposito, M. M., Miller, C. T., Buras, H. S., Laska, S. B., Philippe, R., Peterson, K. J., & Parsons Richards, C. (2014). Sci-TEK: A GIS-based multidisciplinary method for incorporating traditional ecological knowledge into Louisiana's coastal restoration decision-making processes. *Journal of Coastal Research,* 297, 1081–1099. https://doi.org/10.2112/JCOASTRES-D-13-00214.1

Bouizrou, I., Chahinian, N., Perrin, J. L., Müller, R., & Rais, N. (2022). Assessing the effects of urbanization on flood events using hydrological modelling: A case study of the Oued Fez urban catchment (Morocco) (No. IAHS2022-6). Copernicus Meetings.

Calazans Campelo, C. E., Bertolotto, M., & Corcoran, P. (2017). *Volunteered geographic information and the future of geospatial data.* IGI Global.

Carretero, S., Rapaglia, J., Bokuniewicz, H., & Kruse, E. (2013). Impact of sea-level rise on saltwater intrusion length into the coastal aquifer, Partido de La Costa, Argentina. *Continental Shelf Research,* 61–62, 62–70. https://doi.org/10.1016/j.csr.2013.04.029

Chai, L. T., Wong, C. J., James, D., Loh, H. Y., Liew, J. J. F., Wong, W. V. C., & Phua, M. H. (2022). Vertical accuracy comparison of multi-source digital elevation model (DEM) with airborne light detection and ranging (LiDAR). *IOP Conference Series: Earth and Environmental Science, 1053*(1), 012025. https://doi.org/10.1088/1755-1315/1053/1/012025

Church, J. A., Gregory, J. M., Huybrechts, P., Kuhn, M., Lambeck, K., Nhuan, M. T., In, D., & Woodworth, P. L. (2001). Changes in sea level. in: JT Houghton, Y. Ding, DJ Griggs, M. Noguer, PJ Van der Linden, X. Dai, K. Maskell, and CA Johnson (eds.): *Climate Change 2001: The Scientific Basis:*

Contribution of Working Group I to the Third Assessment Report of the Intergovernmental Panel (pp. 639–694).

Diambu, S. M., Osomba, D. W., Mayena, T. K., & Umba-di-Mbudi, C. N. Z. (2023). Contribution of ALOS PALSAR DEM imagery to the study of geological and morphostructural lineaments of Boma Trough Block, onshore coastal basin of DR Congo. *Indonesian Journal of Earth Sciences, 3*(1), A632–A632.

Indian Space Research Organisation. (n.d.). Natural Resource Census Land Use Land Cover Database. https://bhuvan-app1.nrsc.gov.in/2dresources/thematic/2LULC/lulc1112.pdf

Dwarakish, G. S., Vinay, S. A., Natesan, U., Asano, T., Kakinuma, T., Venkataramana, K., Pai, P. J., & Babita, M. K. (2009). Coastal vulnerability assessment of the future sea level rise in Udupi coastal zone of Karnataka state, west coast of India. *Ocean & Coastal Management, 52*(9), 467–478.

Enríquez, A. R., Marcos, M., Álvarez-Ellacuría, A., Orfila, A., & Gomis, D. (2017). Changes in beach shoreline due to sea level rise and waves under climate change scenarios: application to the Balearic Islands (western Mediterranean). *Natural Hazards and Earth System Sciences, 17*(7), 1075–1089.

Ferreira, Z. A., & Cabral, P. (2021). Vertical accuracy assessment of ALOS PALSAR, GMTED2010, SRTM and Topodata digital elevation models. In: *Proceedings of the 7th International Conference on Geographical Information Systems Theory, Applications and Management (GISTAM 2021),* 116–124. https://doi.org/10.5220/0010404001160124

Fonte, C. C., & Martinho, N. (2017). Assessing the applicability of OpenStreetMap data to assist the validation of land use/land cover maps. *International Journal of Geographical Information Science, 31*(12), 2382–2400.

Ministry of Urban Development. (2026). *Formulation of GIS based master plan for AMRUT cities: Design & standards. Town and country planning organisation.* Government of India. https://pib.gov.in/PressReleasePage.aspx?PRID=1885837.

Ganjirad, M., & Bagheri, H. (2024). Google Earth Engine-based mapping of land use and land cover for weather forecast models using Landsat 8 imagery. *Ecological Informatics,* 80, 102498. https://doi.org/10.1016/j.ecoinf.2024.102498

Gautam, A. (2023). DEM AND Comparison of DEM obtained from ASTER, ALOS PALSAR and SRTM.

Gesch, D. B. (2018). Best practices for elevation-based assessments of sea-level rise and coastal flooding exposure. *Frontiers in Earth Science,* 6, 230.

Gopalakrishnan, S., Landry, C. E., Smith, M. D., & Whitehead, J. C. (2016). Economics of coastal erosion and adaptation to sea level rise. *Annual Review of Resource Economics,* 8, 119-139.

Gesch, D. B. (2018). Best practices for elevation-based assessments of sea-level rise and coastal flooding exposure. *Frontiers in Earth Science,* 6. https://www.frontiersin.org/articles/10.3389/feart.2018.00230

Hazra, Sugata & Ghosh, Tuhin & Dasgupta, R. & Sen, G.. (2002). Sea level and associated changes in Sundarbans. *Sci Cult.* 68. 309–321.

Houser, C., Hapke, C., & Hamilton, S. (2008). Controls on coastal dune morphology, shoreline erosion and barrier island response to extreme storms. *Geomorphology, 100* (3–4), 223-240.

J. Jyoti J, P. Swapna, & R. Krishnan. (2023). North Indian Ocean sea level rise in the past and future: The role of climate change and variability. *Global and Planetary Change*, 228: 104205

Jamal, S., & Ahmad, W. S. (2020). Assessing land use land cover dynamics of wetland ecosystems using Landsat satellite data. *SN Applied Sciences, 2*(11), 1891. https://doi.org/10.1007/s42452-020-03685-z

Kanan, A. H., Pirotti, F., Masiero, M., & Rahman, M. M. (2023). Mapping inundation from sea level rise and its interaction with land cover in the Sundarbans mangrove forest. *Climatic Change, 176*(8), 104.

Keenan, J. M., Hill, T., & Gumber, A. (2018). Climate gentrification: from theory to empiricism in Miami-Dade County, Florida. *Environmental Research Letters, 13*(5), 054001.

Leuliette, E. W., & Nerem, R. S. (2016). Contributions of Greenland and Antarctica to global and regional sea level change. *Oceanography, 29*(4), 154–159. https://doi.org/10.5670/oceanog.2016.107

Lincke, D., & Hinkel, J. (2018). Economically robust protection against 21st century sea-level rise. *Global Environmental Change,* 51, 67–73.

Lyons, M. B., Keith, D. A., Phinn, S. R., Mason, T. J., & Elith, J. (2018). A comparison of resampling methods for remote sensing classification and accuracy assessment. *Remote Sensing of Environment,* 208, 145–153. https://doi.org/10.1016/j.rse.2018.02.026

Martínez-Graña, A.; Gómez, D.; Santos-Francés, F.; Bardají, T.; Goy, J.L.; Zazo, C. (2018). Analysis of flood risk due to sea level rise in the Menor Sea (Murcia, Spain). Sustainability, 10, 780. https://doi.org/10.3390/su10030780

Malik, A., & Abdalla, R. (2016). Geospatial modeling of the impact of sea level rise on coastal communities: Application of Richmond, British Columbia, Canada. *Modeling Earth Systems and Environment, 2*(3), 146. https://doi.org/10.1007/s40808-016-0199-2

Mesa-Mingorance, J. L., & Ariza-López, F. J. (2020). Accuracy assessment of digital elevation models (DEMs): A critical review of practices of the past three decades. *Remote Sensing, 12*(16), Article 16. https://doi.org/10.3390/rs12162630

Mitchell, T. D. (2003). Pattern scaling: An examination of the accuracy of the technique for describing future climates, *Climatic Change,* 60, 217–242, 2003.

Mooney, P and Minghini, M. (2017). A review of OpenStreetMap data. In: Foody, G, See, L, Fritz, S, Mooney, P, Olteanu-Raimond, A-M, Fonte, C C and Antoniou, V. (eds.). *Mapping and the citizen sensor.* pp. 37–59. London: Ubiquity Press. DOI: https://doi.org/10.5334/bbf.c. License: CC-BY 4.0

Nicholls, R. J., Marinova, N., Lowe, J. A., Brown, S., Vellinga, P., De Gusmao, D., Hinkel, J., & Tol, R. S. (2011). Sea-level rise and its possible impacts given a 'beyond 4 °C world' in the twenty-first century. *Philosophical transactions of the Royal Society A: Mathematical, Physical and Engineering Sciences, 369*(1934), 161–181.

Nicholls, R.J. and Leatherman, S.P. (1996). Adapting to sea-level rise: Relative sea level trends to 2100 for the USA. *Coastal Management, 24*(4), 301–324.

Nicholls, R.J., 2002. Rising sea levels: potential impacts and responses. In: Hester, R. and Harrison, R.M. (ed.) *Global Environmental Change. Issues in Environmental Science and Technology,* Number 17, Royal Society of Chemistry, Cambridge, pp. 83–107

Nicholls, R.J., Hoozemans, F.M.J., and Marchand, M. (1999). Increasing flood risk and wet land losses due to global sea level rise: Regional and global analyses. Global Environmental Change, 9, pp. S69–S87

National Oceanic and Atmospheric Administration. (2022). *Global and regional sea level rise scenarios for the United States: Updated mean projections and extreme water level probabilities along U.S. coastlines. NOAA technical report NOS 01.* National Ocean Service, Silver Spring, MD, 111p.

National Oceanic and Atmospheric Administration. (1999). *The ocean's role in climate variability and change and the resulting impacts on coasts.* NOAA Report, Vol.23, No.2, NOAA, Silver Spring, M.D., USA, 319p.

Oppenheimer, M., B.C. Glavovic, J. Hinkel, R. van de Wal, A.K. Magnan, A. Abd-EIgawad, R. Cai, M. Cifuentes-Jara, R.M. DeConto, T. Ghosh, J. Hay, F. Isla, B. Marzeion, B. Meyssignac,. & Z. Sebesvari. (2019). *Sea level rise and implications for low-lying islands, coasts and communities.* IPCC Special Report on the Ocean and Cryosphere in a Changing Climate. Intergovernmental Panel on Climate Change.

Otosaka, I. N., Shepherd, A., Ivins, E. R., Schlegel, N. J., Amory, C., van den Broeke, M., & Wouters, B. (2022). Mass balance of the Greenland and Antarctic ice sheets from 1992 to 2020. *Earth System Science Data Discussions,* 2022, 1–33.

Pariartha, I. G. S., Aggarwal, S., Rallapalli, S., Egodawatta, P., McGree, J., & Goonetilleke, A. (2023). Compounding effects of urbanization, climate change and sea-level rise on monetary projections of flood damage. *Journal of Hydrology,* 620, 129535.

Kumar, P., Sardana, D., & Rajni. (2021). Regional sea level changes in the Indian shelf sea and its association with SST anomalies, *Regional Studies in Marine Science,* 47: 101992.

Raman, V. (2023). Determination of parameters for watershed delineation using various satellite derived digital elevation models and its accuracy. *Global NEST Journal,* 1–14. https://doi.org/10.30955/gnj.004202

Remya, R., Nath, A. R., Akhil, T., Babu, S. D., & Ramachandran, K. K. (2018). Assessment of saltwater intrusion and role of sea level rise (SLR) along the coast of Thiruvananthapuram District in Kerala, India. Nature *Environment and Pollution Technology, 17*(4), 1235–1242.

Rotzoll, K., & Fletcher, C.H. (2013). Assessment of groundwater inundation as a consequence of sea-level rise. *Nature Climate Change,* 3, 477–481. http://dx.doi.org/10.1038/nclimate1725

Rwanga, S. S., & Ndambuki, J. M. (2017). Accuracy assessment of land use/land cover classification using remote sensing and GIS. *International Journal of Geosciences,* 08(04), 611–622. https://doi.org/10.4236/ijg.2017.84033

Saintilan, N., Horton, B., Törnqvist, T. E., Ashe, E. L., Khan, N. S., Schuerch, M., & Guntenspergen, G. (2023). Widespread retreat of coastal habitat is likely at warming levels above 1.5 ° C. *Nature,* 1-8.

Santer, B. D., Wigley, T. M. L., Schlesinger, M. E., & Mitchell, J. F. B. (1990). *Developing climate scenarios from equilibrium GCM results,* MPI Report Number 47, Hamburg.

Schneider, P., & Asch, F. (2020). Rice production and food security in Asian Mega deltas—A review on characteristics, vulnerabilities and agricultural adaptation options to cope with climate change. *Journal of Agronomy and Crop Science, 206*(4): 491–503. https://doi.org/10.1111/jac.12415

See, L, Estima, J, Pődör, A, Arsanjani, J J, Bayas, J-C L,. & Vatseva, R. (2017). Sources of VGI for mapping. In: Foody, G, See, L, Fritz, S, Mooney, P, Olteanu-Raimond, A-M, Fonte, C C and Antoniou, V. (eds.) *Mapping and the citizen sensor.* pp. 13–35. London: Ubiquity Press. doi: https://doi.org/10.5334/bbf.b. License: CC-BY 4.0.

Seeteram, N. A., Ash, K., Sanders, B. F., Schubert, J. E., & Mach, K. J. (2023). Modes of climate mobility under sea-level rise. *Environmental Research Letters, 18*(11), 114015.

Sharma, A., Nikam, B. R., & Bagri, D. S. (2021). Comparative evaluation of digital elevation model based on elevation data and terrain attributes leading to their validation. *Asian Conference of Remote Sensing.* https://doi.org/10.1002/essoar.10505887.1

SimCLIM. (2011). *SimCLIM essentials: training book 1,* version 2.0. Climsystems, Hamilton, New Zealand, pp. 210.

Small, C., Sousa, D., Yetman, G., Elvidge, C., & MacManus, K. (2018). Decades of urban growth and development on the Asian megadeltas. *Global and Planetary Change,* 165, 62–89.

Sreeraj P., P., Swapna, R., Krishnan, A. G., Nidheesh, & N., Sandeep. (2022). Extreme sea level rise along the Indian Ocean coastline: observations and 21st century projections. *Environmental Research Letters, 17,* Number 11, doi 10.1088/1748-9326/ac97f5

National Oceanic and Atmospheric Administration. (2022). *Global and regional sea level rise scenarios for the United States.* Center for Operational Oceanographic Products and Services, Silver Spring, MD, USA.

Taherkhani, M., Vitousek, S., Barnard, P. L., Frazer, N., Anderson, T. R., & Fletcher, C. H. (2020). Sea-level rise exponentially increases coastal flood frequency*. Scientific Reports,* 10(1), 6466.

Tariq, M., Najmi, Z., Firdous, M., Saleem, F., Pervez, S., & Riaz, F. (2019). Use of Lidar and Radar technologies for watershed analysis in Feather River near California. In: 2019 *Sixth international conference on aerospace science and engineering* (ICASE). pp. 1-7. IEEE.

Tarboton, D. G., R. L. Bras, & I. Rodriguez–Iturbe. (1991). On the extraction of channel networks from digital elevation data. *Hydrological Processes.* 5: 81–100.

Titus, J. G., Park, R. A., Leatherman, S. P., Weggel, J. R., Greene, M. S., Mausel, P. W., & Yohe, G. (1991). Greenhouse effect and sea level rise: the cost of holding back the sea. *Coastal Management, 19*(2), 171–204.

Taherkhani, M., Vitousek, S., Barnard, P. L., Frazer, N., Anderson, T. R., & Fletcher, C. H. (2020). Sea-level rise exponentially increases coastal flood frequency. *Scientific Reports*, *10*(1), Article 1. https://doi.org/10.1038/s41598-020-62188-4

Urban Climate Change Research Network. (2018). *The future we don't want, How climate change could impact the world's greatest cities,* UCCRN technical report. https://www.c40.org/wp-content/uploads/2023/04/1789_Future_We_Dont_Want_Report_1.4_hi-res_120618.original-compressed.pdf

Unnikrishnan, A. S., Kumar, K. R., Fernandes, S. E., Michael, G. S., & Patwardhan, S. K. (2006). Sea level changes along the Indian coast: Observations and projections. *Current Science, 90*(3), 362–368.

Von Holle, B., Irish, J. L., Spivy, A., Weishampel, J. F., Meylan, A., Godfrey, M. H., & Taylor, N. R. (2019). Effects of future sea level rise on coastal habitat. *The Journal of Wildlife Management, 83*(3), 694–704.

Warrick, R. A., Oerlemans, J., Beaumont, P., Braithwaite, R. J., Drewry, D. J., Gornitz, V., Grove, J. M., Haeberli, W., Higashi, A., Leiva, J. C., Lingle, C. S., Lorius, C., Raper, S. C. B., Wold, B., & Woodworth, P. L. (1990). Sea level rise. In Climate change: *The IPCC Scientific Assessment.* pp. 257–282. Cambridge University Press. https://www.ipcc.ch/ipccreports/far/wg_I/ipcc_far_wg_I_chapter_09.pdf.

Weifeng, X., Jun, L., Dailiang, P., Jinge, J., Hongxuan, X., Hongyue, Y., & Jun, Y. (2024). Multi-source DEM accuracy evaluation based on ICESat-2 in Qinghai-Tibet Plateau, China. *International Journal of Digital Earth, 17*(1), 2297843. https://doi.org/10.1080/17538947.2023.2297843

Werner, A. D., & Simmons, C. T. (2009). Impact of sea-level rise on sea water intrusion in coastal aquifers. *Groundwater,* 47(2), 197–204.

Xie, C., Shao, Y., Xu, J., Wan, Z., & Fang, L. (2013). Analysis of ALOS PALSAR InSAR data for mapping water level changes in Yellow River Delta wetlands. *International Journal of Remote Sensing, 34*(6), 2047–2056.

Yong, E. L. (2021). Understanding the economic impacts of sea-level rise on tourism prosperity: Conceptualization and panel data evidence*. Advances in Climate Change Research, 12*(2), 240–253.

Yu, X., Luo, L., Hu, P., Tu, X., Chen, X., & Wei, J. (2022). Impacts of sea-level rise on groundwater inundation and river floods under changing climate. *Journal of Hydrology,* 614, 128554.

8.Appendices

Appendix 1: Study area and city information

Table A1: Details regarding study area and the considered cities

State	City/town	Area (sq. km)	2011* Population	2022* Population	Infrastructure/economy/eco-sensitivity
Andhra Pradesh	Visakhapatnam	681.96	17,28,128	23,31,000	Fishing industry, port city, petrochemical industries, tourism industry, mangroves, and Kambalakonda Wildlife Sanctuary.
Goa	Panaji	8.72	1,14,759	40,017	Tourism Industry.
Karnataka	Mangaluru	132.5	6,23,841	7,36,000	Port city, religious places, and industrial cities.
Karnataka	Udupi	68.23	1,65,401	1,70,000	Port city, religious places, agriculture and fishing/small scale industries, such as cashew nut.
Kerala	Kochi	440	21,19,724	6,25,345	Kochi port is one of the largest port. Fishing harbour, spices, Mangalavanam Bird Sanctuary, and Gulf of Mannar Marine National Park.
Kerala	Kozhikode	179	4,31,560	40,89,000	City of spices, tourism industry.
Kerala	Thiruvanathapura m	214	16,79,754	28,91,000	Tourism industry, religious places, and Vizhinjam International Seaport
Maharashtra	Mumbai	6,328	1,83,94,912	2,12,96,517	Largest economic hub of India. Eco-sensitive zones within Mumbai Urban Development Authority area are Thane Creek Flamingo Sanctuary, Sanjay Gandhi National Park,

State	City/town	Area (sq. km)	2011* Population	2022* Population	Infrastructure/economy/eco-sensitivity
					Tungareshwar Wildlife Sanctuary, Mumbai and Jawaharlal Nehru ports, textile industry, automotive parts industry, and tourism.
Odisha	Paradip	105	68,585	94,561	Port city, oil refinery, and steel plants.
Odisha	Puri	16.84	2,00,564	2,75,000	Tourism industry, religious places, and agriculture.
Puducherry	Yanam	30	55,626	35,000	Tourism industry.
Tamil Nadu	Chennai	1,189	86,53,521	1,19,33,000	Pallikaranai wetland, Guindy National Park, the Madras Crocodile Bank Trust and Centre for Herpetology, tourism industry, religious places, Royapuram fishing harbour, Chennai port, and Kasimedu harbour.
Tamil Nadu	Kanniyakumari	25.89	16,76,034	29,761	Tourism industry.
Tamil Nadu	Thoothukudi	353.07	2,37,830	Not found	Port city, salt production, thermal power industries, and petrochemical Industries.
West Bengal	Haldia	109	2,00,827	2,76,000	Port city, petrochemical industries.

*Source: Population Census, 2011; World Population Prospects, 2022

Appendix 2: CMIP6 GCMs used in the study

Table A2: Details regarding CMIP6 GCMs used in the study

Sl No.	Model	Reference	Data reference
1	ACCESS-CM2	ScenarioMIP Dix et al. (2019b)	10.22033/ESGF/CMIP6.2285
2	ACCESS-ESM1-5	ScenarioMIP Ziehn et al. (2019d)	10.22033/ESGF/CMIP6.2291
3	BCC-CSM2-MR	ScenarioMIP Xin et al. (2019b)	10.22033/ESGF/CMIP6.1732
4	CAMS-CSM1-0	Rong (2019a); DOI:10.22033/ESGF/CMIP6.1399	10.22033/ESGF/CMIP6.1399
5	CanESM5	Swart et al. (2019m); DOI: 10.22033/ESGF/CMI P6.10205,	10.22033/ESGF/CMI P6.10205
6	CanESM5-CanOE	Swart et al. (2019k); DOI:10.22033/ESGF/CMIP6.10203	10.22033/ESGF/CMIP6.10203
7	CAS-ESM2-0	OMIP Chai (2020c)	10.22033/ESGF/CMIP6.1954
8	CESM2	ScenarioMIP Danabasoglu (2019p)	10.22033/ESGF/CMIP6.2201
9	CESM2-WACCM	Danabasoglu (2019s); DOI:10.22033/ESGF/CMIP6.10024	10.22033/ESGF/CMIP6.10024
10	CIESM	ScenarioMIP Huang (2019b)	10.22033/ESGF/CMIP6.1357
11	CMCC-CM2-SR5	OMIP Fogli et al. (2020b); DOI: 10.22033/ESGF/CMI P6.13162 CMCC:CMCC-CM2-SR5 ScenarioMIP; Lovato and Peano (2020b),	10.22033/ESGF/CMIP6.1365
12	CMCC-ESM2	Lovato et al. (2021b); DOI:10.22033/ESGF/CMIP6.13164	10.22033/ESGF/CMIP6.13164
13	CNRM-CM6-1	ScenarioMIP Voldoire (2019i)	10.22033/ESGF/CMIP6.1384
14	CNRM-CM6-1-HR	Voldoire (2019j); DOI:10.22033/ESGF/CMIP6.1385	10.22033/ESGF/CMIP6.1385

Sl No.	Model	Reference	Data reference
15	CNRM-ESN2-1	Seferian, Roland (2018); DOI:10.22033/ESGF/CMIP6.1391	10.22033/ESGF/CMIP6.1391
16	E3SM-1-1	Bader et al. (2019b); DOI:10.22033/ESGF/CMIP6.11441	10.22033/ESGF/CMIP6.11441
17	EC-Earth3-AerChem	EC-Earth Consortium (EC-Earth) (2020f); DOI:10.22033/ESGF/CMIP6.639	10.22033/ESGF/CMIP6.639
18	EC-Earth3-CC	EC-Earth Consortium (EC-Earth) (2020); DOI:10.22033/ESGF/CMIP6.640	10.22033/ESGF/CMIP6.640
19	EC-Earth3-Veg-LR	EC-Earth Consortium (EC-Earth) (2020); DOI:10.22033/ESGF/CMIP6.4707	10.22033/ESGF/CMIP6.4707
20	FGOALS-g3	ScenarioMIP; Li (2019b)	10.22033/ESGF/CMIP6.2056
21	FIO-ESM-2-0	ScenarioMIP Song et al. (2019c)	10.22033/ESGF/CMIP6.9051
22	GFDL-CM4	Guo et al. (2018a); DOI:10.22033/ESGF/CMIP6.1402	10.22033/ESGF/CMIP6.1402
23	GISS-E2-1-G	ScenarioMIP NASA Goddard Institute for Space Studies (NASA/GISS) (2020)	10.22033/ESGF/CMIP6.2074
24	HadGEM3-GC31-LL	Ridley et al. (2018a); DOI:10.22033/ESGF/CMIP6.419	10.22033/ESGF/CMIP6.419
25	HadGEM3-GC31-MM	Ridley et al. (2019); DOI:10.22033/ESGF/CMIP6.420	10.22033/ESGF/CMIP6.420
26	INM-CM4-8	ScenarioMIP Volodin et al. (2019c); DOI: 10.22033/ESGF/CMI P6.12321 INM:INM-CM5-0 CMIP; Volodin et al. (2019d)	10.22033/ESGF/CMIP6.1423
27	INM-CM5-0	Volodin et al. (2019d); DOI:10.22033/ESGF/CMIP6.1423	10.22033/ESGF/CMIP6.1423
28	IPSL-CM6A-LR	ScenarioMIP Boucher et al. (2019a)	10.22033/ESGF/CMIP6.1532
29	KIOST-ESM	Kim et al. (2019a); DOI:10.22033/ESGF/CMIP6.1922	10.22033/ESGF/CMIP6.1922
30	MIROC6	Tatebe and Watanabe (2018); DOI:10.22033/ESGF/CMIP6.881	10.22033/ESGF/CMIP6.881

Sl No.	Model	Reference	Data reference
31	MIROC-ES2L	CMIP6 VolMIP; Earth System Grid Federation;	10.22033/esgf/cmip6.918
32	MPI-ESM1-2-HR	Jungclaus et al. (2019a); DOI:10.22033/ESGF/CMIP6.741	10.22033/ESGF/CMIP6.741
33	MPI-ESM1-2-LR	Mauritsen et al., 2019. https://doi.org/10.1029/2018MS001400	DOI:10.22033/ESGF/CMIP6.742
34	MRI-ESM2-0	Yukimoto et al. (2019e); DOI:10.22033/ESGF/CMIP6.621	10.22033/ESGF/CMIP6.621
35	NESM3	ScenarioMIP Cao (2019b)	10.22033/ESGF/CMIP6.2027
36	NorESM2-LM	CMIP6 OMIP. Earth System Grid Federation	10.22033/esgf/cmip6.598
37	NorESM2-MM	CMIP6 ScenarioMIP. Earth System Grid Federation	10.22033/esgf/cmip6.608
38	TaiESM1	PAMIP; Hong et al. (2020); DOI: 10.22033/ESGF/CMI P6.15214 AS-RCEC:TaiESM1 ScenarioMIP; Lee and Liang (2020)	10.22033/ESGF/CMIP6.9688
39	UKESM1-0-LL	AerChemMIP Dalvi et al. (2019)	10.22033/ESGF/CMIP6.1741

Appendix 3: IPCC AR6 SSP scenarios

Table A3: Details regarding IPCC AR6 SSP scenarios

SSP scenario	Description	Estimated warming	
		(2041–2060)	(2081–2100)
SSP1-1.9	Very low GHG emissions: CO2 emissions cut to net zero around 2050	1.6 °C	1.4 °C
SSP1-2.6	Low GHG emissions: CO2 emissions cut to net zero around 2075	1.7 °C	1.8 °C
SSP2-4.5	Intermediate GHG emissions: CO2 emissions remain around current levels until 2050, followed by a fall but not reaching net zero by 2100	2.0 °C	2.7 °C
SSP3-7.0	High GHG emissions: CO2 emissions double by 2100	2.1 °C	3.6 °C
SSP5-8.5	Very high GHG emissions: CO2 emissions triple by 2075	2.4 °C	4.4 °C

Appendix 4: Sources of city/town administrative maps

Table A4: Details regarding sources of city administrative maps

Sl No	Tier	Name	Urban limit source	Source link
1	I	Chennai	Chennai Metropolitan Development Authority	https://www.cmdachennai.gov.in/
2		Mumbai	Mumbai Metropolitan Region Development Authority	https://mmrda.maharashtra.gov.in/regional-plan#
3	II	Kozhikode	Town Planning Kerala	https://townplanning.kerala.gov.in/
4		Kochi	Kochi Municipal Corporation	https://kochicorporation.lsgkerala.gov.in/en/map/299
5		Kanniyakumari	Open source (Google)	https://www.google.com/maps/place/Kanniyakumari,+Tamil+Nadu/data
6		Mangaluru	Mangaluru Urban Development Authority	http://www.mangaluru.uda.gov.in/en/master-plan
7		Thiruvananthapuram	Corporation of Thiruvananthapuram	https://tmc.lsgkerala.gov.in/en/master-plan/1282
8		Visakhapatnam	Greater Visakhapatnam Municipal Corporation	https://www.gvmc.gov.in/
9	III	Haldia	Haldia Municipality	https://www.haldiamunicipality.org/town-map
10		Udupi	Udupi Urban Development Authority	http://www.udupi.uda.gov.in/en/LPAM
11		Panaji	North Goa Planning and Development Authority	https://www.goa.gov.in/department/north-goa-planning-development-authority/
12		Paradip	Paradip Municipality	https://www.chilika.com/pdf/ICZM_DPR.pdf
13		Puri	Puri Municipality	https://puri.nic.in/
14		Thoothukudi	Thoothukudi Municipal Corporation	https://doi.org/10.1007/s12594-014-0167-2
15		Yanam	Government of Puducherry	https://yanam.gov.in/about-district/#:~:text=The%20region%2C%20which%20covers%20an,Kms%20towards%20east%20from%20Yanam.

Appendix 5: Adopted LULC classification scheme

Table A5: Details regarding the adopted LULC classification scheme

Sl No.	Level I	Level II	Level III	Remarks
1	Built-up	Urban	Residential	Land used predominantly for housing than for commercial and industrial purposes.
2			Commercial	Land intended for use by for-profit businesses. Examples of such use are office complexes, shopping malls, service stations, bars, and restaurants.
3			Public and semi-public	Public and semi-public zones are formed to recognise that public and semi-public facilities and institutions provide necessary services to the community and have their own unique set of circumstances.
4			Recreational	Land use for leisure time activities undertaken voluntarily and for enjoyment.
5			Road	Road networks
6			Railway	Rail lines
7			Vacant land	Land that may be improved or developed but is not currently in use and has no structures (layouts).
8			Industrial	Land used for industries, factories, power plants, warehouses, etc. Activities performed here are important to that area's economy.
9		Green area	Green belt	Land for planting trees in patterns (such as avenue trees and trees along boundaries).
10			Tree-clad area	Land dominated by clumps of trees.
11			Tree cover	Land with individual trees.
12			Open space	Land reserved for parks, green spaces, including those for plants and water features or blue spaces, and other kinds of natural environment.
13			Road verge	A strip of grass or plants and sometimes trees located between a roadway (carriageway) and a sidewalk (pavement).

Sl No.	Level I	Level II	Level III	Remarks
14		Mining		Land under surface mining operations. The recognisable impacts of these activities on the landscape are unmistakable giant pit mines covering vast areas.
15	Agriculture	Cropland		Land for crops, such as Kharif, Rabi, and Zaid crops
16		Fallow land		Land with an alternation between a cropping period of several years and a fallow period.
17		Plantation		Land under agricultural tree crops planted adopting agricultural management techniques.
18	Wasteland	Gullied/ ravinous land		Gullies are formed as a result of localised surface run-off, which affects the unconsolidated material and leads to the formation of perceptible channels and undulating terrain. They are mostly associated with stream courses, sloping grounds with good rainfall regions, and foothill regions. These are the first stage of excessive land dissection followed by their networking, which leads to the development of ravinous land. Ravines are basically extensive systems of gullies developed along river courses.
19		Land with dense scrubs		Land with shallow and skeletal soils that are chemically degraded at times. These severely eroded extremes of slopes are subjected to excessive aridity. Such lands are dominated by scrubs and have a tendency for intermixing with croplands.
20		Land with open scrubs		Land with sparse vegetative cover or absence of scrubs. These have a thin soil cover.
21		Coastal sandy area		Coastal sands are accumulated as a strip along the seacoast due to seawater action. These are not being used for any purpose, including recreational activities.
22		Riverine sandy area		Riverine sands are accumulated in the flood plain of the river as sheets or as sand bars.

Sl No.	Level I	Level II	Level III	Remarks
23		Barren rocky area		Rock exposures of varying lithology, often barren and devoid of soil and vegetative cover. They occur on steep isolated hillocks/hill slopes, crests, plateau and eroded plains associated with barren and exposed rocky/stony wastes, lateritic outcrops, and mining and quarrying sites.
24	Wetland / Waterbodies	Coastal wetland		Estuaries, lagoons, creeks, backwaters, bays, tidal flats/mud flats, sands/beaches, rocky coasts, mangroves, salt marsh/marsh vegetation area are considered as costal wetland.
25		River/stream/canal		Rivers/streams are natural bodies of water flowing on the land surface along a definite channel/slope regularly or intermittently towards a sea in most cases, into a lake or an inland basin in desert areas, or into a marsh or another river. Canals are artificial water bodies constructed for irrigation and navigation or to drain out excess water from agricultural lands.
26		Lake/pond/tank		Water above ground.
27		Aquaculture		Cultivation of aquatic organisms in controlled aquatic environments for any commercial, recreational, or public purposes.

Appendix 6: Quantifying the accuracy of the ALOS PALSAR DEM

A DEM comprises of both Digital Terrain Model (DTM) and Digital Surface Model (DSM). A DTM represents the ground surface, while a DSM represents the above-ground surface, which includes trees and buildings. A study reviewed the articles on DEM accuracy for around 200 states and reported that there are no standardised guidelines to map the accuracy of DEMs, indicating a challenge for geospatial technology users (Mesa-Mingorance & Ariza-López, 2020). On the basis of projection reference systems (geodic and ellipsoid reference systems), the DEM accuracy is measured in two ways, namely, absolute and relative vertical accuracies (Ihsan & Sahid, 2021). The absolute vertical accuracy is measured with respect to a geodetic cartographic reference system when an official datum has been adopted. Meanwhile, relative vertical accuracy is measured with respect to a local reference system. The DEM accuracy is usually measured using the ground control point references from toposheet maps (Gautam, 2023; Mingorance & López, 2020; Sharma et al., 2021). Mean differences, standard deviation, and root mean-square error (RMSE) statistical indicators are commonly used to indicate the DEM accuracy. RMSE with lower values indicates the higher accuracy of the DEM. The table below provides details of ALOS PALSAR DEM accuracy assessments from other studies, revealing that ALOS PALSAR DEMs are more accurate and precise than other open-source DEMs.

Table A6: ALOS PALSAR DEM accuracy assessment from peer studies

Method/study type	Accuracy	Reference
Watershed delineation compared with ASTER, Cartosat-1, SRTM	R2= 0.998 Vertical low mean error = 19.20 m, compared with ground control points	Raman, 2023
Toposheet elevation as reference	RMSE = 4.76 m	Ferreira & Cabral, 2021
Frequency ratio and random forest	Frequency ratio – Random Forest = 0.917	Arabameri et al., 2019
Used ICESat-2 data	RMSE = 5.05 m	Weifeng et al., 2024
Comparison with LIDER data	RMSE = 9.64 m	Chai et al., 2022
Water storage estimations	NRMSC = 1.3% (lower error)	Bendib, 2021
Comparison of DEM with GCP	Vertical elevation accuracy = + −5 m	Gautam, 2023
Comparison of DEMs with GCP, GNSS	Mean square error = 0.09	Sharma et al., 2021

RMSE: Root mean-square error; GCP: Ground control points; and GNSS: Global Navigation Satellite System

Appendix 7: Accuracy assessment of LULCs

A total of 415 random samples from each city and town (15) were considered to assess the LULC accuracy, while open-source Google Earth Pro and Google map data were used as reference data. Equation 1 was used to perform the calculation. The assessment results revealed the Kappa coefficient to be 0.805, which indicates well-classified LULC maps (Arumugam et al., 2021).

$$\text{Kappa Coefficent} = \frac{\text{TRS} \times \text{TCS} - \sum(\text{Column total} \times \text{Row total})}{\text{TRS} \times \text{TRS} - \sum(\text{Column total} \times \text{Row total})} \quad \text{................ Eq. 1}$$

$$\text{Kappa Coefficent} = \frac{(415 \times 339) - (1{,}40{,}685)}{(1{,}72{,}225 - 1{,}40{,}685)} = 0.85$$

Where, TRS: Total random LULC samples considered across 15 cities and towns; TCS: Total correctly classified samples of TRS.

Table A7: Accuracy assessments of LULCs

LULC	Random sample	Referenced data (Google Earth/ Google map)
Agriculture land	59	62
Commercial	31	32
Forest	2	2
Green space	45	36
Industrial	32	33
Mixed use	23	19
Public and semi-public	54	59
Residential	34	32
Transportation	20	23
Vacant land	30	31
Waste land	38	38
Wetland/ Waterbodies	47	48
Total	415	415

CENTER FOR STUDY OF SCIENCE, TECHNOLOGY & POLICY

Bengaluru
#18, 10th Cross, Mayura Street, Papanna Layout,
Nagashettyhalli, RMV II Stage, Bengaluru 560094

Noida
1st Floor, Tower-A, Smartworks Corporate Park, Sector 125,
Noida 201303, Uttar Pradesh (India)

www.cstep.in | +91-8066902500 | cpe@cstep.in | @cstep_India